Optical and electrical characterisation of threaded molecular wires (TMWs) and related optoelectronic devices

Lisa-Jodie Parrott

A dissertation submitted for the degree of Doctor of Philosophy at the University of London

University College London

July 2007

ProQuest LLC
789 East Eisenhower Parkway
P.O. Box 1346
Ann Arbor, MI 48106-1346

Abstract

Commercial light-emitting devices (LEDs) are currently based on inorganic materials with high processing costs and associated environmental issues. In 1990 Burroughes et al published findings using conjugated polymers (carbon-based chains with single- and double-bonds) as the emissive layer in LEDs.

Organic light-emitting devices (OLEDs) are now commercially available as displays. They have advantages over conventional display technologies; larger viewing angles, lower operating powers and "true" colour display.

OLED device efficiencies and colour purity can be detrimentally altered by close proximity of polymer chains within the device. By separating the chains in the LED film this effect may be lessened. Polyrotaxanes have already found uses in molecular motors, whereas in the materials studied here on the macrocycle is utilised to increase chain separation distance between the conjugated main chains.

Previous work has shown that photoluminescence (PL) and electroluminescence (EL) of the polyrotaxane compared to the unthreaded polyrotaxane shifts to higher energies and polyrotaxane light emission is more efficient, indicating that the macrocycles do increase the distance between adjacent chains.

Different ionic side-groups using metallic and non-metallic ions have been incorporated to the main chain. These side-groups prevent disruption to the electronic structure of the unthreaded and threaded polyrotaxanes when temperature is raised, and the macrocycles provide further stabilisation.

Once an electric field has been applied to the device, the cation is mobile, and the anions remain anchored to the main chain. The ionic mobility allows the devices to emit under forward and reverse bias. This type of device is referred to as a light-

emitting electrochemical cell (LEC). Presence of large metallic cations (e.g. Cs^+) produce LECs which are more stable and exhibit higher PL and EL efficiencies than small metallic cations e.g. Li^+ based LECs. Further studies in to the addition of hole-transport layers for use with the water-soluble polymers has been carried out to boost operating efficiencies.

I, Lisa-Jodie Parrott, confirm that the work presented in this thesis is my own. Where information has been derived from other sources, I confirm that this is indicated in the thesis.

List of Abbreviations

AFM	Atomic Force Microscopy
Bn	Benzylate (CH_2-C_6H_5)
CD	Cyclodextrin
CPD	Contact potential difference
EA	Electron Affinity
EA	Electroabsorption
EL	Electroluminescence
EQE	External Quantum Efficiency
F8	Poly(9, 9-dioctylfluorene)
FWHM	Full-width half-maximum
HOMO	Highest occupied molecular orbital
IMW	Insulated molecular wire
IP	Ionisation Potential
ITO	Indium-tin oxide
K@[2.2.2]	Cryptate-encapsulated potassium
LCD	Liquid crystal display
LEC	Light-emitting electrochemical cell
LED	Light-emitting device
LUMO	Lowest unoccupied molecular orbital
Me	Methyl (CH_3)
NMe_4	Tetrametylammonium
OLED	Organic light-emitting device
PDPV	Poly(4, 4'-diphenylene diphenyl vinylene)
PDV	Poly(4, 4-diphenyl vinylene)
PDV⊂β-CD	Poly(4, 4-diphenyl vinylene) with cyclodextrin non-covalently threaded along its length
PEDOT:PSS	Poly(3, 4-ethylenedioxythiophene):Poly(styrene sulfonic acid)
PEO	Polyethylene (oxide)
PL	Photoluminescence
PPV	Poly(p-phenylene vinylene)
THS	Trihexylsilylate (Si-$(C_6H_9)_3$)
TMW	Threaded molecular wire
TR	Threading ratio
Φ	Work function

Work Outline

As detailed in chapter 1 conjugated polymers are of scientific interest for use in light emitting diodes. Work into adaptation of conjugated polymers to provide optimum device operation has been conducted by tailoring of the polymers as well as improvements of the device structure, either by thorough cleaning of the substrates used or by the use of additional layers in the device. The reader is introduced to polyrotaxanes in chapter 2 and the previous work with these materials for use in light emitting diodes. The further tailoring of these materials by substitution of the counter-cation is described.

Chapter 3 investigates the typical cleaning procedure of using oxygen plasma on ITO, and how effective it is over time in increasing the work function and the effect of placing either PEDOT:PSS or a conjugated polymer immediately on the ITO on the work function after oxygen plasma treatment. Whilst work into how the ITO work function can be increased has been conducted previously, the longevity of this effect has been overlooked in previous work. Measurements of ITO work function was made using a Kelvin Probe. Once this preliminary work into the best way of preparing substrates was completed it was then possible to characterise the optoelectronic properties of the polyrotaxanes and analogue polymers supplied by the Anderson Group. The ion-exchange of the PDV.Li and PDV.Li⊂β-CD was conducted to discover if there was a better choice of counter-cation to aid the optoelectronic properties. Work in to the optical characteristics was conducted to see if the variation of counter ion caused variation in the optical properties. The absorption and PL spectra as well as the photoluminescence efficiency of these materials is discussed in chapter 4, alongside comparison of polyrotaxanes which had been either singly or doubly threaded. The

additional robustness that the CD rings impart to the analogue polymer has already been demonstrated by the increase of PL efficiency and external quantum efficiency of devices in previous work. However the resilience of the materials to temperature had not been investigated so in chapter 5, the thermochromic behaviours of several polyrotaxanes and analogue polymers are compared to other conjugated polymers. After these investigations into the optical properties the electronic properties of the materials were then focused on: studies of devices made of the materials are described in chapter 6. In this chapter characterisation of the device behaviour of all the different counter-cation materials and the possible effect that further threading of the polyrotaxane is considered. The LEC-like behaviour is also demonstrated.

Chapters 7 and 8 cover preliminary work into the improvement of the device characteristics. Chapter 7 details the optoelectronic characteristics of organic soluble polyrotaxanes adapted from the water-soluble polyrotaxanes. Chapter 8 looks at how to improve the device structure whilst maintaining use of the water-soluble polyrotaxanes and analogue polymers. This is typically achieved by the addition of PEDOT:PSS as a hole transport layer. To make it compatible with the water-soluble polymers it was cross-linked. The cross-linking procedure is given as well as prototype device characteristics using F8BT. Finally, conclusions and suggestions for further work are presented in Chapter 9.

Acknowledgements

I would like to thank my supervisors Prof. F. Cacialli and Prof. N. Skipper for their support and guidance over my PhD. Thanks also go to Dr. M. Ellerby, Dr A. Downes, Dr A. Harker, Dr. S. Heutz, Dr. C. Wood, and Dr R. McKendry for help with experimental set-ups and simply pointing me in the right direction both in the metaphorical and physical sense. I am grateful to Prof. H. L. Anderson and Dr. M. Frampton for the provision of my polymers, insightful conversations and a welcoming smile when I visited Oxford. I owe most of my results in the second year to numerous support staff that ordered, lent or gave me materials I desperately needed.

I am thankful that my partner in crime Oliver Fenwick was always an optimistic cheerful and helpful friend, even after countless hours spent in the dark. Dr. G. Latini was a welcome addition (after nearly 2 years working alone on the project) to my one-man band and I hope he enjoyed the many hours stuck in the glovebox with me chatting away at him as much as I did. Thus I come to our group, which over the past 4 years has had many visitors but Prof S. Mian and Eleanor Hall stand out as two people that got me through those periods where *nothing* worked.

My final thoughts are with my family, friends and Alan whose constant support, comfort and most of, belief in my ability to finish my PhD got me here.

TABLE OF CONTENTS

LIST OF FIGURES

Chapter 1. General introduction to OLEDs

Here an overview of conjugated polymers and their properties is given. The use of conjugated polymers in light emitting diodes is introduced along with the physical processes involved.

1.1. Use of Conjugated polymers

Conjugated polymers (CPs) are polymers which have a specific bonding situation (which consists of a mixture of single and double/triple bonds) which leads to interesting properties, namely the ability to conduct electricity and also emit light.

Polymers are long (typically carbon-based) chains of the same base unit repeated many times. Carbon atoms have the ability to form stable bonds with 4, 3, or 2 other atoms and can form single, double or triple bonds Carbon's ability to form these different types of bonds stems from its electronic configuration. Carbon has 6 electrons distributed thus; $1s^2$, $2s^2$ and $2p_{xyz}^2$ when in the ground state. The 2p configuration has the ability to hold 6 (spin pairs in the x, y and z directions) electrons in the same energy level, which is slightly higher in energy than the 2s level.[1, 2]

The electron density in these levels takes on different shapes. In the s-orbitals it is assumed as being spherical whilst in the p-orbital levels it is more akin to a 3D figure of 8 as in Figure1-1.

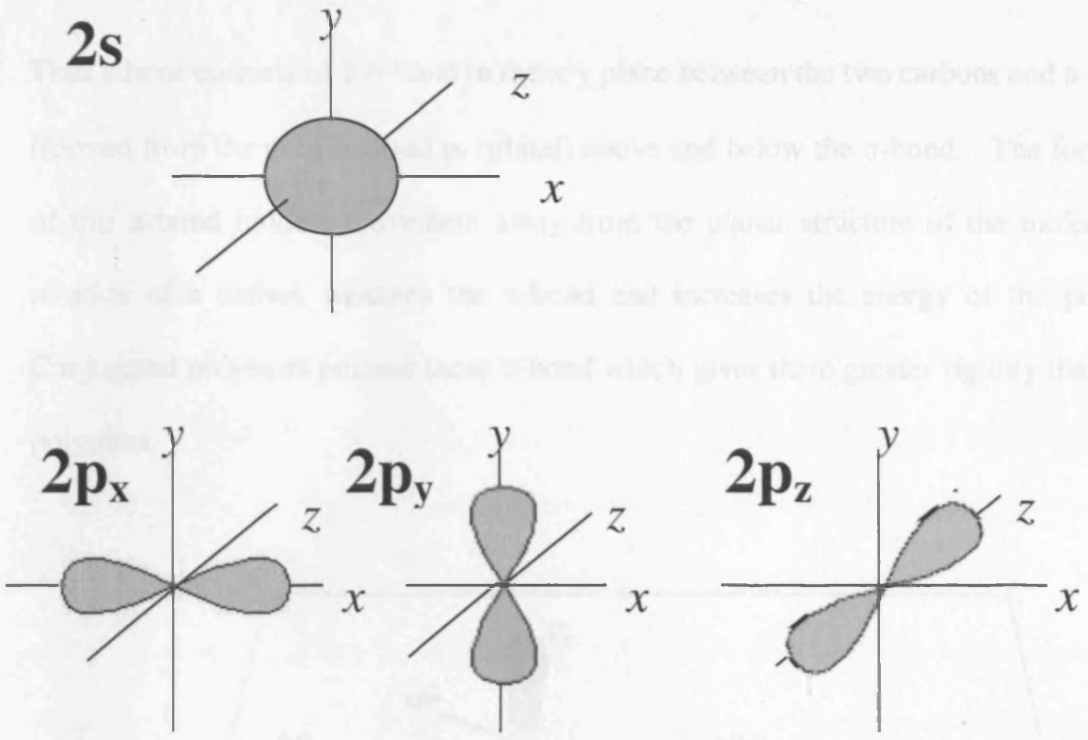

Figure 1-1 Schematic of the 2s and 2 p orbitals of a carbon atom.

In the ground state, carbon has the configuration of $2p^2$ so the electrons are spilt into two p-orbitals. This would lead to the carbon bonding with 2 other atoms. However, it has already been stated that carbon has the ability to form bonds with up to 4 atoms. This is because carbon can promote a 2s electron to a p-orbital as the energy level difference is small. The configuration could be thought of as $2s^1 2p_x^1 2p_y^1 2p_z^1$, which would allow four sigma bonds (σ-bonds) which lie along the chain, so the energy used to promote the electron is recovered by the carbon being able to make 4 rather than 2 bonds. However the electron densities of the s-orbital and p-orbital are able to overlap and thus form new hybrid orbitals (hybridisation). If methane (CH_4) is formed then all 3 p-orbitals are used in four hybrid orbitals (called sp^3) oriented to point towards the corners of a tetrahedron as this the geometry that minimises electron repulsion the most. When forming ethene (C_2H_4) then two p-orbitals (p_x and p_y) hybrise to form three hybrids oriented at 120 degrees to one another in the x-y plane p_z is not included in the hybridisation as this orbital lies perpendicular to the plane in which the hybrids lie.

Thus ethene consists of 1 σ-bond in the x-y plane between the two carbons and a π-bond (formed from the unhybridised p_z orbital) above and below the σ-bond. The formation of this π-bond hinders movement away from the planar structure of the molecule as rotation of a carbon weakens the π-bond and increases the energy of the polymer. Conjugated polymers possess these π-bond which gives them greater rigidity than other polymers.

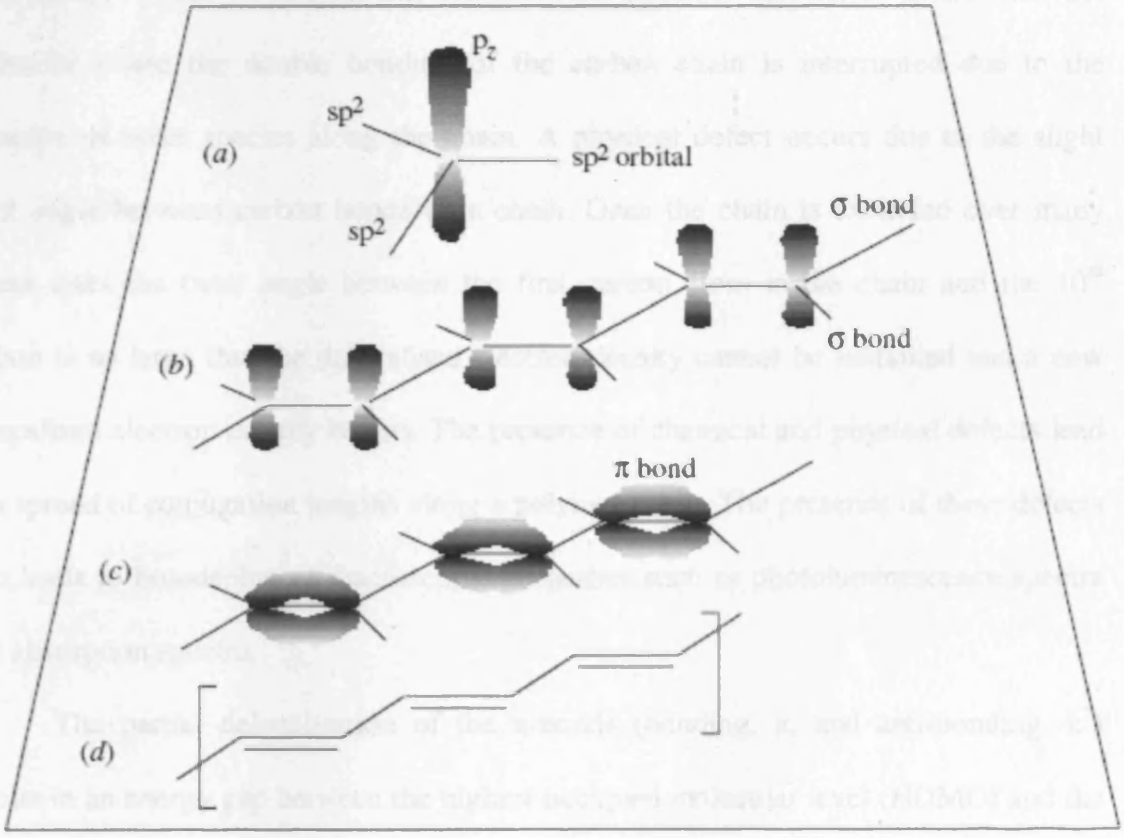

Figure 1-2 Schematic representation of a) A carbon atom which has been sp2 hybridised, note that the hybridised orbitals lie in the plan of the atom whilst the non-hybridised pz orbital is perpendicular to the plane. b) shows the σ-bonds in the plane of a polymer with the pz. In c) the pz atomic orbitals have now formed the diffuse π-bonds of the polymer by forming one π-bonds every two carbon atoms. d) is the conjugated polymer polyacetylene. Taken from [3].

Conjugated polymers have alternating single and double/triple bonds between the carbon atoms. These bonds are formed from σ- bonds (sp^2 hybridised atomic orbitals)

along the chain and π-bonds above and below the chain (the unused p_z orbital lies perpendicular to the chain). The σ-bonds are strong as the overlap between σ-orbitals is large; these σ-bonds thus determine the geometric structure of the molecule. The presence of π-bonds leads to a delocalisation of electron density over several repeat units, as the π-bond occupies a relatively diffuse space away from its original carbon. This development of the bonding in a conjugated polymer is shown in Figure 1-2.

The delocalisation of the π-bonding network is limited by defects within the polymer main chain. These defects include chemical and physical defects; a typical chemical defect is where the double bonding of the carbon chain is interrupted due to the presence of other species along the chain. A physical defect occurs due to the slight twist angle between carbon bonds on a chain. Once the chain is extended over many repeat units the twist angle between the first carbon atom in the chain and the 10^{th} carbon is so large that the delocalised electron density cannot be sustained and a new delocalised electron density begins. The presence of chemical and physical defects lead to a spread of conjugation lengths along a polymer chain. The presence of these defects also leads to broadening of macroscopic properties such as photoluminescence spectra and absorption spectra.

The partial delocalisation of the π-bonds (bonding, π, and anti-bonding, π^*) results in an energy gap between the highest occupied molecular level (HOMO) and the lowest unoccupied molecular level orbital (LUMO) when many polymer chains are closely packed. This development is depicted in Figure 1-3, which also shows the atomic orbitals used to form the π-bonds. This energy gap ranges from 3-5eV in conjugated polymers. Promotion of an electron from the HOMO to LUMO level is therefore possible and if the excited electron decays radiatively it will be as visible light.

Conjugated polymers, via their semiconductor properties, therefore have uses as light emitters if an exciton can be placed on the chain.

If a charge (electron or hole) is placed on the chain the polymer will relax to a new bonding geometry. A typical example is shown below in Figure 1-4 for poly(para-phenylenevinylene), PPV.

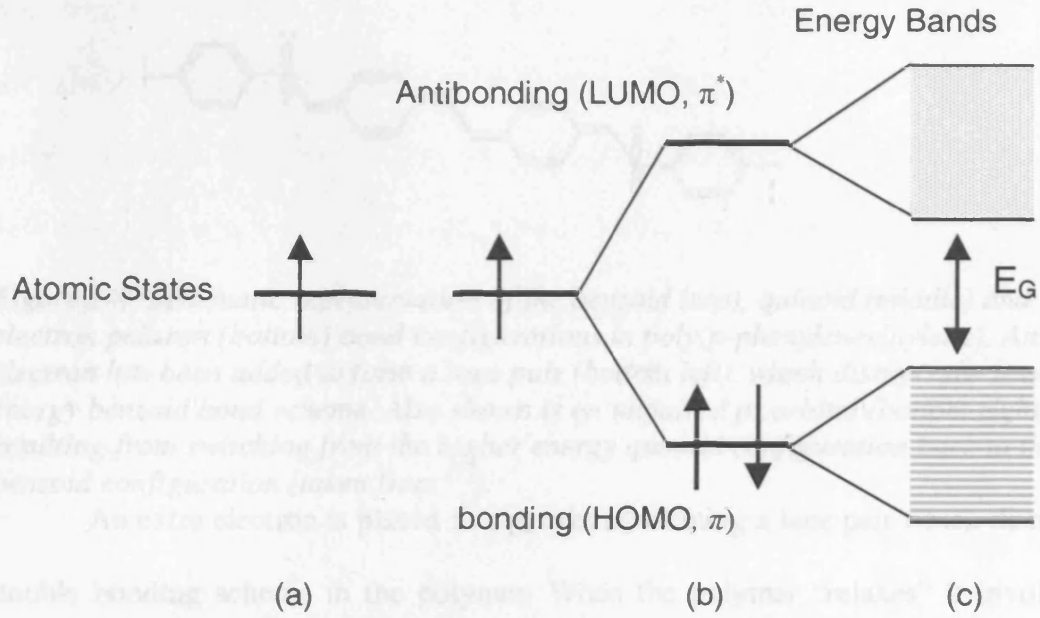

Figure 1-3 Schematic energy diagram showing the formation of band-like electronic states. (a) atomic states; (b) bonding and antibonding states; (c)in a collection of atoms, interactions between orbitals broaden the bonding and antibonding states into energy bands (adapted from references [4-6]).

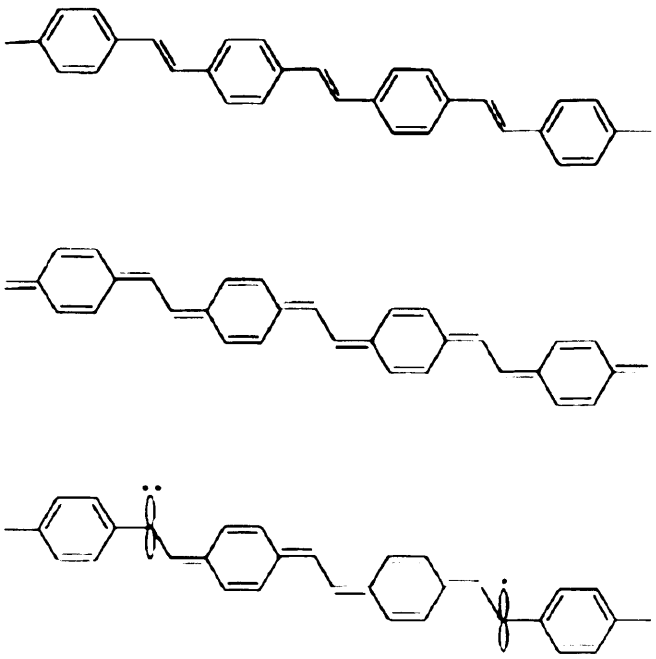

Figure 1-4 Schematic representation of the benzoid (top), quinoid (middle) and electron polaron (bottom) bond configurations in poly(p-phenylenevinylene). An extra electron has been added to form a lone pair (bottom left), which disrupts the lower energy benzoid bond scheme. Also shown is an unpaired pz orbital (bottom right) resulting from switching from the higher energy quinoid configuration back to the benzoid configuration (taken from [7]).

An extra electron is placed in a p_z orbital, forming a lone pair which disturbs the double bonding scheme in the polymer. When the polymer "relaxes" it involves the switching of the carbon double and single bond positions within the chain. This gives rise to a chain that is an admixture of the lower-energy benzoid and the higher energy quinoid PPV configurations. The relaxed negatively charged state is called an electron polaron, if an electron is removed it is a hole polaron. Further addition or removal of electrons result in doubly charged polarons called bipolarons. These polarons and bipolarons lie in new electronic states that are symmetrically located above the HOMO and the LUMO energy levels.

The polaron states are responsible for electronic conduction in conjugated polymers. In the solid state the polymers are packed in an amorphous matrix. Thus as the polymers are closely associated charge transport can occur both along a chain

(intrachain) and between chain segments of two different polymers (interchain). Light emission occurs when two oppositely charged polarons form a bound neutral polaron-exciton and recombine radiatively to emit a photon. This can also be caused by the absorption of a photon with the appropriate energy. If the exciton radiatively decays the energy of the emitted photon is determined by the difference in energy of the lowest-energy excited state and the ground state of the polymer. Emission of the photon always occurs from the lowest vibrational state of the polymer as high energy excitons are unstable and quickly decay to this state. The emission spectra of conjugated polymers is at a lower energy than the absorption spectra because excitons can diffuse between different conjugated segments during their lifetime and will move preferentially to a low energy, better ordered segment from which they then decay. This is known as a Stokes Shift. Figure 1-5 describes this process for an isolated chromophore.

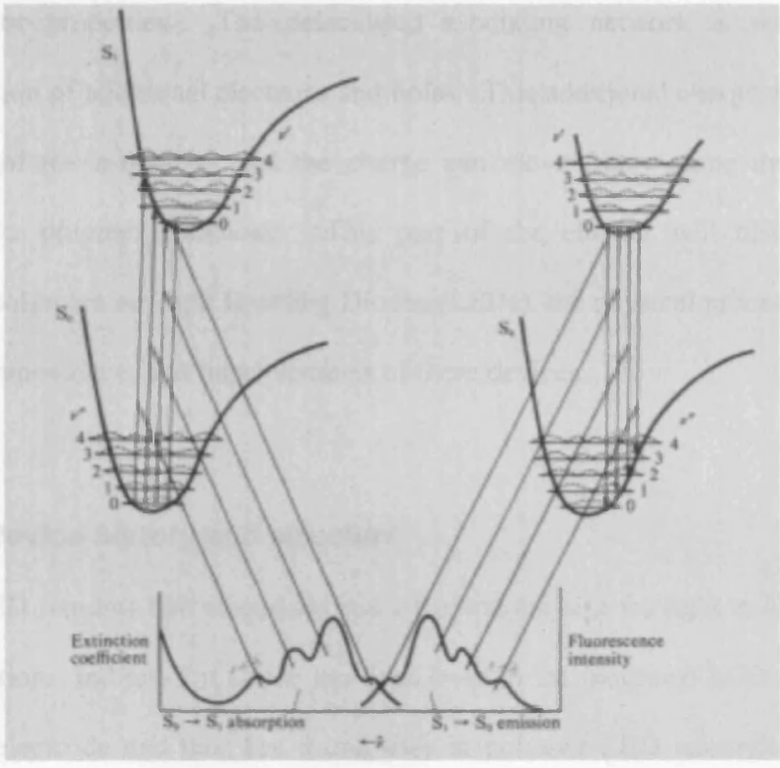

Figure 1-5 Schematic diagram illustrating the energy transitions for emission and absorption in an isolated chromophores. Vibrational relaxation to the lowest energy level of the S1 excited states occurs within 100ps. Emission always occurs from this level. Exciton migration to longer, lower energy segments of polymer introduces an additional energy shift between the 00-0 states of emission and absorption. Taken from reference. [8]

Bound polaron-pairs (excitons) do not only form on a single polymer chain. As polymers are in an amorphous or a crystalline matrix they can form on different chains due to the proximity of polymer chains. If it forms on identical molecular units on separate chains it is known as an excimer and if forms on two different molecular units on separate chains it is a exciplex. Note that when the terms hole, electron and exciton are used in this thesis the accompanying term "polaron" is implied.

1.2. Use of Conjugated Polymers in Light Emitting Diodes

Molecular electronics is used to describe the use of molecules for electronics such as light emitting diodes and electronics at the molecular level. Conjugated polymers are a large area of research in molecular electronics due to their

semiconductor properties. The delocalised π-bonding network is well suited to accommodation of additional electrons and holes. This additional charge causes a local distribution of the π-bonding and the charge can move freely along the conjugated segment of a polymer backbone. This part of the chapter will discuss uses of conjugated polymers as Light Emitting Diodes (LEDs), the physical processes involved in electroluminescence, and improvements of these devices.

1.2.1. Device history and structure

A LED requires two electrodes and a transparent side for light to be emitted via charge injection. Indium-Tin Oxide has been used in the inorganic LCD industry as a transparent electrode and thus has found uses in polymer LED research. The typical polymer LED structure is shown in Figure 1-6a). This "sandwich structure" was first employed by Burroughes and reported in 1990[9] following the work by Tang and Van Slyke on sublimed organic films in the 1980's.[10] The polymer is spun onto the ITO and the other electrode thermally evaporated on top of the polymer layer. The multilayer is made up of thin layers and is typically 300nm thick from the ITO to the metal electrode.

As ITO has a work function of about 4.7 eV before any treatment[11] it is most suited to being the anode (hole injector) and is the substrate for the device. The cathode thus injects electrons and metals such as aluminium and calcium are commonly employed. Radiative recombination of electrons and holes in the polymer film leads to photon production once a bias has been applied across the two electrodes. The cathode and anode are chosen so that the work functions of the electrodes closely match the HOMO and LUMO energy levels of the polymer, if not, the barrier to charge injection is too large.[12] A typical energy level diagram has been given in Figure 1-6b). The work function of the anode (ITO) has been matched to the ionisation potential (IP) of

the PPV polymer whilst the metal cathode (Al) is matched to the Electron Affinity (EA) of the polymer. Note that there is an energy level mismatch between the polymer IP and EA and the electrodes. The mismatch tends to be larger for the injection of electrons. The work functions of calcium and magnesium are closer in value to polymer EAs. These are used but are not desirable for mass production of polymer LEDs due the reactivity of these metals. To prevent reactions, once in air, a capping layer of aluminium is then deposited over the calcium/magnesium layer

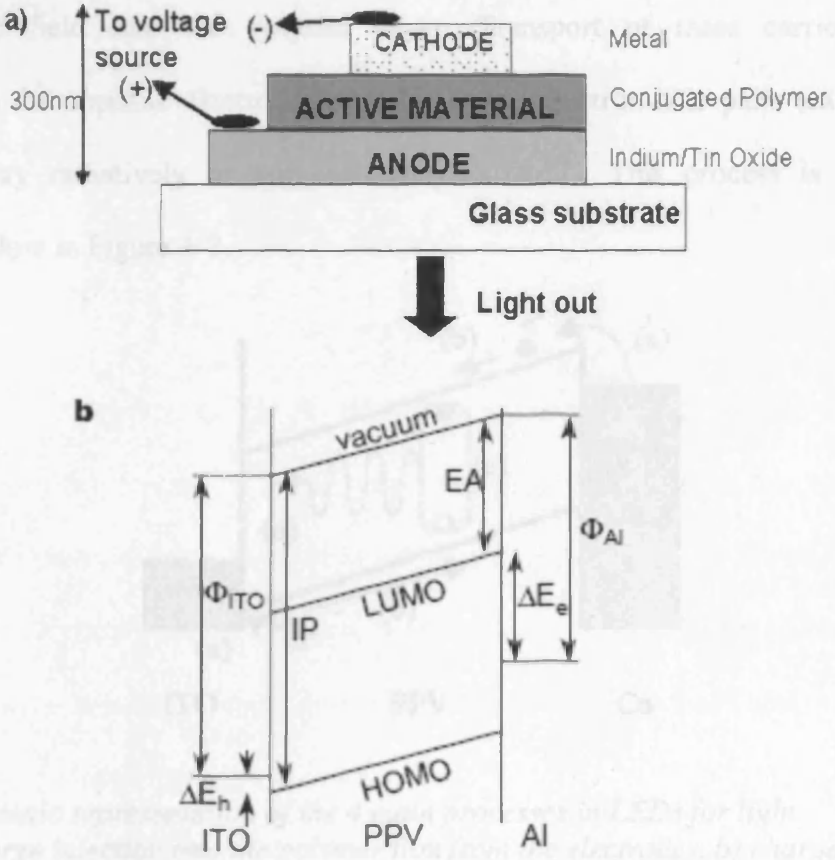

Figure 1-6 a) Polymer light-emitting diode using a multilayer structure; excluding the glass substrate they are typically 300nm in thickness. Once an external bias is applied charge carriers combine in the polymer layer and decay radiatively, producing light - which is emitted through the transparent ITO. b) Energy level diagram of a typical multilayer structure device with a forward bias. It shows the electron affinity (EA) and ionisation potential (IP) of the polymer, the work functions of the electrodes (ΦITO and ΦAl). The barriers to hole (ΔE_h) and electron injection (ΔE_e) are also shown. Figure 1-6b) from Friend et al[13].

1.2.2. Charge Transfer Process

Electroluminescence occurs when excitons produced by the application of electric field decay radiatively and produce photons. The production of electroluminescence can be spilt into four distinct parts; a) Bipolar charge injection into the polymer layer, b) Charge migration in the polymer film, c) Charge combination in the film to form excitons and d) Radiative decay of the exciton. The exciton forms from the injection of holes and electrons from the electrodes under the application of an external electric field into the polymer layer. Transport of these carriers via drift/diffusion to the opposite electrode results in bound electron-hole pairs (excitons) which may decay radiatively or non-radiatively.[3, 13, 14] This process is shown schematically below in Figure 1-7.

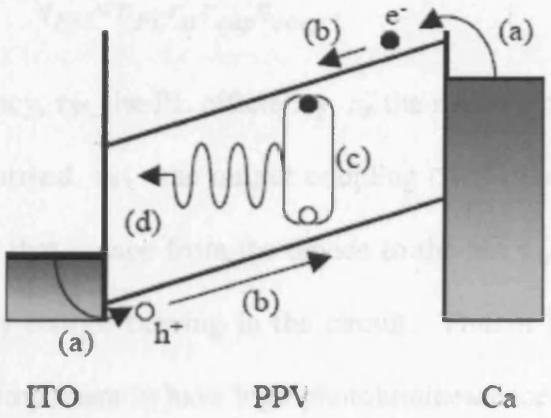

Figure 1-7 Schematic representation of the 4 main processes in LEDs for light emission. a) Charge injection into the polymer film from the electrodes, b) charge migration in the polymer film, c)exciton formation and d) radiative decay of the exciton. Adapted from [15].

There are two possible process for charge injection into the polymer film; 1) Thermonic Emission[16] and 2) Quantum mechanical tunnelling/field emission.[17, 18] Each model has limitations and so are both used in the literature to describe charge injection. Charge transport through the field is normally described by a charge hopping mechanism through numerous localised molecular states. Charge injection is normally

uneven for electrons and holes (which has a higher injection is dependant on the energy level matching between the electrodes and the polymer HOMO/LUMO levels) into the device and then electron mobility through the polymer film is lower than that of the holes and has been attributed to charge trapping of the electrons by oxygen.

Operational performance of LEDs can be classified in various ways some of them include brightness of the LED, lifetime and various operating efficiencies. Firstly the internal quantum efficiency[13, 19] is considered. This is defined as the ratio of the number of photons produced within the device to the number of electrons flowing in the external circuit and is given in Equation 1-1. The efficiency is also frequently expressed by the external quantum efficiency, Equation 1-2.

$$\eta_{\text{int}} = \eta_{PL} r_{st} \gamma_{cap} \qquad \text{Equation 1-1}$$

$$\eta_{EL} = \eta_{PL} r_{st} \gamma_{cap} \eta_{coup}, \qquad \text{Equation 1-2}$$

where η_{EL} is the EL efficiency, η_{PL} the PL efficiency, r_{st} the number of singlets over the total number of excitons formed, η_{PL} the output coupling coefficient is related to the fraction of emitted photons that escape from the device to the air. γ_{cap} is the number of excitons formed per unitary charge flowing in the circuit. Thus it is apparent that to have high efficiencies it is important to have high photoluminescence efficiency as well as having a balanced charge injection into the device.[16]

The external quantum efficiency takes into account that not all photons that are produced are emitted. The output coupling coefficient is needed as due to the refractive index mismatch between the ITO and various layers in the device, a considerable portion of the emitted photons are trapped within the device where they either dissipate or are scattered as edge emission. Other factors that may be included in the external quantum efficiency calculation are the geometry of the measuring apparatus, the sensitivity and quantum efficiency of the photon detector and of course that the human

eye is not uniformly sensitive to light of different wavelengths.[19, 20] If the sensitivity of the human eye is considered then the measured efficiency is the luminous current efficiency. In this work we use luminous current efficiency

1.3. Improvement of polymeric devices

There are many ways in which the operational efficiency of a device may be increased; the charge injection of electrons/holes may be unequal and/or low, recombination of electrons/holes could be low and excitons may decay non-radiatively via the formation of triplets as their decay lifetimes are long and so are more likely to diffuse to a quenching site.[21, 22] Improvements to devices have tried to tackle these issues, by tailoring of polymers so that if triplets are produced they can radiatively decay via by use of heavy atoms even though it is a spin-forbidden transition. Additional layers have been placed in the device at the interface between the emissive polymer and the electrodes to increase charge injection. By the blending of two polymers the charge build-up on segments can be increased so as to increase the probability of recombination within the device rather than the charge passing through the device from one electrode to the other. Ways of guiding the emitted photon in the device have also been suggested. The more common methods are to add a hole transport layer, use a blend of conjugated material and to tailor the polymer.[23]

Hole Transport Layers (HTLs) will be mentioned in more detail below, as after improving electrode work function and polymer HOMO/LUMO energy level match-up to the metal electrode work functions, it is the next step in improving device operation. Tailoring of the polymer is useful as excimer formation can lead to non-radiative decay; thus by imparting a separation between different polymers it may reduce excimer formation. This led to synthesis of conjugated polymers with isolated chromophores,

either by placing spacers along the polymer chain or by introducing steric hindrances to increase the distance between different polymer chains.[24]

1.3.1. Hole Transport Layers

A hole transport layer is often added to the device, to further reduce the barrier to hole injection.[25] The most common hole transport layer is PEDOT:PSS, (Poly (3, 4-ethylenedioxythiophene and Poly(styrene sulfonic acid)), experiments have shown PEDOT:PSS to reduce barrier height by up to 0.5V.[26] This is an ionically bound polymer that is spun onto the ITO surface before the active conjugated polymer layer; its chemical structure is given in Figure 1-8. The PEDOT is ionically bonded to the polyelectrolyte, PSS to render it soluble in water as the PEDOT is insoluble. The PEDOT:PSS is a colloidal suspension in water and as the PSS is the higher molecular weight compound, when films are made, the PSS defines the film morphology.

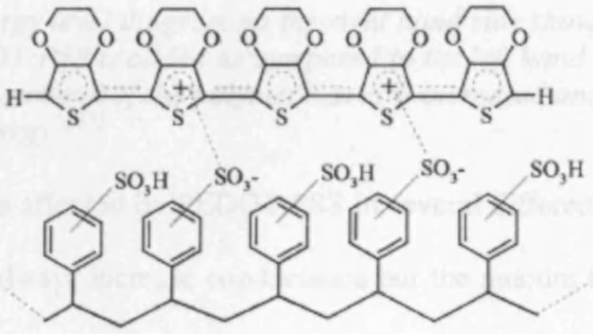

Figure 1-8 The PEDOT is the upper most compound and the PSS is ionically bonded via the side groups. Taken from [27].

The use of PEDOT:PSS also brings other benefits, the conducting polymer makes a repeatable clean interface with the PEDOT:PSS, the PEDOT:PSS suppresses the oxidation of the conducting polymer by suppressing migration of oxygen from the ITO to the conducting polymer.[26, 28-31] The PEDOT:PSS is now effectively the anode and whilst it has lower conductivity than ITO[32, 33] it brings improved device efficiencies,

lifetimes and reduction in the operating voltage.[34] PEDOT:PSS is thus commonly spun onto ITO before the emissive polymer as it increases the device conductivity and increases charge injection by either lowering the energy barrier for hole injection into the polymer film or raising the conduction band level of the emissive polymer . An example of how the energy levels in the device realign in the presence of PEDOT:PSS is presented in Figure 1-9.

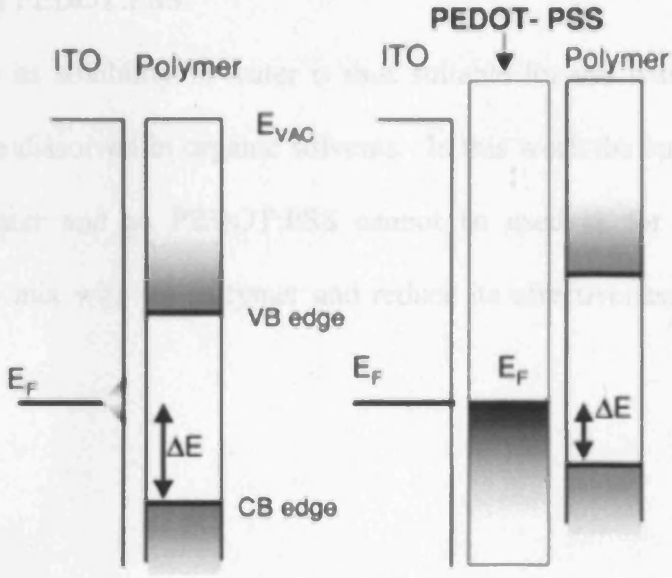

Figure 1-1-9 The energy level diagram on the right hand side shows the energy level alignment after PEDOT:PSS is added as compared to the left hand side diagram. It is seen that the conduction band of the polymer has now increased and is closer in energy to the metal Fermi energy. [25]

Device conductivity is affected by PEDOT:PSS in several different ways (the presence of PEDOT:PSS will always increase conductance but the amount by which conduction is increased can also be adjusted). The conductivity increase may be maximised by variation of a) solvent, b) heat treatment of PEDOT:PSS(and in which conditions), c) ratio of PEDOT to PSS and d) the quality of the interface between the anode and PEDOT:PSS and the active layer and the PEDOT:PSS.[28, 30, 35-37]

The interface between PEDOT:PSS and ITO is thus an important factor in ensuring device stability and good device performance. Whilst the PEDOT:PSS may prevent diffusion of oxygen species from the ITO to the polymer layer the presence of the

PEDOT:PSS may encourage acidic attack of the ITO surface. ITO is known to be sensitive to acidic environments, research has shown that PPV devices made from a sulfonium precursor route has HCL present once the conversion is complete. This HCl etches the ITO and the products of this reaction were found in the PPV layer. PSS is acidic and has been found to etch the ITO surface, resulting in traces of Indium in the emissive layer.[28] However it should be noted that this does not detract from the overall benefits of the use of PEDOT:PSS.

PEDOT:PSS due to its solubility in water is thus suitable for use with most emissive polymers as they are dissolved in organic solvents. In this work the emissive polymers are dissolved in water and so PEDOT:PSS cannot be used as for organic soluble polymers. It would mix with the polymer and reduce its effectiveness as an emissive polymer.

1.4. References

[1] P. W. Atkins, *Physical Chemistry*, Oxford University Press, Oxford **1994**.

[2] K. P. C. Vollhart, N. E. Schore, *Organic Chemistry Structure and Function*, W. H. Freeman and Company, United States of America **1999**.

[3] F. Cacialli, *Philosophical Transactions of the Royal Society of London Series A-Mathematical Physical and Engineering Sciences* **2000**, *358*, 173.

[4] M. Pope, C. E. Swenberg, *Electronic Processes in Organic Crystals and Polymers*, Oxford University Press, New York **1999**.

[5] M. F. Rubner, *Molecular Electronics*, Research Study Press, Somerset **1992**.

[6] R. A. Street, *Hydrogenated Amorphous Silicon*, Cambridge University Press, Cambridge **1991**.

[7] I. H. Campbell, D. H. Smith, *Solid State Physics; Vol 55*, Academic Press, San Diego **2001**.

[8] A. Kearwell, F. Wilkinson, *Transfer and storage of energy by molecules*, Wiley, New York **1969**.

[9] J. H. Burroughes, D. D. C. Bradley, A. R. Brown, R. N. Marks, K. Mackay, R. H. Friend, P. L. Burns, A. B. Holmes, *Nature* **1990**, *347*, 539.

[10] C. W. Tang, S. A. Vanslyke, *Applied Physics Letters* **1987**, *51*, 913.

[11] J. S. Kim, M. Granstrom, R. H. Friend, N. Johansson, W. R. Salaneck, R. Daik, W. J. Feast, F. Cacialli, *Journal of Applied Physics* **1998**, *84*, 6859.

[12] T. Kugler, W. R. Salaneck, H. Rost, A. B. Holmes, *Chemical Physics Letters* **1999**, *310*, 391.

[13] R. H. Friend, R. W. Gymer, A. B. Holmes, J. H. Burroughes, R. N. Marks, C. Taliani, D. D. C. Bradley, D. A. dos Santos, J. L. Bredas, M. Logdlund, W. R. Salaneck, *Nature* **1999**, *397*, 121.

[14] D. Bradley, *Current Opinion in Solid State & Materials Science* **1996**, *1*, 789.

[15] T. M. Brown, **2001**.

[16] N. C. Greenham, R. H. Friend, Vol. 49, Academic Press, San Diego **1995**, p1.

[17] I. D. Parker, *Journal Of Applied Physics* **1994**, *75*, 1656.

[18] R. N. Marks, D. D. C. Bradley, R. W. Jackson, P. L. Burn, A. B. Holmes, *Synthetic Metals* **1993**, *57*, 4128.

[19] N. C. Greenham, R. H. Friend, D. D. C. Bradley, *Adv. Mater.* **1994**, *6*, 491.

[20] J.-S. Kim, P. K. H. Ho, N. Greenham, C., R. H. Friend, *Journal of Applied Physics* **2000**, *88*, 1073.

[21] A. Kohler, J. Wilson, *Organic Electronics* **2003**, *4*, 179.

[22] J. S. Wilson, A. S. Dhoot, A. Seeley, M. S. Khan, A. Kohler, R. H. Friend, *Nature* **2001**, *413*, 828.

[23] M. A. De Paoli, W. A. Gazotti, *Macromolecular Symposia* **2002**, *189*, 83.

[24] A. Kraft, A. C. Grimsdale, A. B. Holmes, *Angew. Chem.-Int. Edit.* **1998**, *37*, 402.

[25] G. Greczynski, T. Kugler, M. Keil, W. Osikowicz, M. Fahlman, W. R. Salaneck, *Journal of Electron Spectroscopy and Related Phenomena* **2001**, *121*, 1.

[26] T. M. Brown, J. S. Kim, R. H. Friend, F. Cacialli, R. Daik, W. J. Feast, *Applied Physics Letters* **1999**, *75*, 1679.

[27] F. Louwet, L. Groenendaal, J. Dhaen, J. Manca, J. Van Luppen, E. Verdonck, L. Leenders, *Synthetic Metals* **2003**, *135*, 115.

[28] M. P. de Jong, L. J. van Ijzendoorn, M. J. A. de Voigt, *Applied Physics Letters* **2000**, *77*, 2255.

[29] T. M. Brown, F. Cacialli, *Journal of Polymer Science Part B-Polymer Physics* **2003**, *41*, 2649.

[30] T. P. Nguyen, P. Le Rendu, P. D. Long, S. A. De Vos, *Surface & Coatings Technology* **2004**, *180-81*, 646.

[31] J. C. Scott, S. A. Carter, S. Karg, M. Angelopoulos, *Synthetic Metals* **1997**, *85*, 1197.

[32] S. A. Carter, M. Angelopoulos, S. Karg, P. J. Brock, J. C. Scott, *Applied Physics Letters* **1997**, *70*, 2067.

[33] G. Gustafsson, Y. Cao, G. M. Treacy, F. Klavetter, N. Colaneri, A. J. Heeger, *Nature* **1992**, *357*, 477.

[34] J. S. Kim, R. H. Friend, F. Cacialli, *Applied Physics Letters* **1999**, *74*, 3084.

[35] M. M. de Kok, M. Buechel, S. I. E. Vulto, P. van de Weijer, E. A. Meulenkamp, S. de Winter, A. J. G. Mank, H. J. M. Vorstenbosch, C. H. L. Weijtens, V. van Elsbergen, *Physica Status Solidi A-Applied Research* **2004**, *201*, 1342.

[36] H. J. Snaith, H. Kenrick, M. Chiesa, R. H. Friend, *Polymer* **2005**, *46*, 2573.

[37] P. J. Brewer, J. Huang, P. A. Lane, A. J. deMello, D. D. C. Bradley, J. C. deMello, *Physical Review B* **2006**, *74*.

Chapter 2. Polyrotaxanes as molecular wires

The supramolecular structures which are studied in this work, polyrotaxanes, are introduced as well as some of uses they have already found in industry. The concept of molecular wires is introduced and related to polyrotaxanes. The materials used in this work are then presented along with their synthesis route. Previous work and findings on these polymers are then summarised.

1.1. Polyrotaxanes

Polyrotaxanes are a type of supramolecular structure. They have a polymer backbone which is threaded non-covalently through several macrocycle (organic molecules that are circular in shape) units. The macrocycle may be prevented from unthreading from the polymer chain by the addition of large side or end groups to the polymer backbone. The polymer backbone on its own may be referred to as the analogue polymer, reference polymer or as a polydumbbell (because of its shape). In this work it is referred to as the analogue polymer. This broad description of polyrotaxanes allows many materials to be classed as polyrotaxanes. For consistency, in this work we will use polyrotaxane to refer to an organic polymer backbone specified by the term "analogue polymer" threaded with organic macrocycles.

Synthesis of rotaxanes has been conducted for many years[1-5] and from this, if the "dumbbell" guest is threaded through several macrocycles it leads to a main-chain pseudopolyrotaxane or a polyrotaxane. The stages in the synthesis of rotaxanes are shown in Figure 2.1. If the analogue polymer guest is threaded through only one macrocycle a pseudorotaxane is created, if threaded through several macrocycles a main-chain pseudopolyrotaxane is formed. To be a true polyrotaxane there must be

end-groups which are sufficiently large to prevent the macrocycles from unthreading as in Figure 2.1c).

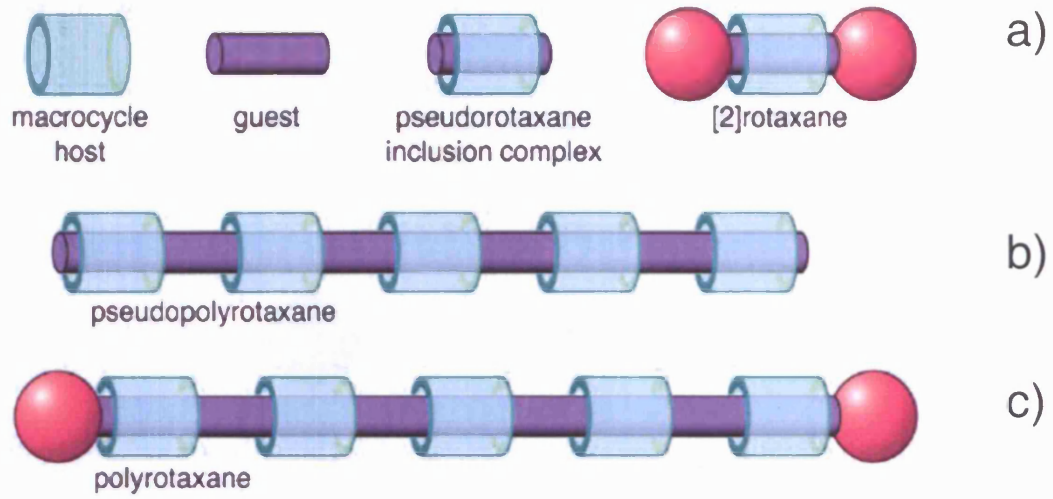

Figure 2-1 The terms used to describe polyrotaxanes. In this example the polyrotaxane is a [6] rotaxane. To be a true polyrotaxane (bottom image) there must be large end-groups to prevent the macrocycle host from unthreading otherwise it is a pseudopolyrotaxane as in the middle image. Taken from [6].

The typical polyrotaxane and its generic shape is shown at the bottom of Figure 2-1. The rings represent the macrocycle guest at regular intervals along the chain. The large spherical objects at either end of the polyrotaxane are the bulky end groups used to prevent unthreading. The ability to thread small molecules around much larger polymers has been known to organic chemists for many years. It is normally a delicate synthetic process and until 20 years ago was not thought to have any technological use, however recent research has proved this not to be so.

With the increasing desire to be able to manipulate at the mesoscale, research into using polyrotaxanes, rotaxanes, psuedopolyrotaxanes and psuedorotaxanes as molecular motors and drug delivery systems, via the use of a molecular motor, has been extensively studied[7, 8]. All make use of the presence of the macrocycle. In a molecular motor it can shuttle from one end of the polyrotaxane to another, perhaps allowing the backbone to undergo a conformation change and thus change the energy of the system.

Rotaxanes in which there is only one macrocycle per two dumbbell units, can act as a molecular switch. The macrocycle is present at either the site of dumbbell "0" or dumbbell "1" in response to external stimulus as in Figure 2-2 from [8].

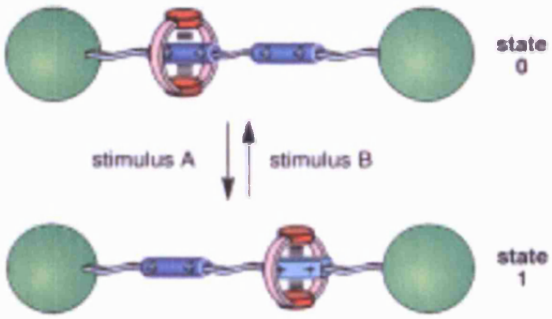

Figure 2-2 The macrocycle is able to "slip" from one unit to another under external stimulus, resulting in two different states. Taken from [8].

In drug delivery the macrocycle may protect the drug until it is needed and the macrocycle is then removed from the polymer backbone at the drug delivery site by the molecular motor action. The motion in these artificial molecular motors can be activated via electrochemical, photochemical and binding environments dependant on the design and anticipated use of the motor. There are possibilities of use in molecular electronics to further scale down circuitry size by using these wires to pass electrons along.

More recently new uses of the polyrotaxanes as insulated molecular wires have been developed, which raises the possibility of utilising polyrotaxane structures in conducting and luminescent capacities. A molecular wire typically describes a conjugated polymer which has efficient charge transport along its length such as poly(phenylenevinylene).[9] This charge transport along the wire is of importance in the application of molecular wires for molecular electronics. However, as previously discussed, issues with the use of "molecular wires" arise from modification of the optoelectronic properties due to inter-chain interactions: the resulting loss of singlet decay in devices, for example, leads to lower light emission unless the polymer is

adapted to make use of triplet decay. Separating the chains with an insulating sheath, to create an insulated molecular wire (IMW), can lessen and even block these interactions. Encapsulation of the conjugated polymer can also reduce the chemical instability[10] which is a common problem when operating organic semiconductors in devices what can lead to rapid degradation of the device.

When designing an IMW it is important to keep the solution processability of the initial polymer as this is one of the key benefits of organic semiconductors over inorganic semiconductors. Frampton and Anderson have written a comprehensive review of IMWs[6] where they study three types of IMWs in depth:

1) polyrotaxanes, as described in this work,

2) polymer-wrapped molecular wires,

3) dendronized conjugated polymers.

Polymer wrapped molecular wires encapsulate the wire by wrapping it with another polymer. It then becomes the guest inside the axial cavity of a helix. Amylose is a common choice for this encapsulation. This type of encapsulation is difficult to structurally characterise and thus perhaps not the best solution for molecular electronics. Understanding the charge transfer process in an undefined characterised material which is likely to undergo structural changes (such as unwrapping) is extremely challenging

Dendrimers[11-16] consist of a number of regularly branched substituents (dendrons) attached to a central core, with terminal groups at the surface. Polymeric cores can be encapsulated by attaching dendrons laterally to a polymer chain. If this core is a conjugated polymer the material may be described as an IMW. There are few examples of dendronised conjugated polymers as, due to steric hindrances, there is incomplete coverage. So the insulation is poor and not uniform along the polymer backbone.

Polyrotaxanes offer a relatively simple synthesis route in comparison to wrapped molecular wires and dendrimers as well as being able to polymerise further than dendrimers, increasing the conjugation length. The additional of the macrocycle is well defined and the threading of the polymer is known. To use polyrotaxanes in molecular electronics Prof. H.L Anderson and his co-workers have developed conjugated polyelectrolytic polyrotaxanes[17-20]. This class of polyrotaxane satisfies the criteria for molecular electronics (delocalised π-π^* system, low aggregation tendencies and light emission in the visible range). The polyrotaxanes they have developed are based on common, well researched light emitting polymers, such as polyfluorenes to exploit their desirable optoelectronic characteristics and cyclodextrin molecules (CD) are used as the macrocyclic hosts.

1.2. Polyrotaxanes for use in OLED

Investigations to develop polyrotaxanes as molecular electronic materials have been conducted because it is hoped that the problems of red-shifted and partially quenched luminescence (caused by intermolecular interactions and solid-state packing effects) may be reduced by insulating the conducting structure. Shielding the molecular wire should also help limit luminescence quenching (which reduces EL efficiency) and prevent red-shifting of the luminescence caused by aggregation of the molecular wires.

Interstrand charge trapping causes light emitting device efficiency to drop dramatically because it provides a non-radiative way for the exciton to decay. It has been suggested that the presence of the insulating CD macrocycle should prevent steric interactions because strand separation will be limited by the diameter of the CD ring. This gap is probably too large for an exciton to travel between polymers and thus encourages charge to travel along the strand, extending its lifetime and likelihood to decay radiatively.

The polyrotaxanes studied here on average have one cyclodextrin unit per repeat unit.[21] This shields the π-bond from undergoing photo-oxidation reactions, allowing electronic devices using the polyrotaxane to be made in air. This does not totally insulate the chain, allowing the charges to migrate. Whilst the electrostatic nature of the CD macrocycle means polyrotaxanes are normally soluble in water, by adapting end groups and adding side chains to the cyclodextrins they may also become organic-soluble, which will be discussed in Chapter 7. This ease of processability and potential to manipulate the solubility characteristics of polyrotaxanes makes them compatible with a wide range of substances and useful in a diverse range of applications.

Cyclodextrin is also desirable for use as a macrocycle host as it will form inclusion complexes with a wide variety of organic guests in both aqueous and the solid state.[22, 23] Cyclodextrin is readily available in both high purities and large quantities and can be functionalized by a wide variety of synthetic methods.[24] Polymers such as the polyelectrolyte, Poly(ethylene oxide) and poly(ethylene glycol) readily thread through cyclodextrin to form polyrotaxanes.[25-29]

There are three variations in the cyclodextrin; it can be made up of 6, 7 or 8 glucose units. These are referred to as α, β and γ respectively as in Figure 2-3. The inner wall of the cyclodextrin is hydrophobic whilst the outer wall is hydrophilic, which can aid threading. It is toroidal in shape and as the number of glucose units present increases, the diameter of the cyclodextrin increases. The Anderson lab uses α- and β-cyclodextrin as macrocycle hosts. In this work we use β-cyclodextrin rings as the molecular wire's sheath. They have a diameter of 1.5nm and are chosen as they should be wide enough not to inhibit charge transport but narrow enough that it is unable to pass over the analogue polymer's side or end groups.

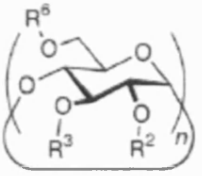

α-CD (n = 6; $R^2 = R^3 = R^6 = H$)
β-CD (n = 7; $R^2 = R^3 = R^6 = H$)
γ-CD (n = 8; $R^2 = R^3 = R^6 = H$)

Figure 2-3 Structure of α-,β- and γ-cyclodextrin.

2.1. Synthesis of polyrotaxanes

There are two widely used synthesis routes to make rotaxanes with CD:

1) CD is threaded onto the analogue polymer unit and then the endgroups are attached.

2) The endgroups are attached to the analogue polymer and the CD is slipped over the endgroups.

The second method often results in pseudorotaxanes as the CD can slip both on and off the chain. The first method is thus more suitable for formation of true polyrotaxanes. The ease of threading with cyclodextrin comes from the hydrophobic nature of the inner wall of the cyclodextrin. Anderson *et al* have developed an aqueous polymerisation reaction to take advantage of the hydrophobic interactions. The hydrophobic monomer is non-covalently bound inside the CD and polymerised by Suzuki coupling with a water-soluble monomer to form a pseudopolyrotaxane.[30] The chains are terminated with bulky stoppers to prevent the CD from slipping off. This is shown schematically in Figure 2-4.

Suzuki coupling is widely used for the synthesis of conjugated polymers. Via the use of a palladium catalyst, a boronic acid R^1-$B(OH)_2$ is coupled with a organo-halide R^2-Halide. R^1 and R^2 are generally aryl or vinyl which leads to the formation of biphenyl or stilbene links, R^1-R^2.[30]

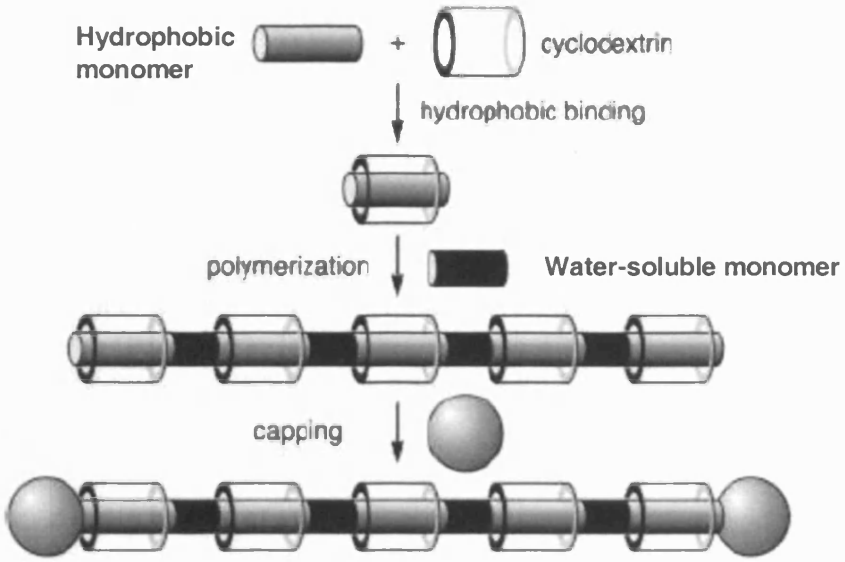

Figure 2-4 Polymerisation reaction to make polyrotaxanes. The base unit is threaded through the CD and polymerised at the same end. The reaction is terminated by the addition of the end caps which then bond to the ends of the polymer and prevent unthreading of the polyrotaxanes. Adapted from [18].

The degree of threading (the threading ratio) is determined by H^1-NMR, (Nuclear Magnetic Resonance detects the chemical environment in a material via the use of magnetic nuclei, such as protonated hydrogen, for example, to identify the functional groups within a molecule[31]) the signals from the aromatic portion of the polyrotaxane and the cyclodextrin are integrated and the ratio of them calculated, typically this is one CD per repeat unit but it will not extend over the whole of the unit. It leaves part of the backbone uninsulated. Doubly threaded polymers will have most of the repeat unit covered. This implies that the conjugated polymer is only partially insulated leaving some of the backbone exposed. Due to the toroidal shape of the cyclodextrin they will have an orientation along the chain but this is unknown in these polyrotaxanes.

To check the polyrotaxane stability (absence of unthreading) it is subjected to dialysis. A polyrotaxane solution in aqueous solution is dialyzed through a thin membrane. The threading ratio is measured as water passes through the dialysis

ultrafiltration. If it does not decrease with increasing volume of water through the cell, then no unthreading of the cyclodextrin occurs. This method verified which end groups prevent unthreading of the cyclodextrin.

Determining the molecular weight of these polyrotaxanes is difficult as they are polyelectrolytes and so the normal techniques employed, such as gel permeation chromatography (GPC), are not always suitable for them. This is because the materials can adsorb on to the GPC column, giving unrealistic molecular weights. Analytical ultracentrifugation (AUC) has been used: it is more commonly applied to biological materials but gives a realistic molecular weight for the polyrotaxanes. However the analogue polymer molecular weights were higher than expected, perhaps due to aggregation during AUC.[18]

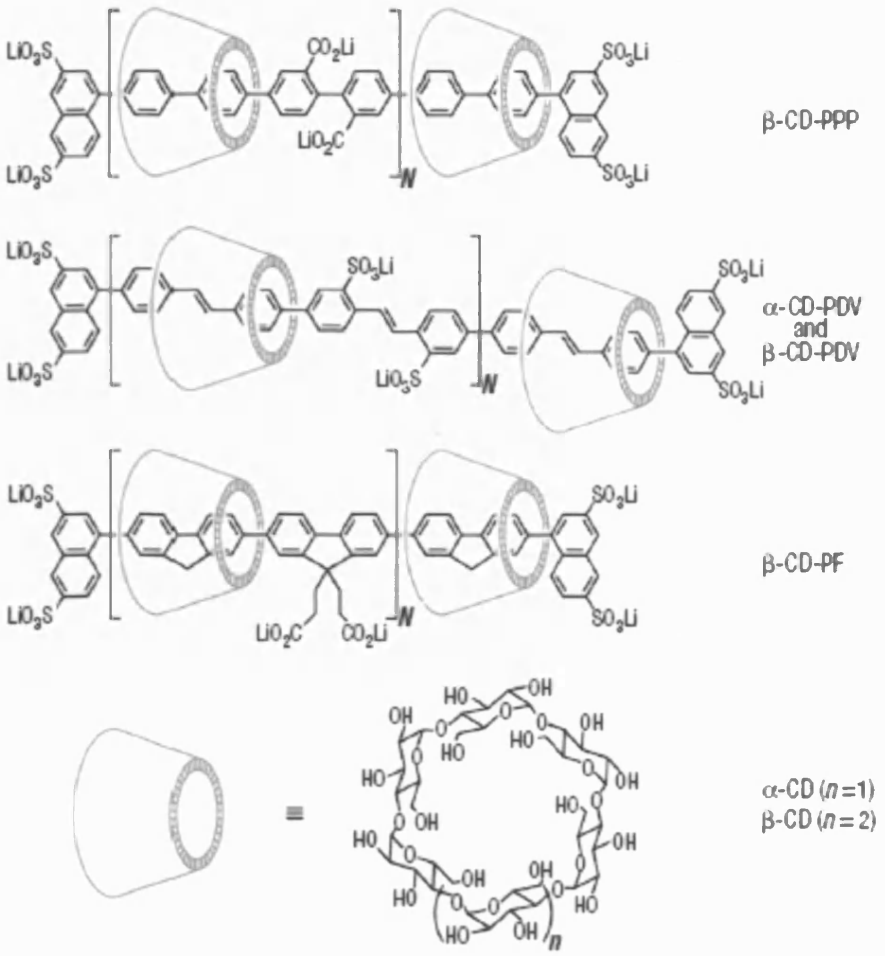

Figure 2-5 Three examples of polyrotaxanes suitable for molecular electronics. Taken from [21]. The side-groups are ionic and may be varied. The cyclodextrin is shown at the base of the figure as a truncated cone, the sugar groups may be varied and nomenclature is given in the figure.

As the full names of the polymers are cumbersome, abbreviations are often used. Cyclodextrin is commonly referred to as CD and by the number of glucose units present, and the polyrotaxanes are known by the name of the analogue polymer. Polyfluorene is known as PF, poly(4,4 –diphenyl vinylene) as PDV and Poly (para-phenyl-phenylene) as PPP. The ionic side-groups in the conjugated polyelectrolytes are referred to by their counter-cationic salt, i.e. PDV.Li and all polyrotaxanes are denoted as ⊂*β*-CD. Thus the poly(4,4 –diphenyl vinylene) polyrotaxane with $LiSO_3$ side-groups

would be referred to as PDV.Li⊂β-CD. The chemical structure of the polymer along with the counter-cations is given in Figure 4-6.

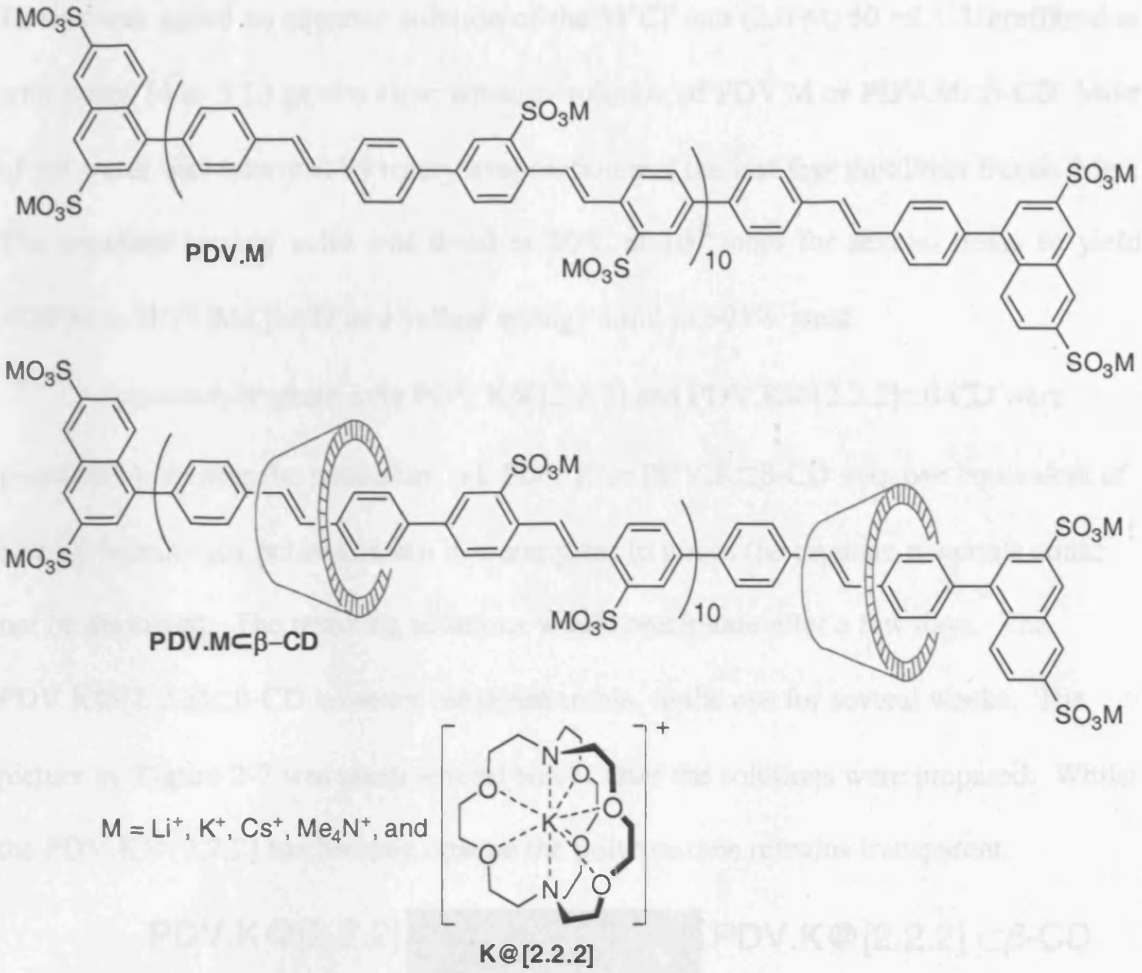

Figure 2-6 Chemical structure of poly(4,4'-diphenylene vinylene) with different cationic groups and large end groups. The polymer is typically ten repeat units long and the β-cyclodextrin is 1.5nm in diameter.

2.1.1. Ion-exchange

The counter-cation exchange was performed at the Chemical Research Laboratory, University of Oxford. The counter-cations chosen had to be monovalent to be used with the sulphate group that was attached to the main chain. Caesium, potassium, and two non-metallic based cations; tetrametylammonium (NMe_4) and cryptate-encapsulated potassium (K@[2.2.2]) were chosen.

PDV.Li or PDV.Li⊂β-CD (100 mg) was dissolved in water (50 mL) and added to a 200 mL ultrafiltration cell, fitted with a 5000 NMWL polyethersulfone membrane. To this was added an aqueous solution of the M^+Cl^- salt (2.0 M, 50 mL). Ultrafiltration with water (4 to 5 L) gave a clear aqueous solution of PDV.M or PDV.M⊂β-CD. Most of the water was removed by rotary evaporation and the last few millilitres freeze-dried. The resultant spongy solid was dried at 50°C at 10^{-2} mbar for several hours to yield PDV.M or PDV.M⊂β-CD as a yellow spongy solid in >95% yield.

Potassium cryptate salts PDV.K@[2.2.2] and PDV.K@[2.2.2]⊂β-CD were prepared by stirring the potassium salt PDV.K or PDV.K⊂β-CD with one equivalent of [2.2.2]cryptand per potassium ion in water prior to use as the cryptate materials could not be dissolved. The resulting solutions would precipitate after a few days. The PDV.K@[2.2.2]⊂β-CD however remained stable, to the eye for several weeks. The picture in Figure 2-7 was taken several weeks after the solutions were prepared. Whilst the PDV.K@[2.2.2] has become opaque the polyrotaxane remains transparent.

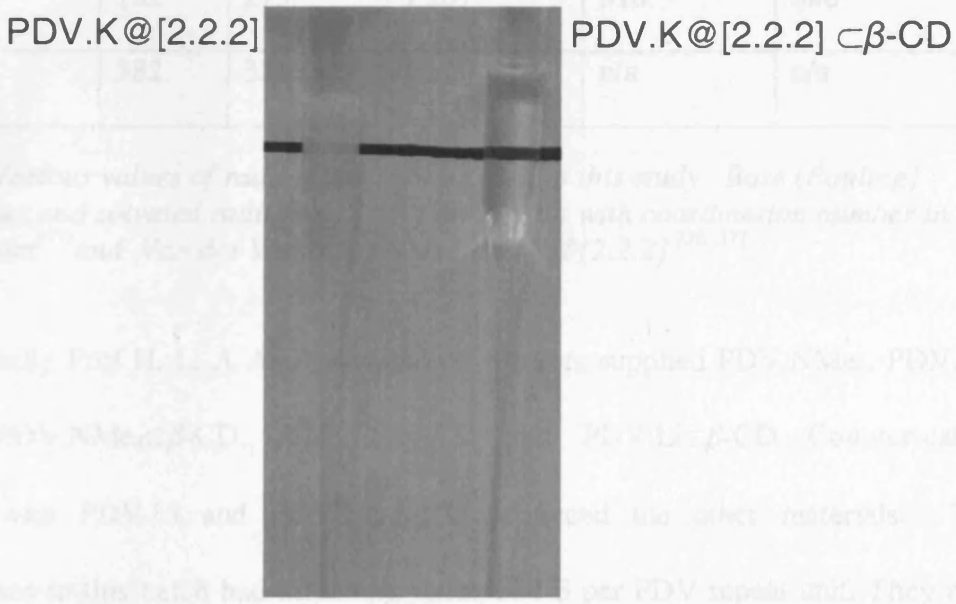

Figure 2-7 Photograph of PDV.K@[2.2.2], left-hand of figure, and PDV.K@[2.2.2]⊂β-C, right-hand of figure, solutions after storage for several weeks. The PDV.K@[2.2.2] is now opaque whilst the polyrotaxane remains transparent.

Table 2-1 reports values for the bare (Pauling), ionic, solvated and Van der Waals radii of the cations used, where available. The bare radii have been given using the Pauling radius as the coordination nature of the cations in the polymer film is undetermined. Here it was determined that the cationic radius should best be classified by their Van der Waals radius as a full dataset is available and has been experimentally verified in the case of the two largest cations. The general trend is for Li<K<Cs<NMe_4<K@[2.2.2] regardless of radius classification. The only time this scheme is not followed is for the Van der Waals and solvated radii of the K and Cs ions however the Van der Waals radii of the K and Cs ions are very similar in size. A previous investigation by Hu *et al* [32] into the use of alkali perchlorates in LECs made use of the ionic radii as, for these compounds they are well defined: for NMe_4 and K@[2.2.2] they are not, hence here the Van der Waals radius was more appropriate.

	Li	**K**	**Cs**	**NMe_4**	**K@[2.2.2]**
Bare radius/pm	60	133	169	350	n/a
Ionic radius/pm	73 (4)	151 (4)	181 (6)	n/a	n/a
Van der Waals/pm	182	275	267	310	580
Solvated radius/pm	382	331	329	n/a	n/a

Table 2-1 Various values of radii of the cations used in this study. Bare (Pauling) radius values and solvated radii from [33, 34], ionic radii with coordination number in brackets from [35] and Van der Waals for NMe4 and K@[2.2.2] [36, 37].

Initially Prof H. L. A Anderson and co-workers supplied PDV.NMe_4, PDV.Cs, PDV.Li, PDV.NMe_4⊂β-CD, PDV.Cs⊂β-CD and PDV.Li⊂β-CD Counter-cation exchange with PDV.Li and PDV.Li⊂β-CD produced the other materials. The polyrotaxanes in this batch had threading ratios of 1.3 per PDV repeat unit. They next sent new materials produced from a new batch of PDV.Li and PDV.Li⊂β-CD which were used to make PDV.K, PDV.K⊂β-CD, PDV.Cs⊂β-CD, PDV.NMe_4⊂β-CD,

PDV.K@[2.2.2] and PDV.K@[2.2.2]⊂β-CD. The polyrotaxanes in this batch had an unintentionally higher threading ratio of 2.3. It has been suggested that possible reasons for this discrepancy could be catalyst activity, reaction rate, heating rate, mixing rate and the degree of dissolution of reagents variations in the ambient temperature of the synthesis laboratory.

1.3. Previous work

The benefits and adaptation of the optoelectronic properties of conjugated polymers by encapsulation have been documented previously by Cacialli, Anderson and co-workers in [21, 38]. Here the findings will be given as a prelude to the work presented in this thesis. The polymers investigated were those presented in Figure 2-5. Firstly Cacialli and co-workers characterised the effect of insulation on the optoelectronic properties [21] and they then explored the polyelectrolytic nature of the polymers and their behaviour when blended with polyethylene (oxide), PEO, another polyelectrolyte. [38]

2.1.2. Optical Properties

Cyclic voltammetry measurements of the PDV.Li and PDV.Li⊂β-CD showed little variation (5.36 and 5.20nm respectively) in the ionization potentials, however there are differences in the optical absorption and emission spectra of the analogue polymer and its associated polyrotaxane which are present for all materials in Figure 2-5. The linear absorption coefficient for the insulated material is always smaller than for the uninsulated materials, due to dilution of the conjugated material because of the CD rings. The absorption and emission spectra of the polyrotaxanes are blue-shifted in comparison to their analogue polymer as seen in Figure 2-8 from [21].

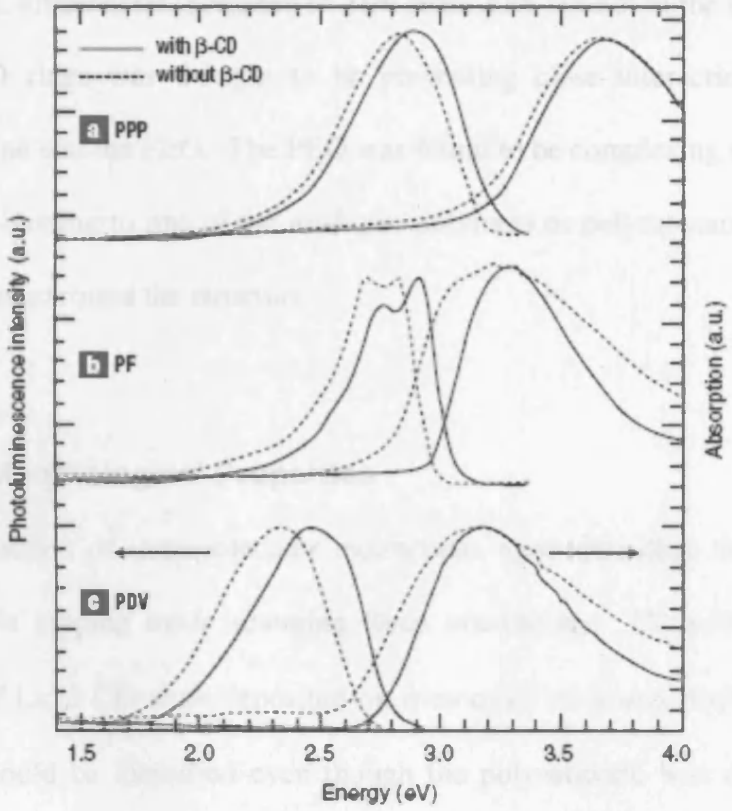

Figure 2-8 Optical properties of the polyrotaxanes and of the uninsulated wires. Absorption (right y axis) and photoluminescence spectra (left y axis) of thin films of the rotaxane (solid lines) and of the non-threaded cores (dashed lines),spun-coated on spectrosil substrates.a) PPP; b)PF; c)PDV. Taken from reference [21].

This has been attributed to reduced interchain interactions in the polyrotaxanes or in the case of PPP.Li⊂β-CD it could be due to a sterically induced increase in twist angle of the adjacent phenylene units. The vibronic structure of the photoluminescence spectra alters upon addition of CD. This is most apparent in the PF.Li⊂β-CD spectra in Figure 2-8 where the strongest peak is the 0-0 transition rather than the 0-1 transition for the PF.Li.

The photoluminescence efficiencies of the polyrotaxanes were found to always be larger than their analogue polymers due to reduced luminance quenching. Upon blending the materials with PEO the PL efficiencies of the uninsulated materials were increased nearly to the value of the insulated polymers at a value of 49% from 5%, as well as blue-shifted in comparison to the unblended spectra. The insulated materials

also had their PL efficiencies increased to 51% from 20% but not to the same extent: the presence of CD rings was thought to be preventing close interaction between the polymer backbone and the PEO. The PEO was found to be complexing with the Li; one PEO chain was binding to one of the analogue polymers or polyrotaxanes by wrapping in a helical manner around the structure.

2.1.3. Morphological Properties

The reduction of intermolecular interactions upon threading through CD was demonstrated via tapping mode scanning force microscopy. Ultra-thin films of the PPP.Li and PPP.Li⊂β-CD were deposited on muscovite mica and studied. Individual polyrotaxanes could be identified even though the polyrotaxane was densely packed. However the PPP.Li assembled into domains with a constant thickness and individual strands could not be identified.

Blends of conjugated polymers suffer from phase separation which can limit their effectiveness in LEDs. Studies of thin films of the analogue polymers or polyrotaxanes blended with the PEO showed smooth and featureless surfaces, indicating that these two polymers do not separate. Pure PEO tends to crystallize, so the blend not only exhibits no phase separation, it also suppresses crystallisation of PEO. This has been attributed to the PEO coiling around the conjugated polyelectrolyte (cf 2.3.1) and this supposition is borne out by the results of titration experiments documented in [38].

In the synthesis section (2.2.1) it was mentioned that the singly threaded polymers were only partially insulated. The reduction of intermolecular interactions demonstrated by the blue-shift in absorption/emission spectra and the AFM images may have been so great as to prevent charge transport. Light emitting devices (as described

in Chapter 1) using the ITO/polymer/Ca/Al structure and a polyrotaxane as the electroluminescent polymer layer proved to exhibit diode-like character and light emission. The polyrotaxane emits at higher voltages than the analogue polymer perhaps due to the insulation and has higher operating efficiencies resulting from lower current densities than the analogue polymer.

Upon addition of PEO the external quantum yields of the LEDs for both the analogue polymer and the polyrotaxane are increased. This is making use of the ionic groups in the polymer blend they also added Lithium Triflate sidegroups to increase conductivity in the device. From Figure 2-9 it seems that Lithium Triflate is not needed to increase the external quantum yield. The use of mobile cations in the devices lends these conjugated polyelectrolytes to use as light-emitting electrochemical cells (LECs).[39, 40]

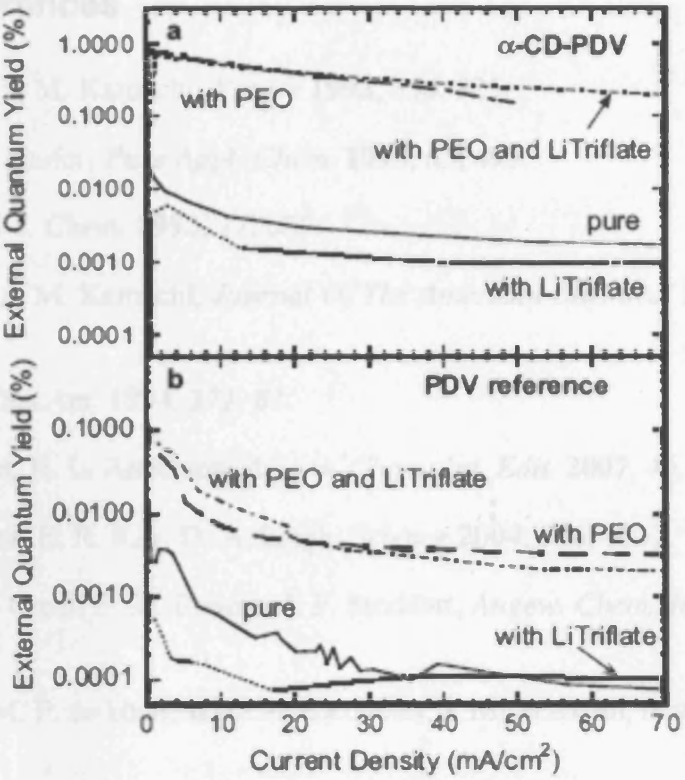

Figure 2-9 a) Comparison of the external EL efficiency of light-emitting cells with different compositions of the a-CD-PDV-based active layers.b) EL efficiency versus current density for the same type of cells as in (a), but based on the PDV reference polymer instead of the polyrotaxane. In both panels solid lines correspond to active layers made of the pure materials, whereas dotted lines refer to an active layer consisting of blends of polyrotaxane and lithium triflate (3.8% lithium triflate), dashed thick lines refer to active layers made of PEO/polyrotaxane blends (17% PEO), and dash–dotted lines refer to active layers consisting of blends of PEO/polyrotaxane/lithium triflate with weight concentrations of 16% PEO and 3.2% lithium triflate. Taken from [38].

2.2. References

[1] A. Harada, J. Li, M. Kamachi, *Nature* **1992**, *356*, 325.

[2] R. Isnin, A. E. Kaifer, *Pure Appl. Chem.* **1993**, *65*, 495.

[3] H. Ogino, *New J. Chem.* **1993**, *17*, 683.

[4] A. Harada, J. Li, M. Kamachi, *Journal Of The American Chemical Society* **1994**, *116*, 3192.

[5] K. Leutwyler, *Sci.Am.* **1994**, *271*, 87.

[6] M. J. Frampton, H. L. Anderson, *Angew. Chem.-Int. Edit.* **2007**, *46*, 1028.

[7] J. V. Hernandez, E. R. Kay, D. A. Leigh, *Science* **2004**, *306*, 1532.

[8] V. Balzani, A. Credi, F. M. Raymo, J. F. Stoddart, *Angew. Chem.-Int. Edit.* **2000**, *39*, 3349.

[9] R. Hoofman, M. P. de Haas, L. D. A. Siebbeles, J. M. Warman, *Nature* **1998**, *392*, 54.

[10] M. R. Craig, M. G. Hutchings, T. D. W. Claridge, H. L. Anderson, *Angew. Chem.-Int. Edit.* **2001**, *40*, 1071.

[11] K. T. Al-Jamal, C. Ramaswamy, A. T. Florence, *Adv. Drug Deliv. Rev.* **2005**, *57*, 2238.

[12] D. A. Tomalia, *Prog. Polym. Sci.* **2005**, *30*, 294.

[13] S. C. Zimmerman, L. J. Lawless, in *Dendrimers Iv*, Vol. 217, **2001**, 95.

[14] P. E. Froehling, *Dyes Pigment.* **2001**, *48*, 187.

[15] F. Vogtle, S. Gestermann, R. Hesse, H. Schwierz, B. Windisch, *Prog. Polym. Sci.* **2000**, *25*, 987.

[16] J. Roovers, B. Comanita, in *Branched Polymers I*, Vol. 142, **1999**, 179.

[17] S. Anderson, R. T. Aplin, T. D. W. Claridge, T. Goodson, A. C. Maciel, G. Rumbles, J. F. Ryan, H. L. Anderson, *Journal of the Chemical Society-Perkin Transactions 1* **1998**, 2383.

[18] J. J. Michels, M. J. O'Connell, P. N. Taylor, J. S. Wilson, F. Cacialli, H. L. Anderson, *Chemistry-A European Journal* **2003**, *9*, 6167.

[19] P. N. Taylor, M. J. O'Connell, L. A. McNeill, M. J. Hall, R. T. Aplin, H. L. Anderson, *Angew. Chem.-Int. Edit.* **2000**, *39*, 3456.

[20] J. Terao, A. Tang, J. J. Michels, A. Krivokapic, H. L. Anderson, *Chemical Communications* **2004**, 56.

[21] F. Cacialli, J. S. Wilson, J. J. Michels, C. Daniel, C. Silva, R. H. Friend, N. Severin, P. Samori, J. P. Rabe, M. J. O'Connell, P. N. Taylor, H. L. Anderson, *Nature Materials* **2002**, *1*, 160.

[22] S. A. Nepogodiev, J. F. Stoddart, *Chem. Rev.* **1998**, *98*, 1959.

[23] J. F. Stoddart, *Angewandte Chemie-International Edition In English* **1992**, *31*, 846.

[24] G. Wenz, B. H. Han, A. Muller, *Chem. Rev.* **2006**, *106*, 782.

[25] A. Harada, *Acta Polymerica* **1998**, *49*, 3.

[26] K. Miyake, S. Yasuda, A. Harada, J. Sumaoka, M. Komiyama, H. Shigekawa, *Journal Of The American Chemical Society* **2003**, *125*, 5080.

[27] T. Takata, *Polymer Journal* **2006**, *38*, 1.

[28] M. Tamura, D. Gao, A. Ueno, *Chemistry-A European Journal* **2001**, *7*, 1390.

[29] D. Tuncel, J. H. G. Steinke, *Macromolecules* **2004**, *37*, 288.

[30] A. Suzuki, *Journal of Organometallic Chemistry* **1999**, *576*, 147.

[31] K. P. C. Vollhart, N. E. Schore, *Organic Chemistry Structure and Function*, W. H. Freeman and Company, United States of America **1999**.

[32] Y. F. Hu, J. Gao, *Applied Physics Letters* **2006**, *89*.

[33] M. Colic, G. V. Franks, M. L. Fisher, F. F. Lange, *Langmuir* **1997**, *13*, 3129.

[34] H. Matsuoka, T. Yamamoto, T. Harada, T. Ikeda, *Langmuir* **2005**, *21*, 7105.

[35] R. D. Shannon, C. T. Prewitt, *Acta Crystallographica Section B-Structural Crystallography And Crystal Chemistry* **1969**, *B 25*, 925.

[36] J. G. Breitzer, A. I. Smirnov, L. F. Szczepura, S. R. Wilson, T. B. Rauchfuss, *Inorg. Chem.* **2001**, *40*, 1421.

[37] William W. Brennessel, V. G. Y. Jr, J. E. Ellis, *Angewandte Chemie International Edition* **2002**, *41*, 1211.

[38] J. S. Wilson, M. J. Frampton, J. J. Michels, L. Sardone, G. Marletta, R. H. Friend, P. Samori, H. L. Anderson, F. Cacialli, *Adv. Mater.* **2005**, *17*, 2659.

[39] Q. B. Pei, G. Yu, C. Zhang, Y. Yang, A. J. Heeger, *Science* **1995**, *269*, 1086.

[40] L. Edman, *Electrochim. Acta* **2005**, *50*, 3878.

Chapter 3. Optimisation of substrates and freezing of work function

When producing LEDs, improvement of the operating efficiencies can be achieved by tailoring of the emissive polymer, adaptation of the cathode or addition of further polymer layers. Before these steps are undertaken it is important to ensure that the substrate is well cleaned producing sharp interfaces between materials.

Typically an indium-tin oxide substrate is used as it has been studied extensively for use in liquid crystal displays and for semiconductors. The desired properties of the substrate have been detailed before; transparency, conductivity and low resistivity. Tin doped indium-oxide, ITO, is conductive, transparent (90% at 550nm) and it is easy to pattern. ITO is also employed as the anode because it has a relatively high work function which can be matched to the highest occupied molecular orbital or the polaron level of the emissive layer to improve hole injection. For OLEDs the emissive polymer ionisation potential tends to be higher than 5eV so contact materials with a work function of over 5eV are sought to minimise charge injection barriers.

The ITO can undergo cleaning preparations which also have been shown to increase its work function and smooth the surface. In this chapter preparatory work on the substrates is discussed along with its importance and how, by placing polymer films on to these prepared substrates the work function value may be semi-permanently fixed.

3.1. Preparation of substrates for LEDs

ITO is usually sputter deposited onto a glass substrate, which leads to high surface roughness. This is not desirable for LEDs made from polymer films as it can lead to device instabilities and lower operating efficiencies. This has previously been

attributed to poor adhesion of the polymer film to the ITO due to the large surface roughness leading to a decrease in the effective area available for charge injection.[1]

The chemical structure of ITO may be written as $In_{2-y}Sn_yO_{s-x}(V_o^{\cdot\cdot})_xe_{2x-y}$.[2] The oxygen vacancy content x is normally less than 0.01. $V_o^{\cdot\cdot}$ denotes doubly-charged oxygen vacancies and e denotes electrons which are needed for charge neutrality on the macroscopic scale. The typical surface structure is shown in Figure 3-1.

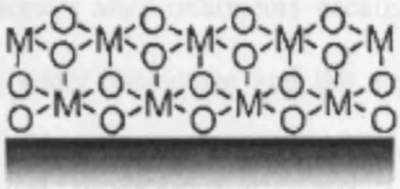

Figure 3-1 Schematic of a metal-oxide surface where M indicates the metal. ITO has this structure after oxygen plasma treatment. Taken from[2].

The bulk contains more In/Sn than the surface, whilst the surface has a higher oxygen content[3]. These oxygen atoms are reactive and allow contaminants and water to adsorb readily onto the ITO surface. The work function of metals strongly depends on the surface conditions, and so hydrocarbons and water need to be removed from the surface of the ITO to give a sharp interface between the ITO and the polymer layer.

Various groups have studied different methods of cleaning the ITO including such methods as wet cleaning, chemical cleaning, ozone and oxygen plasma treatments.[1-8] It is now a common strategy to use a wet clean (acetone followed by isopropanol in an ultra sonic bath) to degrease the substrate which precedes an ozone/oxygen plasma clean. This (i) removes adsorbed material on the ITO surface, (ii) decreases the surface roughness, (iii) provides an adsorbed layer of oxygen and (iv) increases the polarity of the surface.[1, 2, 6-12] These four factors have been shown to raise the work function of ITO. The increase of work function is useful as hole injection into OLEDs is typically low and this will limit efficient charge recombination

within the device.[13] Neither the timescale over which this rise in work function occurs, nor the subsequent decrease in work function following cleaning has been well documented. Kim *et al* [1] have reported a sustained increase in the work function of ITO over a period of months but they note that soon after the treatment the work function is even higher. However they did not study the ITO work function decay in detail.

The work function decays after treatments because the adsorption of oxygen will, in air, be replaced by water molecules and the surface be recontaminated by organic materials. It is unknown how long this takes and if the work function will revert to its original value or remain at a higher value due to the other benefits of ozone/plasma treatments such as reduced surface roughness.

The oxygen plasma cleaner works by creating a plasma of ionised gases at low pressures, which erode surfaces, with rates of around 1 - 100 nm per minute. The oxygen is admitted to the oven chamber at low flow rates and kept at low pressure through use of a vacuum pump. The gases are subjected to induced radio frequency (RF) magnetic and electric fields generated by a solenoid coil current. The plasma is then generated by the subsequent RF/collsional heating of the electrons in the gas. Powers of between 5-400W for times of 5-20min are employed with varying results. Oxygen plasma treatments in our group are performed in a Harrick PDC-002.

3.2. Use of Kelvin Probe as measure of work function

Determination of work functions is important to understand physical processes involved in charge transfer by efficient energy level line up, and to suggest possible methods how to improve these processes. There are various ways of studying the work function of metallic surfaces: Ultraviolet photoelectron spectroscopy (UPS),[14] X-ray

photoemission spectroscopy (XPS)[2] and Kelvin Probe[6, 12] have been utilised previously. Electroabsorption studies (EA)[9, 15-17] provide work function information on operational LEDs. UPS and XPS must be conducted in high vacuum and probe the immediate surface (to depths of 10nm) of the metal. UPS also measures the lowest work function area on the surface even if it is a small part of the total surface area. EA is typically used on devices and is conducted under low pressures unless the device is encapsulated to prevent alterations of the work function during measurement. Kelvin Probe experiments may be performed in air or under vacuum on conductive substrates or substrates with a film (metallic or polymer) deposited on them. The Kelvin probe provides the average work function difference under the probe. These experiments are thus relatively simple in comparison to EA, UPS and XPS as there is no need for vacuum operation.

The Kelvin Probe has a mesh electrode (typically a gold electrode) positioned in front of the sample being studied and is driven electromagnetically by a solenoid or by piezoceramics.[18, 19]

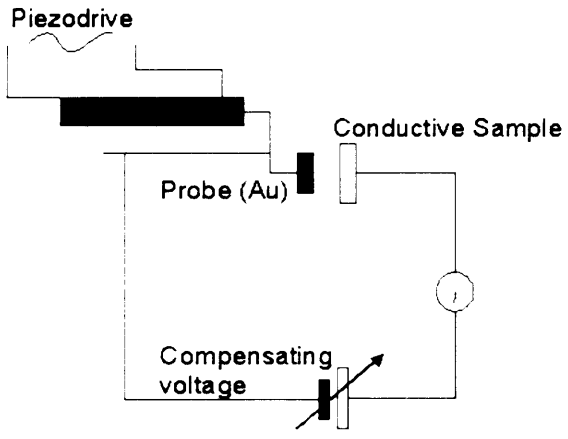

Figure 3-2 Schematic of a Kelvin probe used to measure the work function of a conductive sample. The probe and conductive sample are effectively parallel plate capacitors which can be at placed varying distances from each other. Measurements may be taken in air or vacuum.

The Kelvin probe operates like a parallel plate capacitor, the probe and sample distance may be varied in a periodic manner as shown in Figure 3-2. This vibration gives rise to an oscillating current:

$$i = \frac{dC}{dt}\left(\frac{\Delta\phi}{e} - V^{comp}\right) \tag{3.1}$$

where V^{COMP} is the external compensation voltage. $\Delta\phi$ arises from the contact potential difference which exists between the two conducting plates and is equal to the difference between the sample surface work function studied (ϕ^S) and of the reference probe (ϕ^P). V^{COMP} can be adjusted to null the current, and at this particular value of the compensating voltage gives the difference in work function of the two conducting plates:

$$eV^{COMP} = \phi^S - \phi^P \tag{3.2}$$

Thus to find the absolute value of the surface work function the absolute value of the reference probe work function (ϕ^P) must be known. Here we use a Besocke DeltaPhi Kelvin probe with a gold mesh electrode. To determine the precise work function of the gold mesh the measurements should be made in ultra-high vacuum, as the work function of gold, like most metals, depends strongly on the surface state. A study has shown that the work function of gold decreases in air/nitrogen compared to the value in ultra-high vacuum (UHV). In air/nitrogen the work function has been quoted as 4.7-4.8eV[20] whilst in UHV it is 5.1eV.[12] Thus as our Kelvin Probe system operates in air it should be assumed that the gold work function is in the lower regime of 4.7-4.8eV. As the work function is not absolutely determined, contact potential differences (CPD) are quoted where needed, however they are a good approximation of the work function and are treated as such in this thesis. It should be noted that relative

work function differences (between different surfaces) are quoted as these are independent of the reference used.

3.3. Studies of the longevity of plasma treatment of ITO

Work on achieving higher work functions of ITO by oxygen plasma cleaning has been well documented[1-3, 6-9, 12, 14]however there is little literature detailing how long the effect lasts or how it declines, so that aspect is studied here. The Kelvin probe was used for the ease of measurement and as it allows multiple measurements in a short time scale.

1.3.1. Experimental and Results

ITO supplied by Merck was subjected to a wet clean process (ultrasonic cleaning in acetone and isopropanol with nitrogen drying between changing of the solvents) before oxygen plasma cleaning. Once the plasma procedure was completed it took approximately 2 minutes from bringing the chamber to air to recording the first measurement. The sample is then kept in the Kelvin probe chamber for the successive measurements in air.

Several untreated ITO substrates were measured and the work function determined to be 4.7eV for these particular substrates. Work function values for ITO are typically between 4.6 and 4.8 eV[12, 16] depending also on the ITO supplier. It was found that the ITO substrates from the particular batches in our possession gave the same KP readings within 0.05-0.1V. The value of ϕ(ITO) = 4.7 eV is a satisfactory estimate [~ ± (0.1-0.15) eV], and also supported by EA measurements of the built-in potential by Brown *et al*[16, 21]. The experimental error on CPD measurements is estimated to be equal to oscillations in the CPD that are detected during measurement over a day, i.e. ±

0.05 eV. Each experiment had a wet cleaned piece of ITO measured to act as a reference point.

The work function measured after the wet clean and plasma treatment steps are presented in Figure 3-3. The oven chamber was used at a pressure of 10^{-1}mbr and samples were oxygen plasma cleaned for typically 5 minutes at a medium RF value. This procedure was found experimentally to be optimal for our particular oven. The plasma oven at our disposal operates at 7.2, 10.2 and 29.6W which correspond to an RF level of low, medium and high respectively in figures presented in this chapter.

Wet cleaning increases the work function by 0.1eV but the oxygen plasma treatment raises the work function by over 1eV.

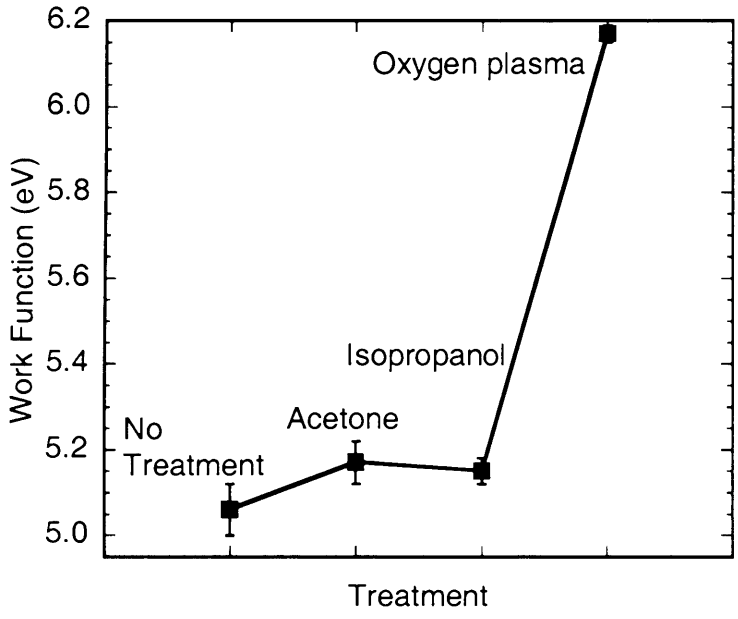

Figure 3-3 Work function measurements taken in air by a Kelvin probe after no treatment, ultra sonic cleaning with acetone/isopropanol and oxygen plasma treatment. Measurements were conducted up to 2 minutes after completing the treatment.

This effect is not permanent but even though the work function decreases the samples do not return to the initial work function value in a period of days. The decay

in work function is rapid initially and after 30 minutes the work function value plateaus as depicted in Figure 3-4. The sample may be retreated in the oxygen plasma oven and the high work function regained.

The initial work function would be a few tenths higher with a shorter less powerful plasma (5min, RF = 10.2W/medium) than a long exposure to a high plasma (10min, RF= 29.6W/high). Both would plateau to approximately the same value, which is higher than for untreated ITO but lower than measured immediately after treatment.

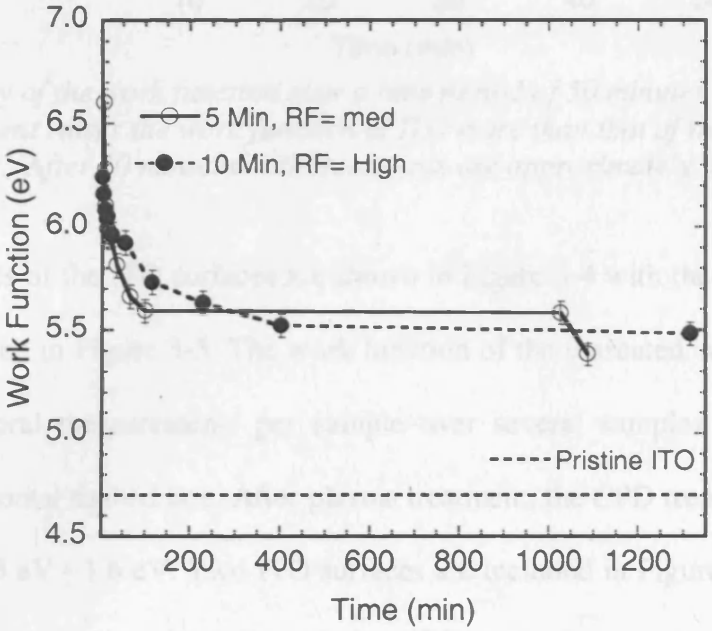

Figure 3-4 Decay of work function of treated ITO with time. Two treatments were used: 5 minutes at RF = med (10.2W) and 10 minutes at RF = high (29.6W). The reference measurement of pristine ITO (neither wet cleaned or oxygen plasma treated) is also given. After many days the work function will return to a value close to that of the unplasma treated ITO.

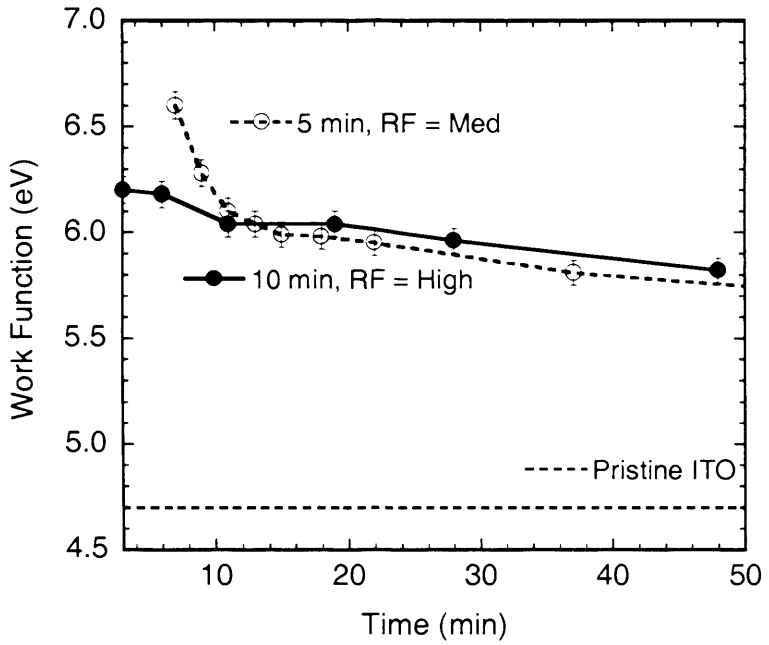

Figure 3-5 Decay of the work function over a time period of 50 minutes. The 5 minute, RF= med treatment raises the work function of ITO more than that of the 10 minute, RF = high treatment. After 10 minutes both treatments are approximately the same value and decay slowly.

KP measurements of the ITO surfaces are shown in Figure 3-4 with the first 50 minutes of this decay given in Figure 3-5. The work function of the untreated surface was set at 4.7eV after several measurements per sample over several samples of ITO, and is shown as a horizontal dashed line. After plasma treatment, the CPD measured by the KP increases by ~1.3 eV - 1.6 eV. Two ITO surfaces are included in Figure 3-4 and Figure 3-5 to show that the reproducibility of the CPD enhancement due to the plasma treatment, just after its completion, is a few tenths of an eV. Once the ITO surfaces were left in air, the CPD decreased by ~ 0.7 V within 100 - 400 mins towards a lower plateau in the work function. Whilst the shorter less powerful plasma clean (5min at RF = med) gives a higher CPD value initially both treatments converge in the first 10 minutes to within tenths of an eV of each other.

Note that the plateau is still 0.5 eV – 0.7 eV higher than the work function of the initial untreated surface. The work function (t >1000 minutes, not shown) actually continues to decrease slowly with time.

3.4. Freezing/pinning of CPD upon addition of PEDOT:PSS or an emissive polymer.

Further investigations into stabilising the work function of the ITO by addition of a polymeric film have been conducted. It was thought that covering the ITO soon after the plasma treatment would slow and even prevent the adsorption of materials such as organic contaminants which decrease the work function.

PEDOT:PSS is a polymeric colloidal suspension that is employed as a hole transport layer in OLEDs. It has a work function value of around 5eV, but can vary from 4.7[22] to 5.4eV[23] dependant on batch and treatment. The supplier markets several variations of PEDOT:PSS depending on the ratio of PEDOT to PSS and %wt in the solvent. We were supplied with BAYTRON® P VP AI 4083 and BAYTRON® P VP CH 8000 from H.C. Starck whose properties are presented in Table 3-1.

	Solid content (%)	Viscosity (mPa.S)	Particle Size (nm) d50 d90	PEDOT:PSS ratio	Resistivity (Ωcm^{-1})
BAYTRON® P VP AI 4083	1.3-1.7	5-12	80 100	1:6	500-5000
BAYTRON® P VP CH 8000	2.5-3	9-20	35 50	1:20	$1x10^5$-$3x10^5$

Table 3-1 Physical properties of the two types of PEDOT:PSS supplied by H.C. Starck as detailed by H.C. Starck Taken from H.C.Starck website.[24]

The two batches of PEDOT:PSS will thus have different surface composition, roughness and PSS content. The particle size of BAYTRON® P VP CH 8000 is smaller

than its counterpart. As PEDOT:PSS is a conductive polymer, the Kelvin probe will measure the work function of PEDOT:PSS and its work function evolution over time.

I also report KP measurements on conductive surfaces covered by a poly(9,9-dioctylfluorene), F8, overlayer. F8 is a polyfluorene employed in the fabrication of efficient optoelectronic devices[25]. It was chosen mainly for its high purity and high ionisation potential so that space charge in the semiconductor, band bending and strong pinning of the conductor Fermi level occurring at the HOMO (bi)polaronic levels of the semiconductor[26] would not occur. Polyfluorenes have in fact been shown to be high purity materials devoid of significant charge over the ≤ 100nm film thickness under consideration[25, 27, 28]. Therefore, it is sensible to assume that these CPD measurements of the F8/ITO layer probe the work function of the contact/polymer structure, rather than the CPD of the ITO layer or the surface of the F8 layer. All KP measurements reported here were taken in air.

3.4.1. Experimental and Results

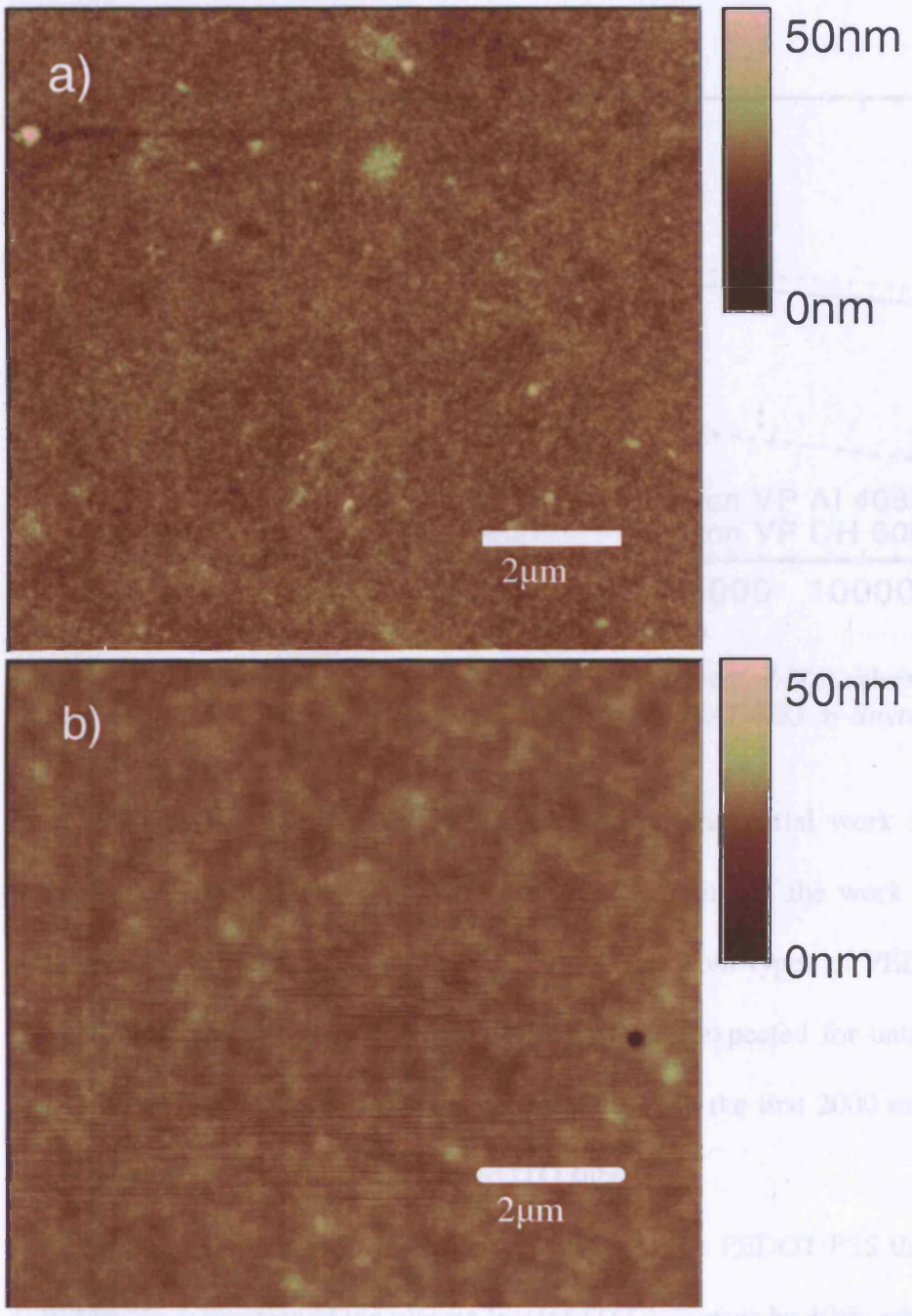

Figure 3-6 Tapping mode topographical AFM images of a) BAYTRON® P VP AI 4083 and b) BAYTRON® P VP CH 8000 spincoated onto ITO substrates.

Atomic force microscopy on two thin films (approximately 100nm thick) of the PEDOT:PSS revealed very little surface differences as seen in Figure 3-6. Mean surface roughness measurements of the film were performed using the Nanoscope software on

an area of 5x2μm from the AFM images. Baytron® P VPAI 4083 is rougher, 22.6nm, than the Baytron® VPCH 8000 which has an average roughness of 11.7nm.

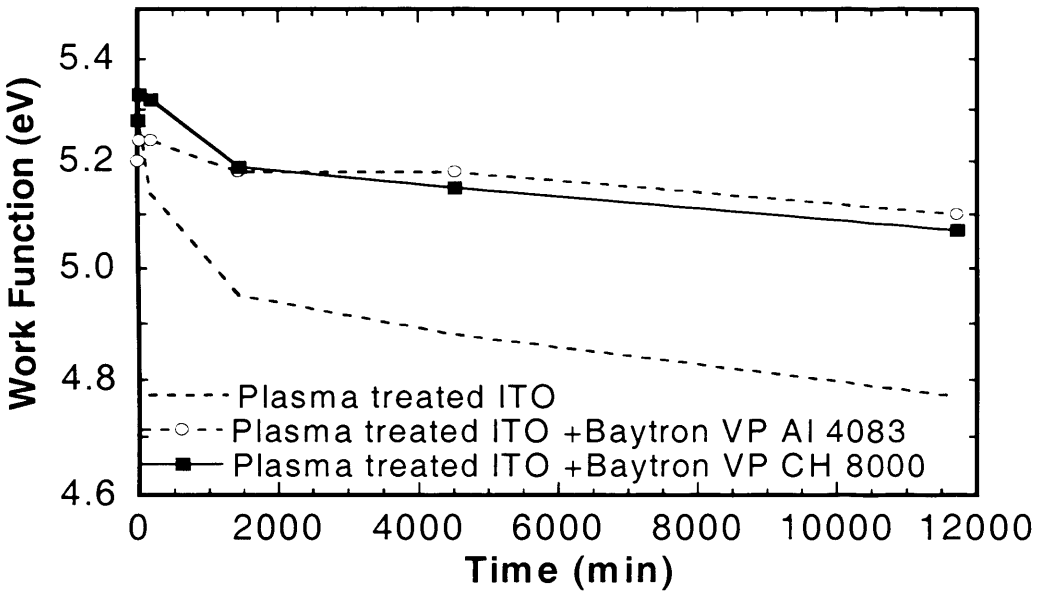

Figure 3-7 Evolution of the work function of a plasma treated ITO substrate, and a plasma treated ITO substrate with either Baytron® VP AI 4083 or Baytron® VP CH 8000.

The addition of PEDOT:PSS does increase the initial work function of the electrode by 0.15eV as seen in Figure 3-7 but a decline in the work function of the substrate and PEDOT:PSS combined is evident for both types of PEDOT:PSS. The work function values measured here are higher than expected for untreated ITO and PEDOT:PSS thin films and the work function decay in the first 2000 minutes is slower than that of the uncoated plasma treated ITO substrate.

The decrease in work function is slower for the PEDOT:PSS than ITO (Figure 3-7). The work function of the plasma treated ITO decreases by 10% whilst it decreases by 2% for the Baytron® P VP AI 4083 and by 4% for the Baytron® P VP CH 8000 coated ITO in the first 60 minutes after deposition. This is a typical example of the work function decay. The work function is increased by up to 0.1eV by the use of Baytron® P VP CH 8000 coated ITO rather than Baytron® P VPAI 4083. It is worthwhile noting

that the first measurement of the Baytron® P VP CH 8000 occurs some 5 minutes later than the first measurement of the Baytron® P VP AI 4083 coated ITO in Figure 3-7. This indicates that the work function of the Baytron® P VP CH 8000 would be even higher if measured sooner after spincoating.

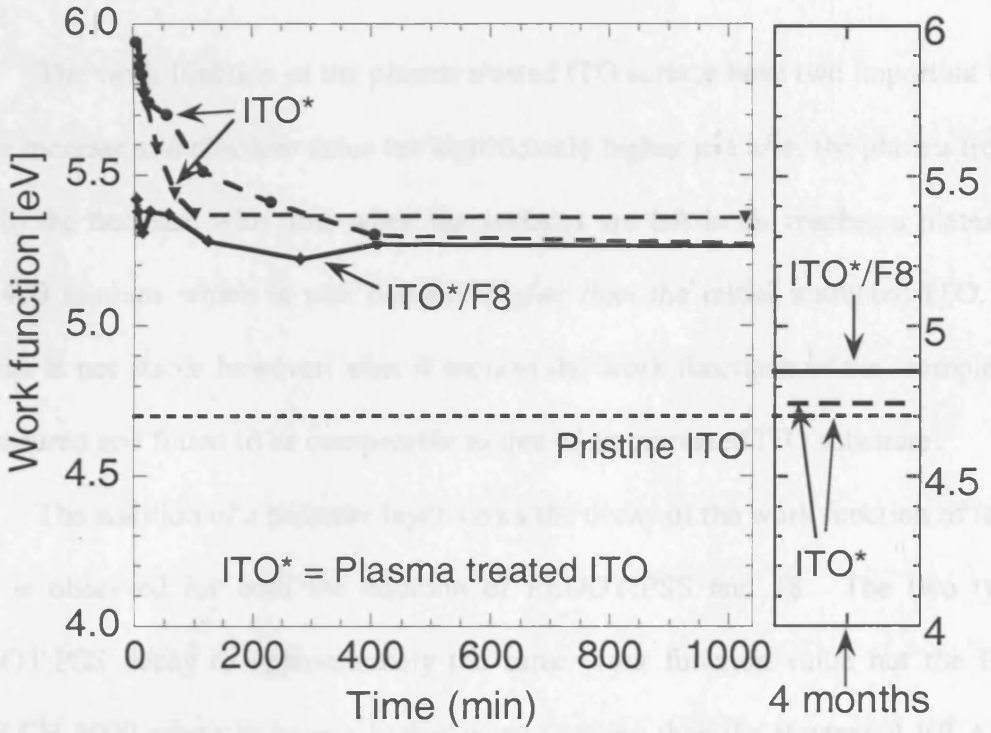

Figure 3-8 A thin film (75nm) of F8 as spun onto a ITO sample and the work function measured by Kelvin probe in over 1000 minutes. Two ITO substrates that were subjected to the same type of plasma treatment as the ITO/F8 are also plotted for comparison. The pristine work function of the ITO substrate used is also given. The work function of the samples after 4 months is given on the right of the graph.

Shown in Figure 3-8 is a graph of work function measurements of an ITO surface which was covered with a 75nm film of F8 two minutes after being treated with the oxygen plasma. Here the initial work function enhancement due to the plasma is still significant (0.6 - 0.7 V) but reduced compared to the uncoated plasma treated ITO surface. There is also some work function evolution - an overall small decrease (0.1-0.15V) within the first 400 minutes. The work function tends to a plateau value of ~0.5

eV higher than the untreated ITO surface. After 4 months the plasma treated ITO surfaces and the ITO/F8 work function values decayed. The plasma treated ITO surfaces have a work function value that is comparable to the "pristine" ITO whilst the ITO/F8 substrate remains 0.15eV higher than the "pristine" ITO.

3.5. Discussion

The work function of the plasma treated ITO surface have two important factors: a) the increase and absolute value are significantly higher just after the plasma treatment and b) the decrease with time when the surfaces are left in air reaches a plateau after 100-400 minutes which is still sizeably higher than the initial untreated ITO. This plateau is not stable however: after 4 months the work functions of the samples were remeasured and found to be comparable to that of an untreated ITO substrate.

The addition of a polymer layer slows the decay of the work function of the ITO. This is observed for both the addition of PEDOT:PSS and F8. The two types of PEDOT:PSS decay to approximately the same work function value but the Baytron ®VP CH 8000 seems to have a higher work function than the Baytron® VP AI 4083. This could be due to the Baytron ®VP CH 8000 having a more homogeneous dispersion than the Baytron ®VP AI 4083 as verified by surface roughness calculations of the AFM images. A more homogeneous dispersion, one that is less PSS-rich at its surface, should have the greatest rise in anode work function and hole injection, as the PSS acts as a barrier.[29, 30] The addition of PEDOT:PSS seems to pin the conducting polymer/ITO interface to a work function value closer to the work function value of PEDOT:PSS rather than that of ITO. This may have been expected as it is already known that if the work function of ITO is varied whilst other conditions such as surface morphology are constant then energy barrier to hole injection is determined wholly by

the work function of PEDOT:PSS.[22, 31] PEDOT:PSS is thought to act as a protective layer as well as increasing the work function of the anode. It lessens the diffusion of chemical species (Indium and oxygen) in to the emissive polymer layer and these species then act as traps for the charge decreasing photon emission. It is also known that PEDOT:PSS etches the ITO surface producing a smoother interface due to its acidic nature. However the work function decay is akin to that seen for uncoated ITO, implying that this Fermi Level pinning is still subject to degradation of the interface between the ITO and PEDOT:PSS and by exposure to air due to the hygroscopic nature of PEDOT:PSS.

Although higher than that of the untreated ITO, the work function of the ITO/F8 sample is still lower (by ~ 0.5 eV) than that of the respective uncoated plasma treated ITO. This suggests that either: a) a simple Schottky vacuum-level alignment does not occur and a significant dipole (that shifts the levels by 0.5eV) is formed at the ITO/F8 interface and/or b) any reactive chemical species left on the ITO surface after the oxygen-plasma and likely to contribute to the work function increase after the plasma treatment are instead quenched much more rapidly by application of the polymer layer. Figure 3-8 shows that any chemical, physical and electronic process or interaction between F8 and ITO continue even some time (~ 200 mins) after deposition of the polymer overlayer. Although in previous work[3, 6-8, 12, 14] the increase of the ITO work funcion upon plasma treatement has mainly been ascribed to the removal of surface contaminants such as hydrocarbons and to chemical modification (e.g. oxidation) of the ITO, it would be worthwhile to consider the role of reactive, unstable species left on the surface after an oxygen plasma treatment. This would require a chemistry-sensitive technique such as X-ray photoelectron spectroscopy (XPS).

A consideration that arises when analysing these results is that the time elapsed between the completion of the plasma treatment and the deposition of PEDOT:PSS or F8, can be crucial in determining the energy level alignment. A dipole that actually decreases the separation of the semiconductor HOMO and the Fermi level of the high work function conductor is rare. It thus becomes important to overlay the organic semiconductor before the work function of the underlying contact has decreased much beyond the ionization potential of the semiconductor in order to minimise the hole injection barrier.

Whilst the effect of the plasma is long lasting in the case of ITO, it does not permanently fix the work function. Figure 3-8 shows that the work function of the ITO surfaces has returned to its initial value after leaving the samples 4 months idle in air. Even the work function of the ITO/F8 sample has decreased very sizeably, although it remains 0.15 eV higher than untreated ITO surface. The F8 layer carries out some protective action on the electronic properties of the underlying interface, but not on the time scale of months. This large decrease in the KP reading over time can either be ascribed to chemical/electronic variations at the electrode/polymer interface or in the bulk of the semiconductor. Either way, this will have a strong and detrimental impact on the performance and lifetime of any device built with these materials and is mainly due to molecules from the air environment diffusing into and through the semiconducting polymer. Thus encapsulation of the device whilst still in an inert atmosphere should be employed if devices are to be stable over a time period of months or years. However the encapsulation process has not been developed in this group yet and as such the stability of an encapsulated device has not been proven here.

3.6. Conclusions

The usefulness of cleaning the ITO substrate which is commonly used for OLEDs has been previously acknowledged: the important effects are smoothing the substrate surface, removing contaminates and increasing the work function. However the extent to which the various treatments lasted prior to device making had not been explored. Here it has been determined that the oxygen plasma treatment is most useful if polymer layers are spun rapidly onto the ITO after the plasma treatment, preferably in the first ten minutes. During these ten minutes the work function decays rapidly, increasing the hole injection barrier. When PEDOT:PSS is applied the ITO work function appears to be pinned to the PEDOT:PSS work function and decays slower than for pure ITO whilst F8 (or another similar emissive polymer) freezes the ITO work function at a value lower than that of the plasma treated ITO but, ultimately is more stable, decaying slowly in comparison.

3.7. References

[1] J. S. Kim, M. Granstrom, R. H. Friend, N. Johansson, W. R. Salaneck, R. Daik, W. J. Feast, F. Cacialli, *Journal of Applied Physics* **1998**, *84*, 6859.

[2] J. S. Kim, P. K. H. Ho, D. S. Thomas, R. H. Friend, F. Cacialli, G. W. Bao, S. F. Y. Li, *Chemical Physics Letters* **1999**, *315*, 307.

[3] S. M. Tadayyon, K. Griffiths, P. R. Norton, C. Tripp, Z. Popovic, *J. Vac. Sci. Technol. A-Vac. Surf. Films* **1999**, *17*, 1773.

[4] H. W. Choi, S. Y. Kim, K. B. Kim, Y. H. Tak, J. L. Lee, *Applied Physics Letters* **2005**, *86*.

[5] Y. L. Shen, D. B. Jacobs, G. G. Malliaras, G. Koley, M. G. Spencer, A. Ioannidis, *Adv. Mater.* **2001**, *13*, 1234.

[6] T. A. Beierlein, W. Brutting, H. Riel, E. I. Haskal, P. Muller, W. Riess, *Synthetic Metals* **2000**, *111*, 295.

[7] J. S. Kim, R. H. Friend, F. Cacialli, *Journal of Applied Physics* **1999**, *86*, 2774.

[8] J. S. Kim, R. H. Friend, F. Cacialli, *Applied Physics Letters* **1999**, *74*, 3084.

[9] T. M. Brown, F. Cacialli, *Journal of Polymer Science Part B-Polymer Physics* **2003**, *41*, 2649.

[10] M. P. de Jong, L. J. van Ijzendoorn, M. J. A. de Voigt, *Applied Physics Letters* **2000**, *77*, 2255.

[11] H. J. Kim, J. W. Bae, J. S. Kim, K. S. Kim, Y. C. Jang, G. Y. Yeom, N. E. Lee, *Thin Solid Films* **2000**, *377*, 115.

[12] J. S. Kim, B. Lagel, E. Moons, N. Johansson, I. D. Baikie, W. R. Salaneck, R. H. Friend, F. Cacialli, *Synthetic Metals* **2000**, *111*, 311.

[13] J. C. Scott, G. G. Malliaras, W. D. Chen, J. C. Breach, J. R. Salem, P. J. Brock, S. B. Sachs, C. E. D. Chidsey, *Applied Physics Letters* **1999**, *74*, 1510.

[14] K. Sugiyama, H. Ishii, Y. Ouchi, K. Seki, *Journal Of Applied Physics* **2000**, *87*, 295.

[15] I. H. Campbell, S. Rubin, T. A. Zawodzinski, J. D. Kress, R. L. Martin, D. L. Smith, N. N. Barashkov, J. P. Ferraris, *Physical Review B* **1996**, *54*, 14321.

[16] T. M. Brown, J. S. Kim, R. H. Friend, F. Cacialli, R. Daik, W. J. Feast, *Applied Physics Letters* **1999**, *75*, 1679.

[17] T. M. Brown, R. H. Friend, I. S. Millard, D. J. Lacey, J. H. Burroughes, F. Cacialli, *Applied Physics Letters* **2000**, *77*, 3096.

[18] K. Besocke, S. Berger, *Rev. Sci. Instrum.* **1976**, *47*, 840.

[19] W. R. Zisman, *Rev. Sci. Instrum.* **1932**, *3*, 367.

[20] W. N. Hansen, K. B. Johnson, *Surf. Sci.* **1994**, *316*, 373.

[21] T. M. Brown, **2001**.

[22] G. Greczynski, T. Kugler, W. R. Salaneck, *Journal of Applied Physics* **2000**, *88*, 7187.

[23] K. Z. Xing, M. Fahlman, X. W. Chen, O. Inganas, W. R. Salaneck, *Synthetic Metals* **1997**, *89*, 161.

[24] http://www.baytron.com, **2006**.

[25] Y. He, S. Gong, R. Hattori, J. Kanicki, *Applied Physics Letters* **1999**, *74*, 2265.

[26] I. H. Campbell, T. W. Hagler, D. L. Smith, J. P. Ferraris, *Phys. Rev. Lett.* **1996**, *76*, 1900.

[27] T. M. Brown, R. H. Friend, I. S. Millard, D. J. Lacey, T. Butler, J. H. Burroughes, F. Cacialli, *Journal of Applied Physics* **2003**, *93*, 6159.

[28] G. Greczynski, M. Fahlman, W. R. Salaneck, *Chemical Physics Letters* **2000**, *321*, 379.

[29] G. Greczynski, T. Kugler, M. Keil, W. Osikowicz, M. Fahlman, W. R. Salaneck, *Journal of Electron Spectroscopy and Related Phenomena* **2001**, *121*, 1.

[30] G. Greczynski, T. Kugler, W. R. Salaneck, *Thin Solid Films* **1999**, *354*, 129.

[31] T. Kugler, W. R. Salaneck, H. Rost, A. B. Holmes, *Chemical Physics Letters* **1999**, *310*, 391.

Chapter 4. Optical Characterisation

This chapter discusses the optical characterisation of polyrotaxanes and the corresponding analogue polymers. The polymers have different monovalent counter-cations on the side-chains of the main polymeric chain. These cations vary in size and charge density. The effect of the change of cation on the optical properties such as absorption maxima, PL spectra and PL efficiency are discussed.

4.1. Experimental Details

For the preparation of thin films on Spectrosil B, materials were readily dissolved in ultrapure deionized water at room temperature, stirred for 12 hours at 55°C and passed through a 0.45μm filter prior to spin-coating. Spin-coated films were typically 100 nm thick from the 2%b.w solutions and were annealed at 60°C for 30 minutes under nitrogen to remove residual water. Film and solution absorption spectra were taken at room temperature, in air, with an Agilent UV-Vis Spectrophotometer. Photoluminescence (PL) was measured with excitation from an UV LED with spectrum peak of 370nm using an Ocean Optics spectrograph. PL efficiency was measured with the aid of an integrating sphere and using a He-Cd laser (325nm).

4.2. Change in counter-cation group

Previous experimental investigations concentrated on variations of the polyrotaxane and analogue polymer main chain with a $[Li]^+$ cation side group, and either $[SO_3]^-$ or $[CO_3]^-$ anions attached to the main chain. The threading of the polymer through the cyclodextrin resulted in reduced interchain interactions which manifest themselves in higher photoluminescence (PL) efficiency, blue-shifted

absorption/emission spectra,[1] and reduced luminescence quenching when compared to the unthreaded conjugated polyelectrolytes.[2]

Further investigations into the role of the counter-cation in regards to the optoelectronic properties of the conjugated polyelectrolytes have been conducted in this work. Frampton *et al* (Unpublished) have exchanged the lithium ion for caesium (Cs), potassium (K) and two non-metallic based cations; tetrametylammonium (NMe_4) and cryptate-encapsulated potassium (K@[2.2.2]), as described in Chapter 2. PDV has been used in conjunction with β -cyclodextrin, β-CD, to provide the threaded wire as in previous investigations.[2-6] Threading ratios (TR) of 1.3 and 2.3 β-CD per repeat unit have been prepared (as determined by H^1 NMR) and the effect of further insulation of the backbone on the optical properties of the polymers has been studied.

Figure 4-1 shows the chemical structure of the polymer with the different counter-cation groups and cyclodextrin. The synthesis, determination of threading ratios and ion-exchange procedures were discussed in Chapter 2.

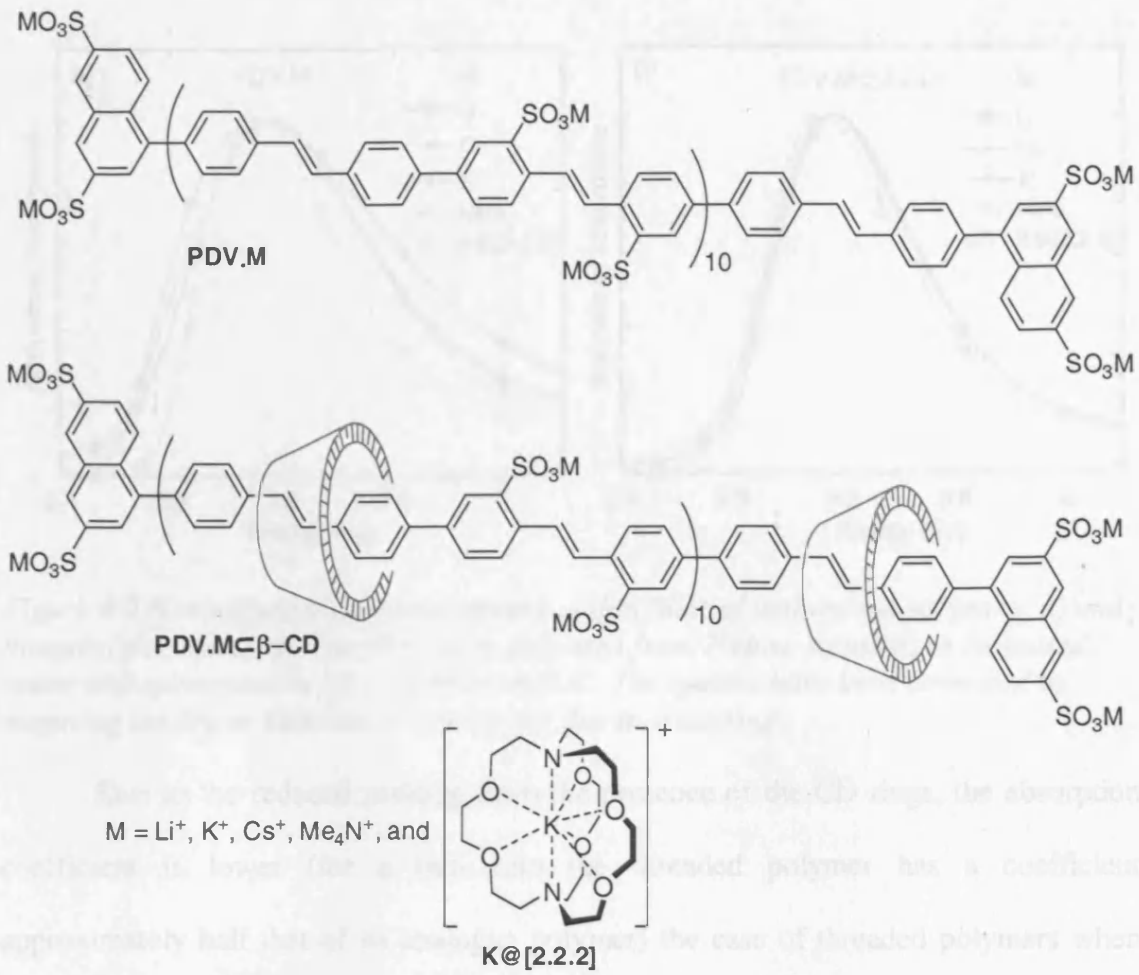

K@[2.2.2]

Figure 4-1 Chemical structure of poly(4,4′-diphenylene vinylene) with different cationic groups and large end groups. The polymer is typically ten repeat units long and the *β*-cyclodextrin is 1.5nm in diameter.

4.2.1. Absorption Studies

It was already known that the polyrotaxanes' absorption spectra blue-shift in comparison with their unthreaded polymers.[2] It has been further observed that the absorption spectra differ for threaded and unthreaded polymers upon addition of counter-cations with larger radii, as in Figure 4-2. The spectra of the threaded polymers experience a slight red-shift which is more apparent for the NMe_4- and K@[2.2.2]-substituted polyrotaxanes with no significant change of shape whilst the unthreaded polymer spectra narrow with increasing cation size as well is also slightly red-shifting. This indicates that the interchain distances are increased.

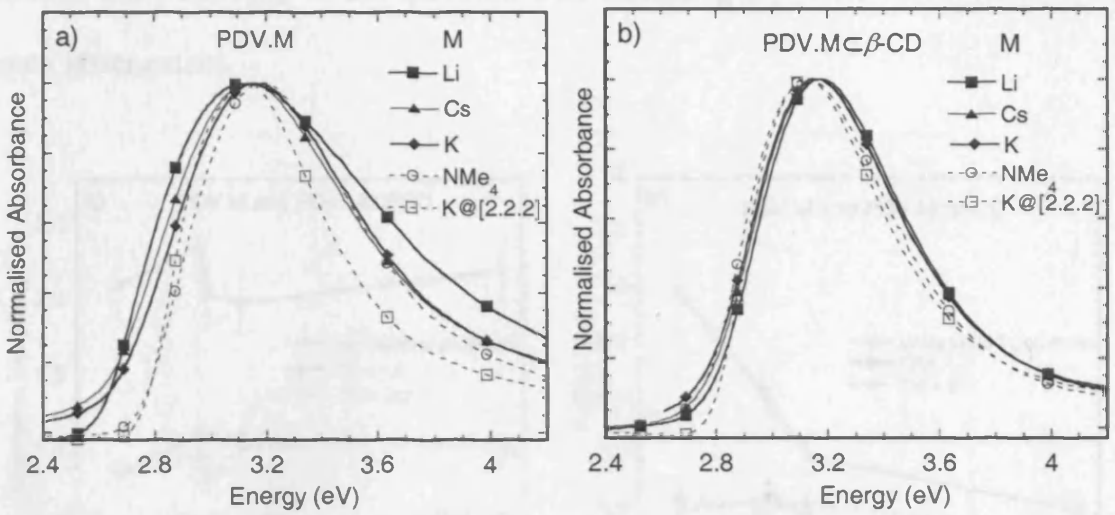

Figure 4-2 Normalised absorption spectra of thin films of unthreaded polymers, a) and threaded polymers, b). The films were prepared from 2%b.w. solutions in deionised water and spincoated in air onto Spectrosil B. The spectra have been corrected by removing the linear baseline at low energy due to scattering.

Due to the reduced packing from the presence of the CD rings, the absorption coefficient is lower (for a thin film the threaded polymer has a coefficient approximately half that of its analogue polymer) the case of threaded polymers when compared to their unthreaded counterparts. However Figure 4-3a) shows that the cation-exchange does not further alter the absorption intensity as all measurements are within experimental error of each other. The increase of threading ratio from TR = 1.3 to TR = 2.3 per repeat unit appears not to further alter the absorption intensity of the spectra or further shift the spectral peak (not depicted) or indeed affect the full-width half maximum (FWHM) as illustrated in Figure 4-3a) and b). For Li-, Cs- and NMe_4-polyrotaxanes the absorption intensity and FWHM values for both TRs either coincide or are within experimental error.

As the counter-cation radius increases from Li to K@[2.2.2], the unthreaded polymer FWHM as shown in Figure 4-3b) decreases and the low energy edge of the spectrum moves progressively to higher energies. The threaded polymer FWHM also

exhibits this narrowing of the spectrum with increasing counter-cation radii but to a much lesser extent.

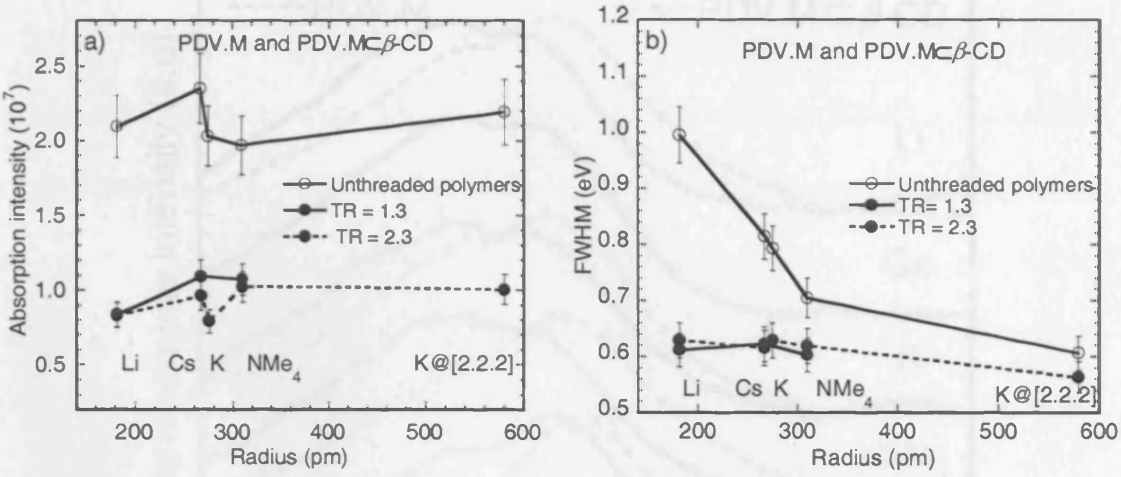

Figure 4-3 Optical density of the films integrated between 275 and 496nm is reported in a). The full width half maximum (FWHM) of each spectrum have been plotted in b). The optical density and FWHM of the two threading ratios (1.3 and 2.3) of β-CD have also been plotted. a) and b) are plotted as a function of the ionic (Li^+, Cs^+ and K^+) and Van der Waals ($NMe4^+$ and $K@[2.2.2]^+$) radius.

4.2.2. Photoluminescence Spectra

Photoluminescence (PL) spectra, Figure 4-4, of the materials show that for the PDV.M and PDV.MC⊂β-CD the main peaks occur at approximately 2.40eV and 2.50eV respectively apart from K@[2.2.2]-substituted polymers. All are Stokes shifted by ~0.8eV from the absorption spectra. K@[2.2.2] substituted PL spectra present a more pronounced vibronic structure and the spectra are further in the blue with respect to the other cations. The K@[2.2.2]- unthreaded polymer and polyrotaxane spectra differ to the other spectra. The unthreaded polymer has spectra peaks at approximately 0.15eV further in the blue and the polyrotaxane a few hundredths of an eV further in the blue r when compared to the corresponding Li, Cs, K and NMe_4^+ unthreaded polymer/polyrotaxane. The TR=1.3 data are plotted in Figure 4-4 alongside the unthreaded polymer spectra and the TR = 2.3 data showed no significant spectral

differences to the TR = 1.3 and are not presented apart from PDV. K⊂β-CD and PDV. K@[2.2.2]⊂β-CD.

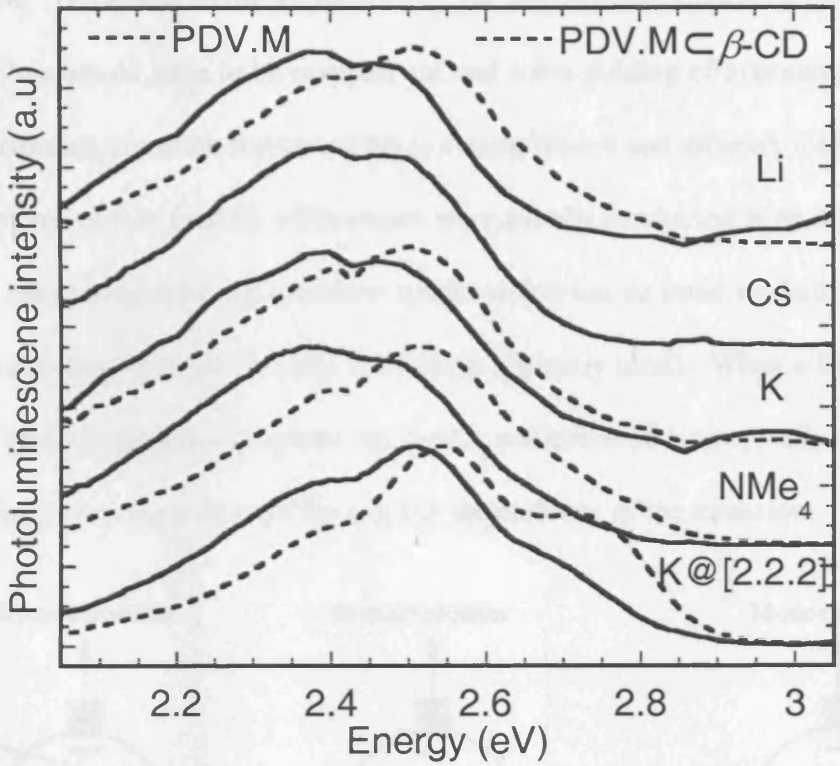

Figure 4-4 Normalised photoluminescence spectra of thin films performed in air using an Ocean Optics Spectrograph, unthreaded and threaded polymers are plotted alongside each other.

4.2.3. Photoluminescence Efficiency measurements

The external photoluminescence quantum yield of thin polymeric films is obtained using a method developed by de Mello *et al* [7] at Cambridge University. This method takes into account that thin films do not have an isotropic angular distribution for the emission, unlike solutions. If the emission were isotropic then the measurement would be relatively simple and the external quantum efficiency, η, defined thus in Equation 4-1:

$$\eta = \frac{\text{number of photons emitted}}{\text{number of photons absorbed}}$$

Equation 4-1

could be used. To be able to use Equation 4-1, the angular distribution of the emission of the thin films would have to be mapped out and wave-guiding effects can modify the angular distribution emission further. This is a complicated and difficult measurement so measurements of thin film PL efficiencies are typically conducted in an integrating sphere. An integrating sphere is a hollow sphere which has its inner surface coated with a diffusely reflecting material (barium sulphate is typically used). When a light-source is placed in an ideal integrating sphere the light is redistributed isotropically over the interior of the sphere regardless of the angular dependence of the emission.

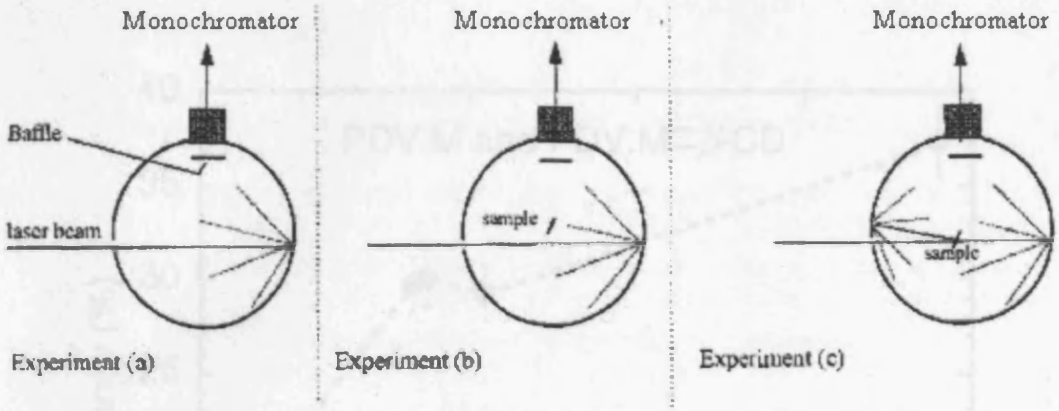

Figure 4-5 Diagram illustrating the 3 configurations of the sphere required for the efficiency measurement: (a) NO sample, (b) OFF sample, (c) ON sample.

deMello *et al* made use of an integrating sphere in the setup shown in Figure 4-5, however they used a CCD spectrometer in place of the monochromator. The basic experimental set-up has a baffle coated in barium sulphate in front of the monochromator slot to prevent direct illumination of the monochromator. Laser illumination of an appropriate wavelength is directed through a small entrance hole.

Three measurements are made using the sphere. In the first measurement the sphere is empty and just laser light is directed into the sphere, in the second the sample

is mounted inside the sphere and the laser beam is directed onto the sphere wall near the sample, the last measurement directs the laser onto the sample. The sample is orientated as to prevent reflected laser light from coming back through the entrance hole and ensure it lands on the sphere wall. The PL efficiency is then calculated by the ratios of laser light and the photoluminescence. Further discussion of the PL efficiency calculation can be found in the paper by deMello *et al.*[7]

Here PL efficiency measurements have been conducted on thin films of PDV.M and PDV.M⊂β-CD, where M = Li, Cs, K, NMe_4 and K@[2.2.2]. The PDV.M⊂β-CD had *β*-CD TRs of either 1.3 or 2.3 per repeat unit. PL efficiencies of PPV and MEH-PPV[7] have been supplied to act as reference points.

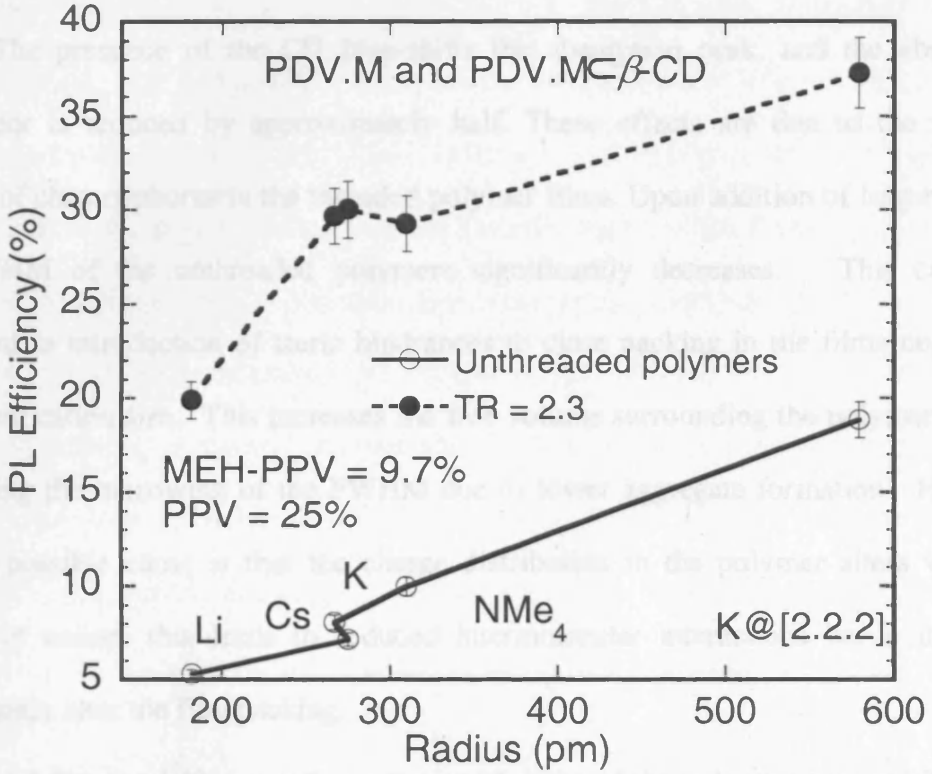

Figure 4-6 PL Efficiency of the unthreaded polymer and double threaded (TR = 2.3) polymers as a function of the ionic (Li^+, Cs^+ and K^+) and Van der Waals ($NMe4^+$ and $K@[2.2.2]^+$) radius. The PL efficiencies of MEH-PPV and PPV have been supplied as reference values.

The PL efficiency values have been plotted in Figure 4-6 as a function of increasing counter-cation radii for TR = 2.3 as there was a larger sample set than for the TR = 1.3. As the radii increase the PL efficiency increases overall for all polymers and the unthreaded polymers all have lower PL efficiencies than their threaded counterparts. An increase of the PL efficiency with respect to cation radii is observed from 5% for PDV.Li to 19% for PDV.K@[2.2.2] for the unthreaded polymers.

The threaded polymers exhibit two sharp increases in the PL efficiency in Figure 4-6: 1) Change in cation from Li to K and 2) Change from NMe_4 to K@[2.2.2]. The PL efficiency varies little between Cs and NMe_4 before the large increase to 37% seen for K@[2.2.2] counter-cation threaded polymers.

4.3. Discussion

The presence of the CD blue-shifts the absorption peak, and the absorption coefficient is reduced by approximately half. These effects are due to the reduced content of chromophores in the threaded polymer films. Upon addition of larger cations the FWHM of the unthreaded polymers significantly decreases. This could be attributed to introduction of steric hindrances to close packing in the films due to the increasing cation size. This increases the free volume surrounding the polymer chains, so causing the narrowing of the FWHM due to lower aggregate formation. However another possible cause is that the charge distribution in the polymer alters with the change in cation: this leads to reduced intermolecular interactions but it does not significantly alter the film packing.

In Figure 4-3b) the different cation-substituted peaks of the polyrotaxanes, whilst blue-shifted with respect to their unthreaded counterparts, only slightly alter with increasing cation size in FWHM. This suggests that the more probable reason for this effect in the analogue polymers and the polyrotaxanes is a change in the film packing and the effect

is lessened in the polyrotaxanes due to the presence of the CD rings which have already led to an altered packing formation to the analogue polymer. The movement of the absorption spectra to the red regime for the polyrotaxanes and analogue polymers also suggests that packing in the films is altered by the increased size of the cations as it adds another large bulky group to the chain alongside the CD.

The unthreaded polymers have larger absorption intensities than the polyrotaxanes as they have more conjugated material but they remain constant, as do the threaded polymers, with changes in cation (within experimental errors).

PL spectra on the different materials demonstrated that the addition of larger side-groups does not further change the emission process, apart for the case of K@[2.2.2] substituted ions which are extremely large. It is already known that the 0-1 transition is stronger in the PDV.M whilst the 0-0 transition is strongest in the PDV.M⊂β-CD. The K@[2.2.2] spectra have 3 major peaks which are discernible at room temperature compared with the 2 observed for the other cations in Figure 4-4. This change in shape may explain why the PL efficiencies of the K@[2.2.2] substituted materials are considerately larger than their counterparts, as there are different decay processes at work. The increase in PL efficiency may be attributed to either substantial changes in packing or reduced intermolecular interactions. As the absorption intensity does not vary with increase in cation radius while the PL efficiency does it points to intermolecular interactions changing due to variations in charge distribution rather than reduced packing. This may lead to reduced quenching of the photons by non-radiative processes.

It was expected that a further blue-shift and narrowing of the FWHM of the absorption spectra would be seen upon further insulation of the polymer chain. This would have been due to increased shielding of the chain leading to more intrachain

processes than interchain processes. However this did not happen, thus, for optical processes double threading is still a viable option. The effect on the PL efficiencies is harder to identity as there was little data to analyse the singly threaded polyrotaxanes, hence they were not shown.

4.4. Conclusions

The reduced interchain interactions caused by the increased distances between chains in the polyrotaxanes is highlighted by the emission and absorption spectra. Ion-exchange of the cation allows further tuning of the optical properties and introduces variation in the thin film packing as demonstrated by the reduced FHWMs. The substitution of larger cations benefits the PL efficiency by lessening quenching.

4.5. References

[1] J. Cornil, A. J. Heeger, J. L. Bredas, *Chemical Physics Letters* **1997**, *272*, 463.

[2] F. Cacialli, J. S. Wilson, J. J. Michels, C. Daniel, C. Silva, R. H. Friend, N. Severin, P. Samori, J. P. Rabe, M. J. O'Connell, P. N. Taylor, H. L. Anderson, *Nature Materials* **2002**, *1*, 160.

[3] S. Anderson, R. T. Aplin, T. D. W. Claridge, T. Goodson, A. C. Maciel, G. Rumbles, J. F. Ryan, H. L. Anderson, *Journal of the Chemical Society-Perkin Transactions 1* **1998**, 2383.

[4] J. J. Michels, M. J. O'Connell, P. N. Taylor, J. S. Wilson, F. Cacialli, H. L. Anderson, *Chemistry-A European Journal* **2003**, *9*, 6167.

[5] P. N. Taylor, M. J. O'Connell, L. A. McNeill, M. J. Hall, R. T. Aplin, H. L. Anderson, *Angew. Chem.-Int. Edit.* **2000**, *39*, 3456.

[6] J. S. Wilson, M. J. Frampton, J. J. Michels, L. Sardone, G. Marletta, R. H. Friend, P. Samori, H. L. Anderson, F. Cacialli, *Adv. Mater.* **2005**, *17*, 2659.

[7] J. C. deMello, H. F. Wittmann, R. H. Friend, *Adv. Mater.* **1997**, *9*, 230.

Chapter 5. Thermochromism in polyrotaxanes and their analogue polymers

The ease of colour tunability of organic semiconductors is seen as one of the advantages of these materials compared to inorganic semiconductors. For use in displays such as mobile- phone screens,, the colour should be unaffected by changes in the environment such as temperature. However it is known that organic semiconductors may experience shifts in optical absorption and emission spectra with changes in temperature due to variation of the HOMO/LUMO band gap: this phenomenon is called thermochromism. Here, following on from the optical characterisation in Chapter 4, the robustness of the conjugated polyelectrolytes is further tested with respect to temperature variation by following the evolution of the photoluminescence emission and UV-Visible absorption spectra.

5.1. Introduction

Thermochromism describes the ability of a material to change colour due to changes in temperature. This effect is observed in liquid crystals (LCs). Changes in temperature affect the crystalline structure of the LC, this in turn changes the periodic spacing in the crystal lattice (due to thermal expansion) and thus when light is shone on the LC a different wavelength is passed through due to changes in electron-phonon coupling.[1]

In conjugated polymers temperature changes can also affect the optical properties. The wavelength of light emitted is defined by the π-π^* gap. If this energy gap is increased the colour will blue-shift and if it is reduced it will red-shift. The origin of this gap has been explained in Chapter 1, but to recap it is linked to the effective conjugation length of the polymer chain. A longer effective chain length will red-shift

the emission as the overlap of the π-electrons is increased, reducing the π-π^* gap and the opposite will occur in polymers when the effective conjugation length is decreased.

The effective conjugation length is determined by the extent of straight planar chain segments unperturbed by chain twists, bends and other defects. The temperature dependence of conjugated polymers has been rationalised by two different models; 1) structural changes (for example greater torsional freedom) due to variation in temperature[2-6] and 2) electronic changes in the polymer. At higher temperatures the exciton is more likely to remain on smaller chain segments effectively acting as if the conjugation length has been reduced[7, 8]. Both models agree that at higher temperatures the absorption and emission spectra will blue-shift.

The model of structural changes considers that excitations of the vibrational, rotational or librotational modes that may be caused by variation of temperature cause the changes in light emission. These excitations can be observed in the absorption and luminescence spectra as a function of temperature[3]. Upon cooling of a sample, the torsional modes of freedom are frozen out (these reduce the coplanarity of chains) and the conjugation lengths are weighted in favour of longer conjugation lengths leading to the red-shift of the UV-Vis absorption spectra.

This explanation seemed to be verified by other early experiments into the temperature dependence of conjugated polymer optical spectra. Raymond *et al*[4] studied a polythiophene derivative, poly(3,3´-di-(butylthio)-2,2´-bithiophene) which would allow different degrees of freedom in the main chain to regioregular poly(3-alkythiophene). They attributed the greater blue-shift of the UV-Visible absorption spectra in Figure 5-1 of the poly(3,3´-di-(butylthio)-2,2´-bithiophene) to a more twisted conformation of the backbone leading to a reduced conjugation length with increasing temperature.

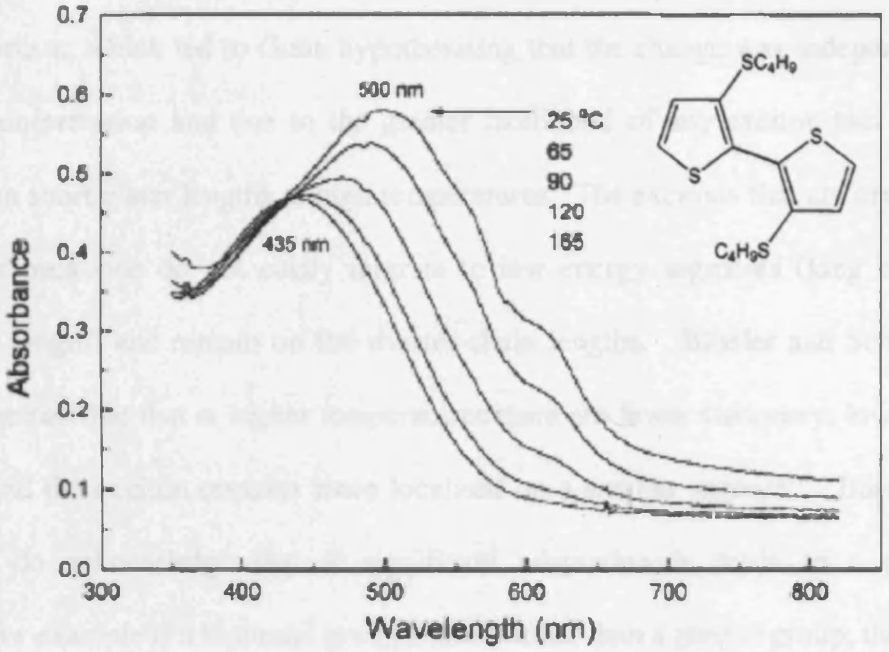

Figure 5-1 Temperature-dependent UV-Visible absorption spectra of poly(3,3´-di-(butylthio)-2,2´-bithiophene) in the solid state, inserted is the chemical structure of the repeat unit used. Adapted from [4].

Many researchers still follow this rationale; recently Kong *et al*[5] published research into the temperature dependence of MEH-PPV and a derivative with aryl-substituted oxadiazole groups (MEH-OPPV) in the backbone. They attributed the lack of blue-shift of the PL spectra of MEH-OPPV compared to MEH-PPV to the differences in dihedral angles of the two compounds. MEH-OPPV has larger dihedral angles at room temperature between adjacent repeat units than MEH-PPV leading to reduced torsional angle changes in the polymer chain upon increases in temperature. Thus the MEH-OPPV is thermally stable in comparison to the MEH-PPV.

The electronic model was first suggested by Bässler and Schweitzer in 1999.[7] They attribute the thermochromic response of conjugated polymers to the temperature dependence of the electronic relaxation in polymer chains rather than the freezing out of torsional modes of freedom. This was also the conclusion of Guha *et al*[8] who also investigated the temperature dependence of polymers which had high levels of torsional

freedom, some torsional freedom and no torsional freedom. All exhibited thermochromism, which led to Guha hypothesising that the change was independent of backbone conformation and due to the greater likelihood of any exciton that formed remaining on short chain lengths at high temperatures. The excitons that are created on the polymer backbone do not easily migrate to low energy segments (long effective conjugation length) and remain on the shorter-chain lengths. Bässler and Schweitzer further suggested that that at higher temperatures there are fewer stationary, low energy trap sites, and the exciton remains more localised on a smaller segment. Bässler and Schweitzer do acknowledge that if significant adaptation is made to a polymer backbone, for example if a biphenyl group is used rather than a phenyl group, then trade offs between steric repulsion and conjugation lead to substantial molecular relaxations after excitation. For example in the ground state biphenyl groups favour a tilted structure so that the rings are at 20^0 to each other whilst in the excited state they are in a planar geometry. Thus it allows both the electronic and structural models to be considered, where appropriate.

The threading of conjugated polyelectrolytes through insulating rings has been shown to reduce interchain interactions, resulting in increased electroluminescence and photoluminescence efficiencies, with blue-shifted emission.[9] These materials are rigid and once threaded cannot interact easily with other polymers. The stability of the electronic structure once CD was added could be studied in part by investigation of the material's thermochromic behaviour. Studies of a prototype polyrotaxane and its analogue polymer (PDV.Li⊂β-CD and PDV.Li) have been conducted alongside analysis of previous work to explore the thermochromic behaviour of these materials.

5.2. Experimental details and results

5.2.1. Experimental Details

For the preparation of thin films, materials were readily dissolved in ultrapure deionized water at room temperature, stirred for 12 hours on at hotplate at 55^0C and filtered through a 0.45μm filter. Spin-coated films were typically 100 nm thick from the 2%b.w solutions, on Spectrosil substrates and were annealed at 60 °C for 30 minutes under nitrogen to remove residual water. Temperature dependent PL spectra measurements were acquired using a time-integrated, temperature-dependent far-field PL spectrometer in a cryostat under a dynamic flow of helium at the Cavendish Laboratory, University of Cambridge. Excitation and detection were provided by a time-correlated single-photon counting system. Samples were excited with a pulsed diode laser emitting at 407 nm. Spectra were recorded from temperatures of 50-400K ramping up with measurements taken either every 2nm or 1nm. Normalised spectra were Gaussian peak fitted.

Polyrotaxanes and analogue polymers were also studied in temperature dependent solution absorption experiments to gain further understanding of their behaviour. The absorption apparatus had a smaller temperature range, from 10K below the room temperature (approximately 288K) to a maximum of 360K. The solution was cooled to the desired temperature and then held at that temperature for 15minutes before the next measurement was taken at a higher temperature.

Previous measurements on a different low temperature PL system by another worker on a polyrotaxane/analogue polymer with a different backbone and side-groups have been compared to these results. Peak fitting and data analysis were performed for the purpose of this thesis.

5.2.2. Temperature dependent Photoluminescence spectra

The vibronic structure of Photoluminescence (PL) spectra of PDV.Li⊂β-CD and PDV.Li are shown in Figure 5-2 and are visibly different in structure. The polyrotaxane spectra are blue shifted with respect to the analogue polymer at the same temperatures as for absorption spectra, seen previously in Chapter 4. The vibronic structure of PDV.Li⊂β-CD is more prominent than that of its analogue polymer, PDV.Li with more than three vibronic peaks assignable in the low temperature spectrum at 150K. Luminescence decreases and peaks broaden with increasing temperature, due to bleaching effects and loss of vibronic structure. PDV.Li⊂β-CD photobleaches more slowly than PDV.Li. In the transition from 150 to 200K the intensity decreases by a quarter for the polyrotaxane compared with the loss of nearly two-thirds intensity for the analogue polymer. The PL spectra intensity increases, but not to the original value, when the temperature is lowered again.

The experiment was repeated to confirm this response. However the vibronic structure was not as well defined as for the previous experiment. It is also worthwhile noting that the initial spectra obtained were red-shifted (0.1eV shift for peak 2 for both polymers) compared to the repeated experiment perhaps due to film quality differences due to thickness variations and order within the film. This better resolved vibronic structure is normally associated with a more ordered film, however it tends to accompany a blue-shift of PL spectra unlike here. To compare the effect of temperature on the photoluminescence of these polymers the largest peak, peak 2, has been followed for the repeated experiment (PL spectra not shown) as this was conducted over a larger temperature range than the initial experiment.

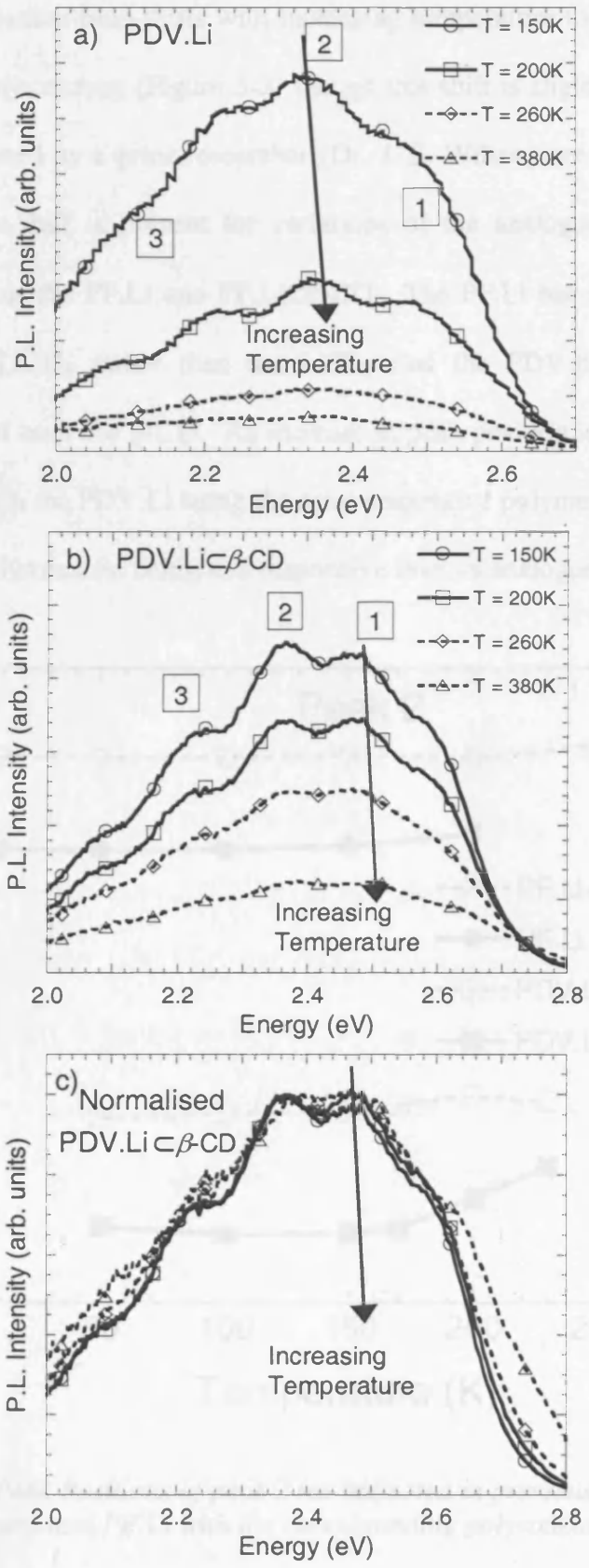

Figure 5-2 Temperature dependent photoluminescence spectra from 150K to 380K of a) PDV.Li, b) PDV.Li ⊂β-CD and c) normalised spectra of the polyrotaxanes.

The peak position blue-shifts with increasing temperature for both the analogue polymer and the polyrotaxane (Figure 5-3) though this shift is slight. Data analysis on experiments conducted by a prior researcher (Dr. J. S. Wilson) are also presented and show that this blue-shift is present for variations of the analogue polymer and the polyrotaxane, such as the PF.Li and PF.Li⊂β-CD. The PF.Li has a PF backbone and the side-group is $LiCO_3$ rather than the $LiSO_3$ that the PDV-based polymers are engineered with, but both use β-CD. An increase in peak position is not observed until 150K is reached, with the PDV.Li being the most responsive polymer to the temperature change and each polyrotaxane being less responsive than its analogue polymer.

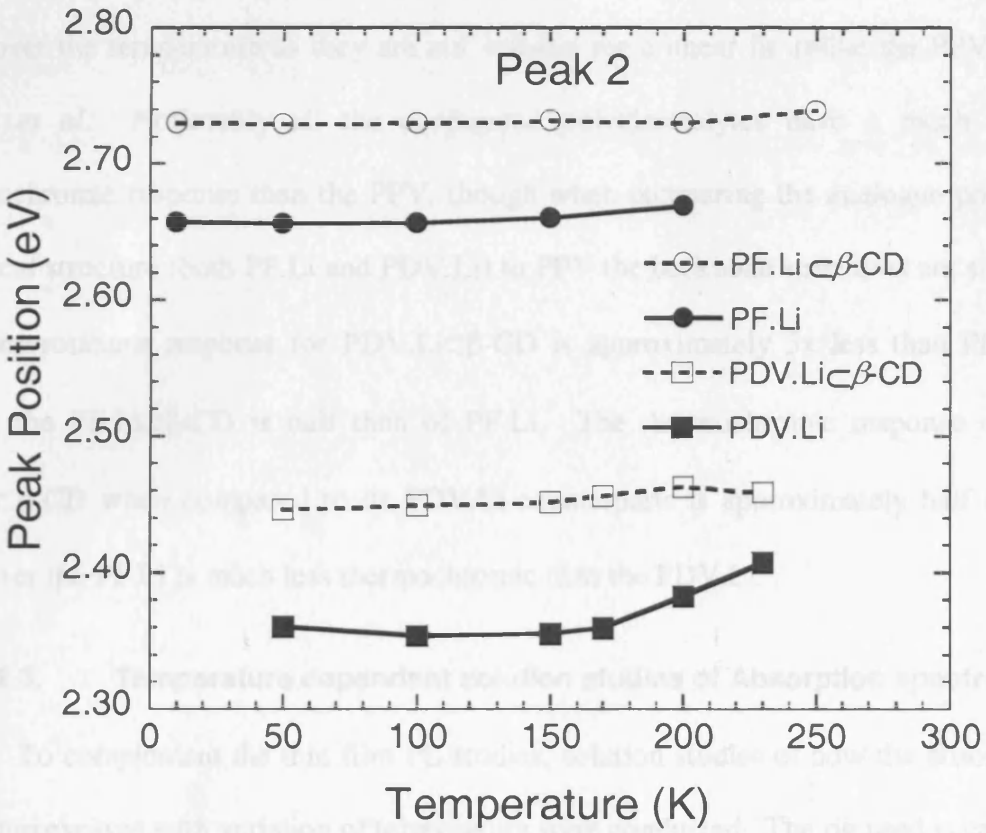

Figure 5-3 Plotted Peak Positions of peak 2 (as indicated in previous graphs) of PDV.Li (PL spectra not shown) and PF.Li with the corresponding polyrotaxanes against temperature.

The peak shift data in meV/K is given in Table 5-1. The peak shift for PDV.Li and PDV.Li⊂β-CD is taken from the data shown above. For comparison with other, similarly structured, conjugated polymers, the peak shift of poly(p-phenylene vinylene),

PPV, measured by Latini et al[10] (where the peak occurs at 2.44eV at room temperature) has been given in Table 5-1.

	Total peak shift (meV/K)
PDV.Li	**0.26**
PDV.Li⊂β-CD	**0.05**
PF.Li	**0.06**
PF.Li⊂β-CD	**0.02**
PPV[10]	**0.5**

Table 5-1 Table of peak shift ratios for temperature dependent photoluminescence measurements of materials studied and analysed during this work, performed Dr. J. S. Wilson but analysed during this work and a reference value.

Peak shifts from the conjugated polyelectrolytes are calculated from total peak shift over the temperature as they are not suitable for a linear fit unlike the PPV from Latini *et al.* Noticeably all the conjugated polyelectrolytes have a much lower thermochromic response than the PPV, though when comparing the analogue polymer chemical structure (both PF.Li and PDV.Li) to PPV the backbone structures are similar. The polyrotaxane response for PDV.Li⊂β-CD is approximately 5x less than PDV.Li whilst the PF.Li⊂β-CD is half than of PF.Li. The thermochromic response of the PF.Li⊂β-CD when compared to its PDV.Li-counterparts is approximately half again. However the PF.Li is much less thermochromic than the PDV.Li.

5.2.3. Temperature dependent solution studies of Absorption spectra

To complement the thin film PL studies, solution studies of how the absorption spectrum evolves with variation of temperature were conducted. The rig used is capable of a 60K temperature range via use of a Peltier cooler. This set-up of the rig meant that only solution studies were possible. This meant that the absorption spectra were broader and that they are more susceptible to small changes in temperature as they are not in film and thus have a larger degree of freedom.

Both the analogue polymer and the polyrotaxane absorption peaks blue-shift with increasing temperature, shown in Figure 5-4. PDV-Li and β-CD-PDV-Li were studied extensively. The PDV-Li polyrotaxane has an absorption maximum at shorter wavelengths than the analogue polymer as seen in PL experiments. This blue-shift in both materials with increasing temperature could be due to either reduced conjugation length from increased torsional angles along the main chain or the result of the exciton remaining localised on a shorter chain length.

The absorbance decreases at high temperatures which indicates that fewer chromophores are available at the absorption maximum. The PDV.Li solution blue-shifts with increasing temperature, and the full width half maximum (FWHM) is temperature insensitive as the whole spectrum blue-shifts. However as the PDV.Li⊂β-CD solution is subjected to higher temperatures the blue edge of the spectrum remains at a constant wavelength whilst the red edge blue-shifts, reducing the FWHM, as seen in Figure 5-4b).

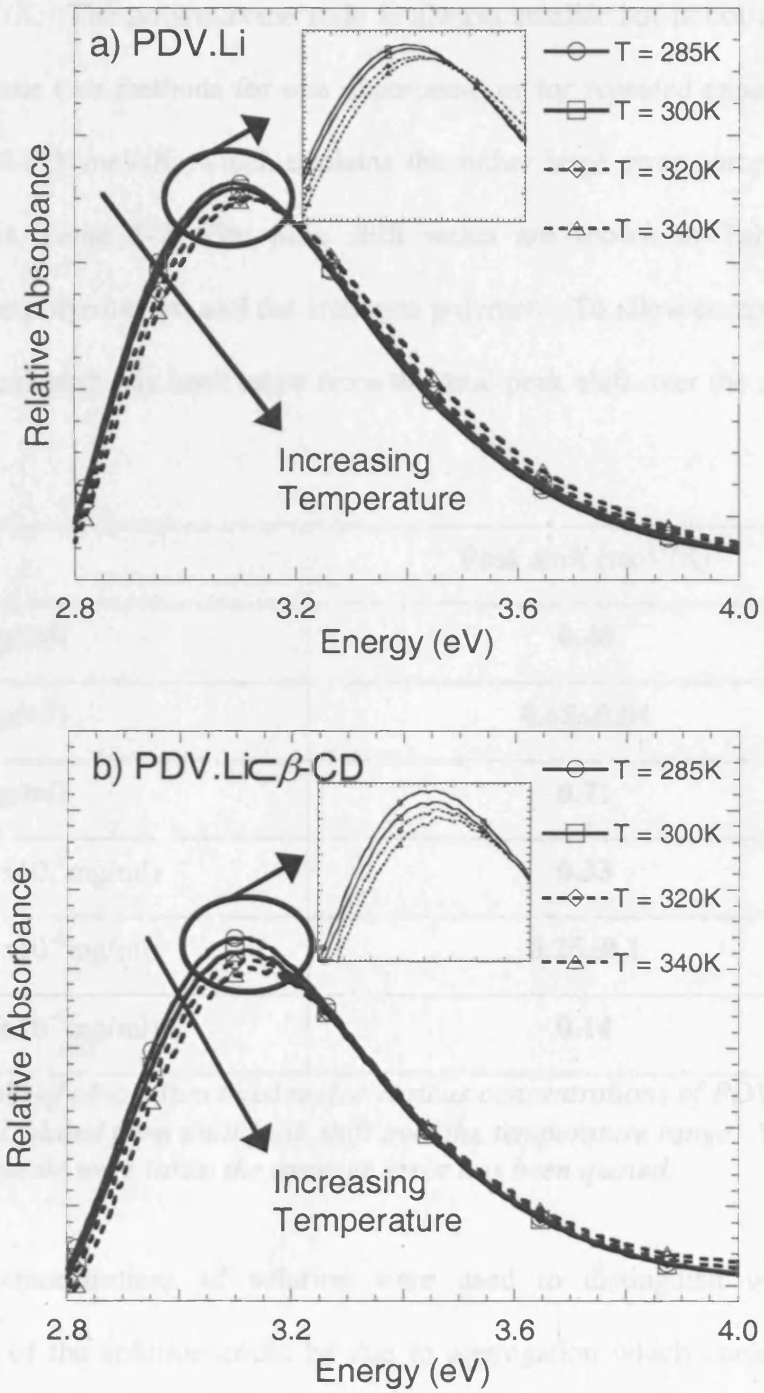

Figure 5-4 Temperature dependent solution studies of absorption spectra for a) PDV.Li and b) PDV.Li⊂β-CD. Inserted in the figures are zooms of the absorption peak to highlight the peak shift.

The peak shift ratio has been measured using the total peak shift over the temperature range, here a liner fit of the peak shift was also possible. Both methods correlate well for the analogue polymers where the peaks shift ratio has been found to

be 0.6 to 07.meV/K. The polyrotaxane ratio is always smaller but is not as constant, whether between the two methods for one experiment or for repeated experiments. It ranges from 0.008-0.31meV/K, which explains the rather large error compared to the other polymers in Table 5-2. The peak shift ratios are shown in Table 5-2 for experiments on the polyrotaxane and the analogue polymer. To allow comparison with the PL data the peak shift has been taken from the total peak shift over the temperature range.

	Peak shift (meV/K)
PDV.Li ($1x10^{-2}$mg/ml)	**0.40**
PDV.Li ($1x10^{-3}$mg/ml)	**0.65±0.04**
PDV.Li ($5x10^{-4}$mg/ml)	**0.71**
PDV.Li⊂β-CD ($1x10^{-2}$mg/ml)	**0.33**
PDV.Li⊂β-CD ($1x10^{-3}$mg/ml)	**0.25±0.1**
PDV.Li⊂β-CD ($5x10^{-4}$mg/ml)	**0.14**

Table 5-2 Peak shift of absorption maxima for various concentrations of PDV.Li and PDV.Li⊂β-CD calculated from total peak shift over the temperature range. Where multiple measurements were taken the average error has been quoted.

Varying concentrations of solution were used to distinguish whether the apparent stability of the solution could be due to aggregation which could mask the effects of the thermochromism in the polymer. This is less important in the photoluminescence studies as the polymers should be "frozen" in place during the spin-coating lessening the possibility of aggregation. If the polymers aggregate readily then the solution would be aggregated at all temperatures investigated reducing the blue-shift. Thus by conducting experiments at three different concentrations this could be discounted. For the PDV.Li⊂β-CD the low and high concentration peak shifts are

within the error of the value given for the medium concentration of $1x10^{-3}$mg/ml. The PDV.Li has a much lower thermochromic response at high concentrations which is outside the error of the initial measurement. This indicates that aggregation may occur in the PDV.Li (the presence of the β-CD limiting this in the polyrotaxane) artificially lowering the thermochromic response, AFM investigations have already shown that the analogue polymer aggregates[9] so it is a plausible reason.

Following on from these results further experiments on conjugated polymers were conducted for comparison purposes. Two more water-soluble conjugated polyelectrolytes (PPP.Li and PF.Li) and an organic soluble polyrotaxane known PF.Me⊂β-CD.Si were studied. Poly (4,4' –diphenylene diphenyl vinylene),PDPV, and poly (9, 9-dioctylfluorene), F8, were also used. The organic soluble polyrotaxane, PDPV and F8 were dissolved in toluene. The structures of the PDV-Li, PPP-Li and PF-Li polymers have been given in Chapter 2 whilst the organic soluble polyrotaxane, PDPV and F8 are reported in Figure 5-5. All of the peak shifts (absorption and PL) are grouped together in Table 5-3.

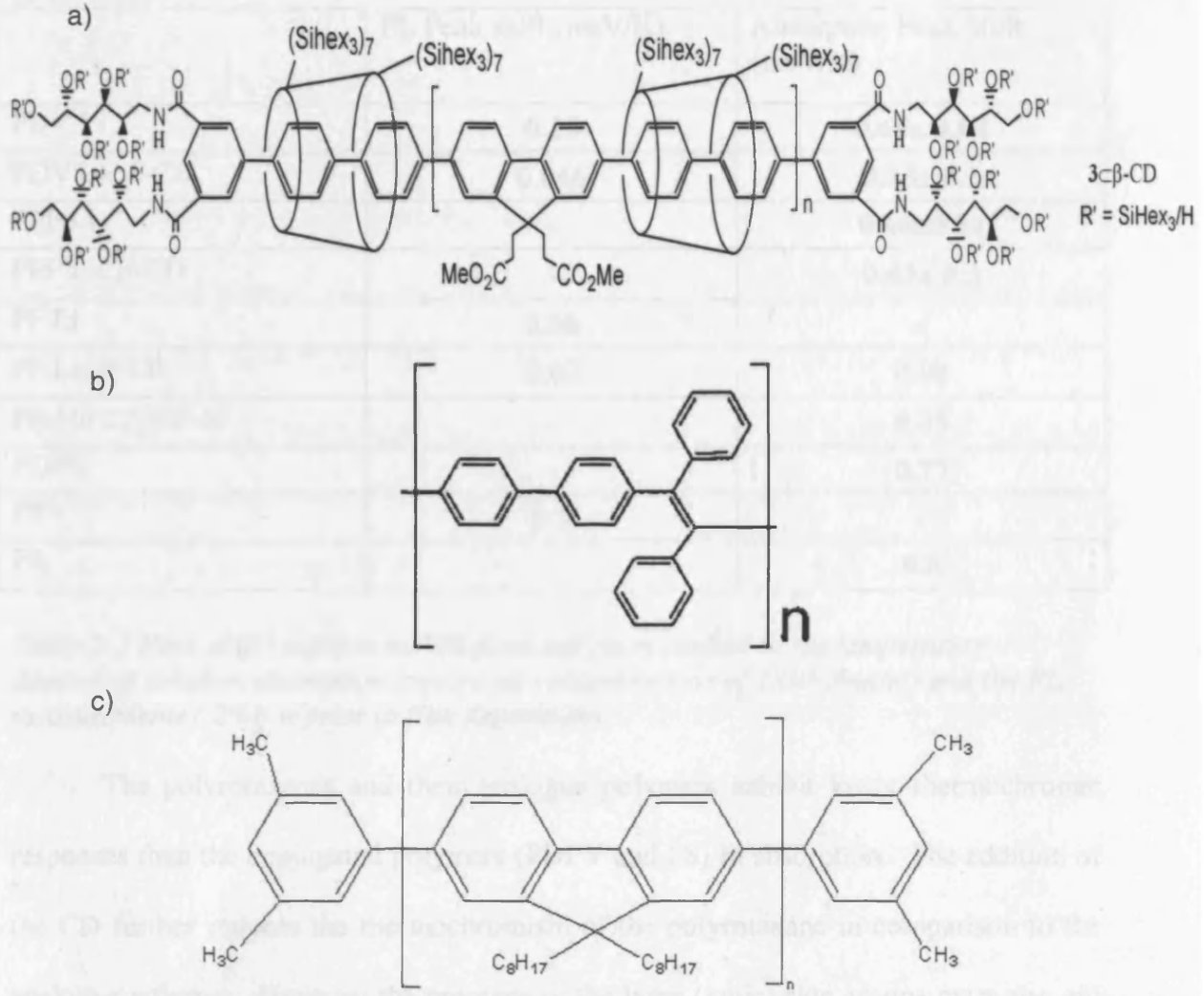

Figure 5-5 a) Structure of the a) organic-soluble polyrotaxane, b) PDPV and c) F8 used in the temperature dependent solution absorption spectra experiments.

	PL Peak shift (meV/K)	Absorption Peak Shift (meV/K)
PDV.Li	**0.26**	**0.65± 0.04**
PDV.Li⊂β-CD	**0.046**	**0.25± 0.1**
PPP.Li	-	**0.46±0.04**
PPP.Li⊂β-CD	-	**0.43± 0.3**
PF.Li	**0.06**	-
PF.Li⊂β-CD	**0.02**	**0.08**
PF.Me ⊂β-CD-Si	-	**0.35**
PDPV	-	**0.77**
PPV	**0.5**	-
F8	-	**0.5**

Table 5-3 Peak shift values in meV/K from polymers studied in the temperature dependent solution absorption spectra (at concentrations of 1x10-3mg/m) and the PL measurements (2%b.w prior to film deposition).

The polyrotaxanes and their analogue polymers exhibit lower thermochromic responses than the conjugated polymers (PDPV and F8) in absorption. The addition of the CD further reduces the thermochromism of the polyrotaxane in comparison to the analogue polymer. However the presence of the large (ionic) side groups must also aid in keeping the electronic structure of the polymer intact as seen for PPP.Li and PPP.Li⊂β-CD as the polyrotaxane and the analogue polymer exhibit very similar thermochromic responses.

The F8, PPV, and PDV.Li may be aggregating leading to the unexpected low thermochromic responses. If the average value is used for each polymer studied the order of thermochromic response (lowest response to highest response) is; PF.Li⊂β-CD, PDV.Li⊂β-CD, PF.Me⊂β-CD.Si, PPP.Li⊂β-CD, PPP.Li, F8 PDV.Li, and PDPV.

5.3. Discussion

The conjugated polyelectrolytes exhibit relatively lower thermochromic responses in both the analogue polymer and the polyrotaxane forms. This was not expected: the thermochromic response of the PDV.Li was expected to be akin to that of the PPV in the photoluminescence measurements but it is a fifth of the value of the PPV. Upon addition of the CD the thermochromic response further reduces by two-thirds. This implies that the addition of CD to the polymer is not its defining quality for thermochromic behaviour. This is also confirmed by two different conjugated polyelectrolytes (PF.Li and PDV.Li) having very low thermochromic responses.

The use of ionic side groups in the main chain dramatically alters the behaviour of PDV compared to PPV. The reduction of the thermochromism could be explained by either sterically driven structural changes caused by the addition of a counter-cation group which reduces the twist angle of each unit, thus preventing large changes in the effective conjugation length and that by further adding the CD it increases the inhibition of the twist angle, further reducing the thermchromism in the material.

However it could be that the electronic structure of the conjugated polyelectrolytes is more stable than that of the more common conjugated polymers. The exciton may be somewhat localised already thus upon temperature increase the additional localisation is not as effective as for PPV. The addition of the CD further localises the exciton that is formed, as shown by the increase in PL efficiency, forcing it to remain on a smaller segment.

The rigidity of each polymer would contribute to its thermochromic response. It would be expected that a rigid polymer would be less thermochromic than a more conformationaly free polymer. The sulfonate group in the PDV-polymers is larger than the carbonate group for the PF- and PPP-polymers so that hinders rotation more (and

thus disruption of the electronic structure). The PF-polymers have a carbonate side-group that is bonded in such a way to prevent rotation around the bonds. However data seems to suggest the contrary which again lies in agreement with Bässler and Schweitzer's idea of molecular relaxation also being important if the main chain is varied significantly. This is the case for PF.Li and PDV.Li as the PF chain is far more rigid, thus the rotational freedom at room temperature in PF-based polyelectrolytes is less than that of the PDV-based polyelectrolytes.

The peak shifts of the conjugated polyelectrolytes in Figure 5-3 exhibit no discernible peak shift until T= 150K and PDV.Li is the most responsive material. The increase in temperature leads to easier segmental motion of the polymer main chain and thus disruption of the effective conjugation length. Hence this effect is lessened in the polyrotaxanes due to the CD causing separation of the strands. The CD inhibits the segmental motion of the polymer.

The solution absorption spectra show the same thermochromic relationships, with the polyrotaxane having a lower thermochromic response. The aggregation of the PDV.Li in solution is also shown by the spectrum's FWHM slightly increasing with temperature whilst the FWHM of the polyrotaxane decreases slightly, though the absorption maximum for both does blue-shift. This decrease in the FHWM of the polyrotaxane spectra can be attributed to lack of self-organisation between the polyrotaxanes and the slight increase in torsional modes of freedom along the chain reducing the effective conjugation length. Here unlike films, torsional modes of freedom will be important as the polyelectrolyte is more mobile as it is suspended in a solution. The thermochromic response of the PPP.Li and the PPP.Li⊂β-CD are quite similar, suggesting that either the addition of the CD does not further localise excitons. This could be because the PPP bond rotations remain energetically similar with or

without the CD, or because the PPP.Li and PPP.Li⊂β-CD self-organise, inhibiting[11] the thermochromic effect.

5.4. Conclusions

The design of the polymer backbone dictates the energy transfer processes in the polymer films with the different side-groups allowing fine tuning of the emission or absorption properties of the film.

The work already undertaken implies that the structure of the polymer backbone is enough to restrict conformational changes which can cause spectral shifts when subjected to varying temperatures. The presence of CD further hinders thermochromism but it does not decrease thermochromism by a large amount compared to the thermochromism in the analogue polymer. The ionic side-groups and polymer backbone contribute most to this quality of the polymers by stabilising the electronic structure of the polyelectrolytes.

5.5. References

[1] D. D.-K. Yang, *Fundamentals of liquid crystal devices*, John Wiley, Chichester **2006**.

[2] J. Cornil, D. Beljonne, Z. Shuai, T. W. Hagler, I. Campbell, D. D. C. Bradley, J. L. Bredas, C. W. Spangler, K. Mullen, *Chemical Physics Letters* **1995**, *247*, 425.

[3] K. Pichler, D. A. Halliday, D. D. C. Bradley, P. L. Burn, R. H. Friend, A. B. Holmes, *Journal Of Physics-Condensed Matter* **1993**, *5*, 7155.

[4] F. Raymond, N. Di Cesare, M. Belletete, G. Durocher, M. Leclerc, *Adv. Mater.* **1998**, *10*, 599.

[5] F. Kong, X. L. Wu, G. S. Huang, R. K. Yuan, C. Z. Yang, P. K. Chu, G. G. Siu, *Appl. Phys. A-Mater. Sci. Process.* **2006**, *84*, 203.

[6] J. L. Bredas, G. B. Street, B. Themans, J. M. Andre, *J. Chem. Phys.* **1985**, *83*, 1323.

[7] H. Bassler, B. Schweitzer, *Accounts Chem. Res.* **1999**, *32*, 173.

[8] S. Guha, J. D. Rice, Y. T. Yau, C. M. Martin, M. Chandrasekhar, H. R. Chandrasekhar, R. Guentner, P. S. d. Freitas, U. Scherf, *Physical Review B (Condensed Matter and Materials Physics)* **2003**, *67*, 125204.

[9] F. Cacialli, J. S. Wilson, J. J. Michels, C. Daniel, C. Silva, R. H. Friend, N. Severin, P. Samori, J. P. Rabe, M. J. O'Connell, P. N. Taylor, H. L. Anderson, *Nature Materials* **2002**, *1*, 160.

[10] G. Latini, A. Downes, O. Fenwick, A. Ambrosio, M. Allegrini, C. Daniel, C. Silva, P. G. Gucciardi, S. Patane, R. Daik, W. J. Feast, F. Cacialli, *Applied Physics Letters* **2005**, *86*, 011102.

[11] P. Baum, W. H. Meyer, G. Wegner, *Polymer* **2000**, *41*, 965.

Chapter 6. Use in OLEDs

The use of polyrotaxanes in light-emitting devices (LEDs) has already been investigated and it was found that the operating efficiencies were higher in the polyrotaxane when compared to its analogue polymer. Here further studies into the behaviour of polyrotaxanes and their analogue polymers are made. The polyelectrolytic nature of these materials modifies their behaviour; light emission is aided by the presence of ions in the material. These devices are typically known as Light emitting electrochemical cells (LECs). The LEC-like nature of the polymers is explored in this chapter.

As well as substitution of the counter-cation, variation of the threading of the PDV repeat unit has also been conducted. Materials of threading ratios 1.3 and 2.3 β-CD per repeat unit have been provided. The effect on current densities and light emission due to the increased insulation will be presented.

6.1. Experimental Details

The procedure detailed here has been followed for all devices unless stated in the text. To fabricate OLEDs, 2%b.w. filtered solutions were spun onto pre-etched, oxygen-plasma-treated ITO substrates[1] to produce ~100nm thick films. The films were annealed and covered with thermally evaporated Al electrodes (~ 100 nm thickness) or LiF (~5nm) with a capping layer of Al (~150nm). Electroluminescent properties of the devices were characterised by measuring the current and light emission against voltage characteristics. These measurements have been carried out in a chamber at ~10^{-2} mbar after being transferred to the chamber under nitrogen.

A source meter (Keithley 2400) source was used to drive the devices and measure current flowing through the device. The luminous output was measured with a calibrated silicon photodiode.

6.2. LEC behaviour

6.2.1. Introduction

LEDs and LECs have the same basic structure but the LEC has mobile ions within the polymer film that alter the properties of the cell, most noticeably lowering the threshold for charge injection. This is possible because, unlike LEDs which normally have a single luminescent polymer, LECs are made from blends of luminescent polymers with ionic materials.

LECs were first reported in 1995 by Pei *et al*[2] and since then two competing models have been presented in the literature to explain the behaviour. Pei *et al*[2-6] developed a model which considers charge injection to occur in LECs through electrochemical reduction and oxidation of the conjugated film; whilst in LEDs charge injection is via interfacial barrier tunnelling. A schematic of the process is shown in Figure 6-1. A typical LEC polymeric film would use poly(1,4-phenylenevinylene), PPV, as the luminescent polymer. A conjugated ionic polyelectrolyte; poly-(ethylene oxide), PEO, which is complexed with a lithium salt is then mixed with the PPV before making the device. The PEO and Li-salt provide the mobile ions.

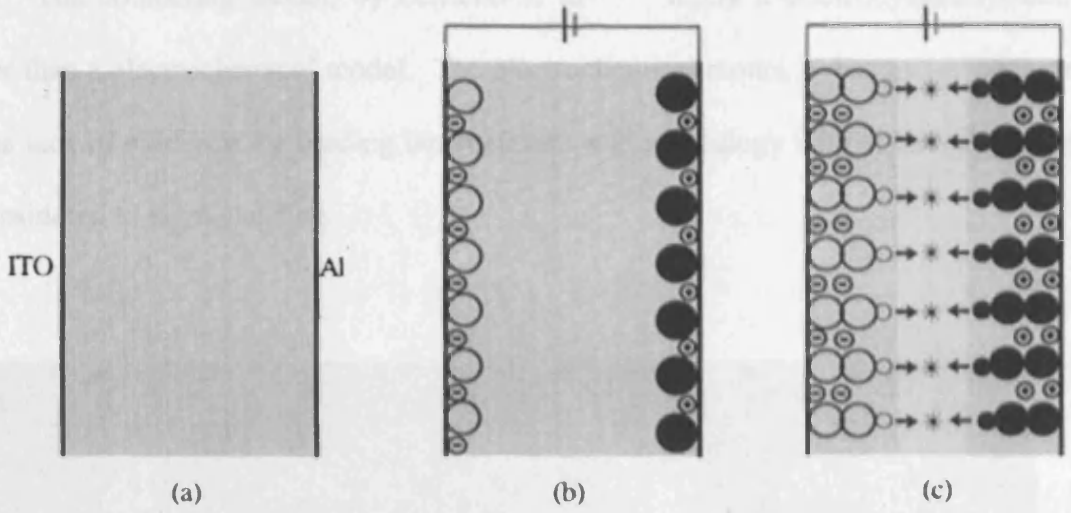

Figure 6-1 Schematic diagram of the electrochemical processes in a solid-state light-emitting electrochemical cell: (large open circle) an oxidized molecule, (large closed circle) a reduced molecule, (circled minus) an anion, (circled plus) a cation, (small open circle) a hole, (small closed circle) an electron, (asterisk) a photon. Taken from Pei[7].

When a sufficiently high bias is applied to the device, charge is injected in to the polymer film. If ITO is the anode and Al the cathode as in Figure 6-1b), the polymer film near the cathode is reduced and the polymer near the anode is oxidised. This charge imbalance causes redistribution of the ionic charge carriers (from the electrolytes) to compensate the charges on the reduced and oxidised polymer film. This doping is symmetrical (for every *p*-doped chain at the anode, a *n*-doped chain is also produced at the cathode) if the Fermi levels of the electrodes and the HOMO/LUMO levels of the polymer are aligned. This is achieved by applying a bias larger than the band gap of the polymer. An *in-situ p-n* junction is formed deep in the polymer film. The *p*-type and *n*-type carriers recombine radiatively in the junction, shown in Figure 6-1c) and decay by emitting a photon as for LEDs. In such a model the electric field is assumed to be high where, due to the doping, a *p-n* junction has formed and to be low in the rest of the device.

The competing model, by deMello *et al*[8, 9] offers a electrodynamic model rather than a electrochemical model. The electrochemical model is discounted because of the lack of evidence for binding between ions and an analogy with chemical doping is considered to be misleading.

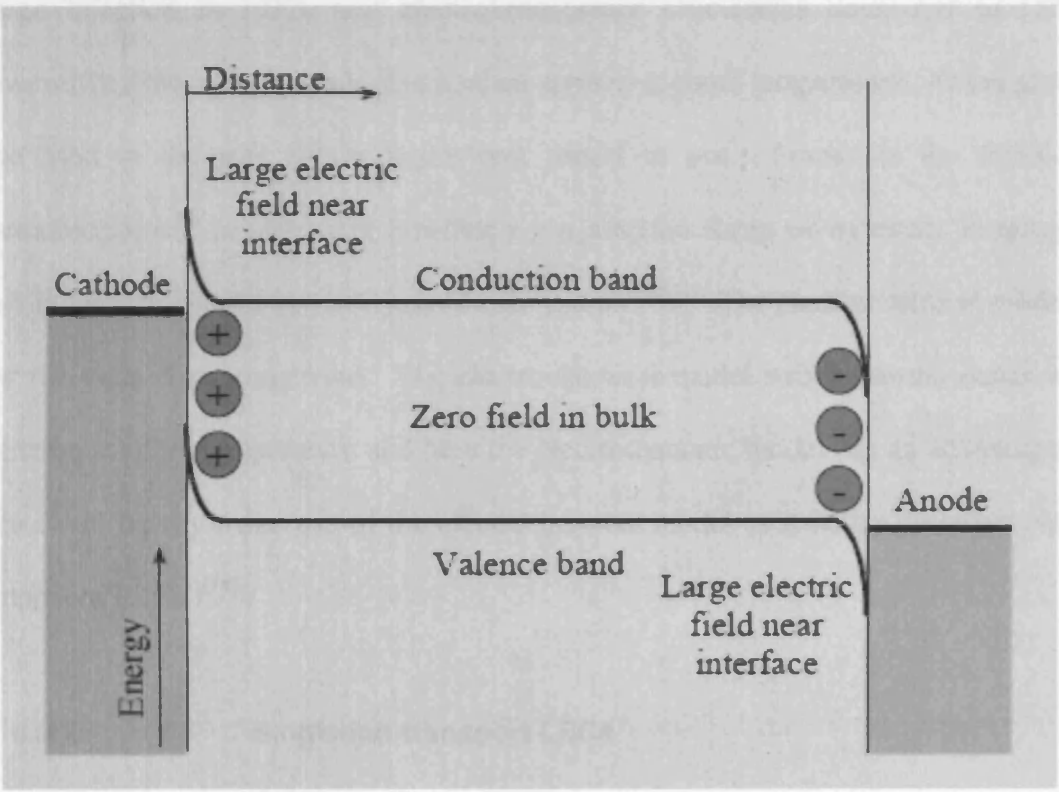

Figure 6-2 Schematic of the band gap diagram for a LEC operating in forward bias in the electrodynamic model. The electric field is redistributed away from the bulk of the film due to ionic space charge accumulation at the electrodes. Taken from [8].

Charge injection occurs via tunnelling, as for LEDs. In this model the luminescent conjugated polymer and electrolytes form a matrix in which both the ionic and electronic charge-carriers are mobile. Once an external field is applied the anions drift towards the positive electrode and the cations to the negative electrode. The density of ions in a LEC is high ($>10^{20}$ cm^{-3}) so small movements of the ions lead to a high electric field. Under constant bias the ionic redistribution continues until the local electric field is zero. A finite electric field is present at the electrodes due to the ionic

motion being blocked by the electrode itself. The band gap diagram of this model is presented in Figure 6-2. This results in a lower barrier to charge injection and then electrons and holes, via diffusion, can recombine within the film and radiatively decay.

Both models allow for the LEC to work in reverse and forward bias (unlike LEDs which emit light only in the forward bias). Pei *et al* and also account for the better charge injection in LECs and electroluminescent efficiencies compared to LEDs. However this theory often falls down when applied at room temperature. Other groups have tried to discover which is the best model to use. Some via the means of electoabsoprtion[4] to determine whether a *p-n* junction forms or by direct imaging of the LEC and discovery of a *p-n* junction formation.[10-12] The electrochemical model is now the more commonly used. The electrochemical model still has some issues with operation at room temperature and here the electrodynamic model has an advantage.[13] Here I will mostly make use of the electrochemical model as it better describes single component LECs .[14]

6.2.2. Single-ion transport LECs

Single-ion transport (or single component) LECs have either mobile anions or cations unlike conventional LECS which use a emissive polymer, polyelectrolyte and a salt. These have advantages over the ternary LECS as they tend to phase segregate over time. This can be due to the mixing of the apolar emissive polymer with the polar electrolytes and results in operational instabilities and slow time responses. As only one ion is mobile in single-ion transport LECs charge will preferentially build at one of the electrodes. This causes a high electric field at that electrode, reducing the charge injection barrier at there.

Single-ion transport LECs have been previously documented by either using a more compatible blend of an emissive polymer and a polyelectrolyte or by the synthesis of conjugated polyelectrolytes which can act as the ion provider and light emitter.

The use of conjugated polyelectrolytes circumvents the phase segregation issue by removing the need for another polymer in the device. This method has been used since 1996 but there are few examples of this type of device.[15-19] By employing single-ion transport it has been shown to quicken time response and to improve lifetimes of the cells.[17]

6.2.3. Conjugated polyelectrolytes as single-ion transport LECs

Previous measurements showed that when these conjugated polyelectrolytes are combined with another polyelectrolyte (PEO) they are able to emit light both in the forward and reverse bias, also that the addition of PEO increased external quantum efficiencies (EQE).[20] This behaviour makes use of the mobile ion transport of the PEO and mobile cations of the analogue polymer/polyrotaxanes. The device is thus behaving as a LEC. The phase segregation in PDV.Li and PDV.Li⊂β-CD has been shown to be minimal as the PEO wraps around the conjugated polyelectrolyte[20] due to its strong affinity with Li. The ether oxygen groups of the PEO complex with the lithium cation.

All of the polyrotaxanes and analogue polymers exhibit this LEC-behaviour without addition of PEO acting as single-ion transport LECs. The cation is mobile so once a forward/reverse bias is applied the cations collect near the cathode, lowering the barrier to electron injection This charge reduction also occurs at the anode as , by the absence of the counter-cation, the polymer has become anodic. The ion build-up involving the polymer will be slower and most probably a larger barrier to hole injection (in the forward bias) will remain.

Asymmetry of light emission and current density with applied voltage is seen for all PDV.M and PDV.M⊂β-CD single-ion transport devices. This asymmetry may be seen in Figure 6-3, and is most apparent for the light emission in all polymers tested. The polymers tend to have lower turn-on voltages (weaker light emission) in the forward bias which follows from the difficulties in migration of the anodic polymer chain to the electrode acting as the anode in reverse bias leading to a mismatch in electron/hole injection.

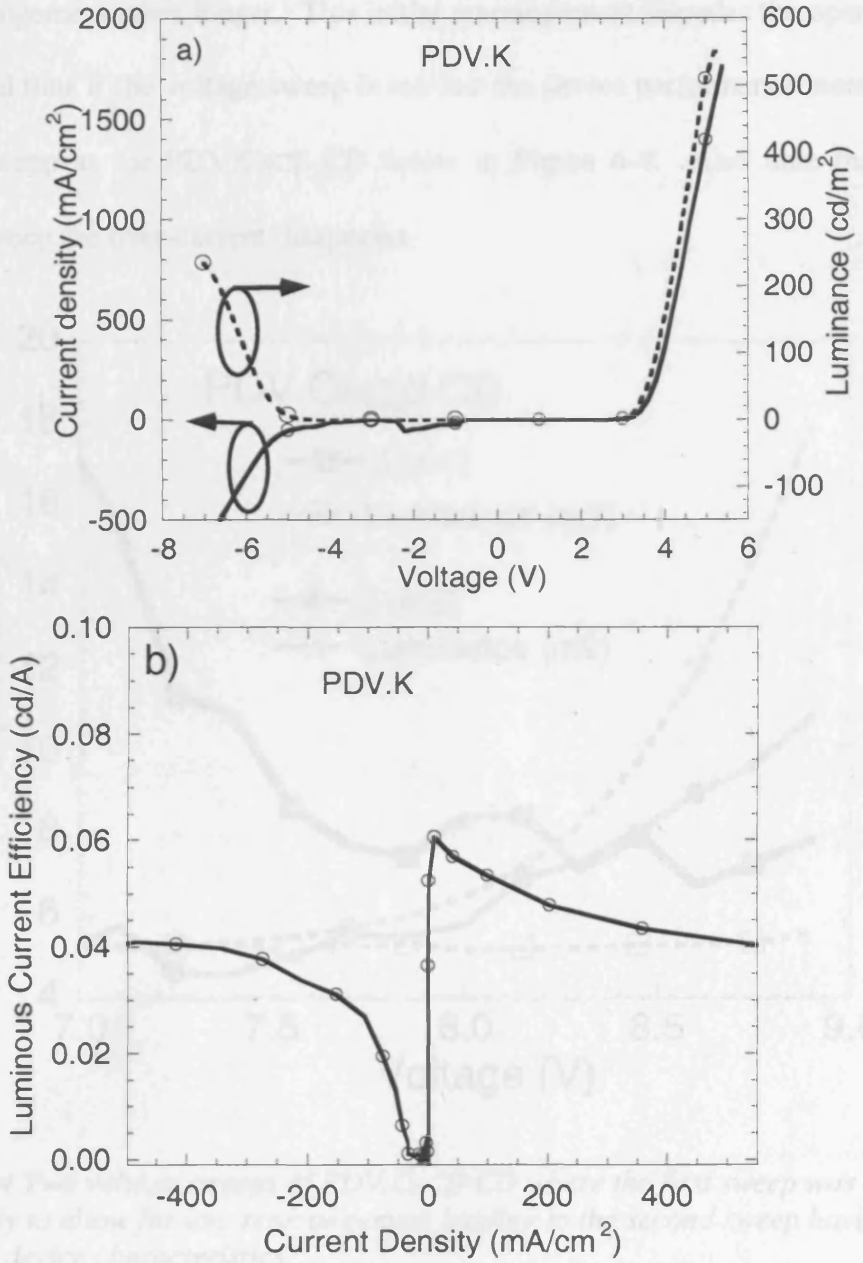

Figure 6-3 Typical asymmetric LEC-like behaviour of PDV.K made from ITO/polymer/Al is shown in a). The luminance is lower under reverse bias leading to the lower efficiency seen in b). These are taken from two different devices and are the first measurement.

The current in these devices has an ionic and electronic component. However, only the electronic component contributes to the luminance. Hence if ionic rearrangement is slow the device efficiency will decrease as most of the current contribution will be from the ionic part.[21] In most cases the device performance is optimal in the first sweep however for the larger ions, the ion mobility is low and thus

the rearrangement takes longer. This initial rearrangement impedes the operation of the device and thus if the voltage sweep is too fast the device performance increases on the second sweep as for PDV.Cs⊂β-CD below in Figure 6-4. Also note that upon the second sweep the over-current disappears.

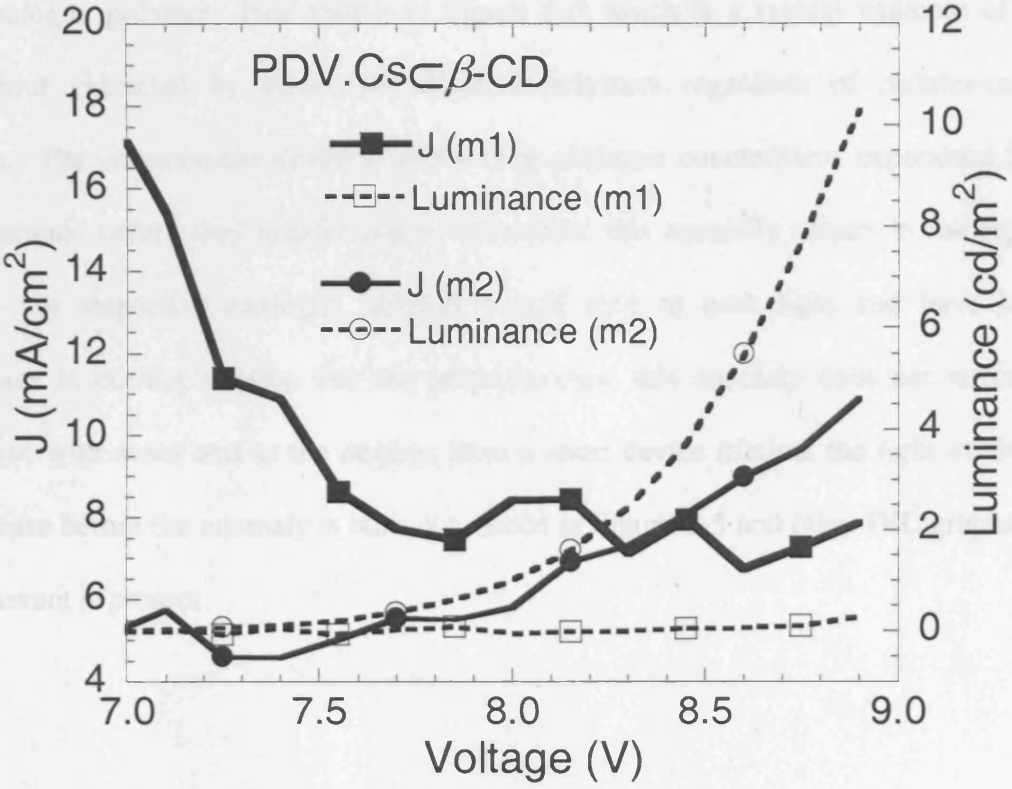

Figure 6-4 Two voltage sweeps of PDV.Cs⊂β-CD where the first sweep was conducted too quickly to allow for ion rearrangement leading to the second sweep having improved device characteristics.

The ionic rearrangement time is highly dependent ion size. Thus the PDV.K@[2.2.2] devices would tend to operate better on a second or third sweep even if the sweep had been conducted slowly. All the PDV.M and PDV.M⊂β-CD devices are capable of light emission in forward and reverse bias, however K@[2.2.2] devices are poor in both forward and reverse bias.

6.3. Differences in device performace

6.3.1. Analogue polymer vs. polyrotaxane

The insulation of the polymer leads to reduced current densities and light emission coupled with a light emission which commences at higher voltages than for the analogue polymer. This shown in Figure 6-5 which is a typical example of the behaviour exhibited by these two different polymers regardless of counter-cation choice. The polyrotaxane devices, unlike their analogue counterparts, experience high overcurrents before they exhibit diodic behaviour: this normally occurs in the region where the respective analogue polymer would start to emit light and have large increases in current density. For the polyrotaxanes, this anomaly does not normally decrease with scans and as the devices have a short device lifetime the light emission will cease before the anomaly is burn out, hence in Figure 6-5 and other IVL graphs the overcurrent is present.

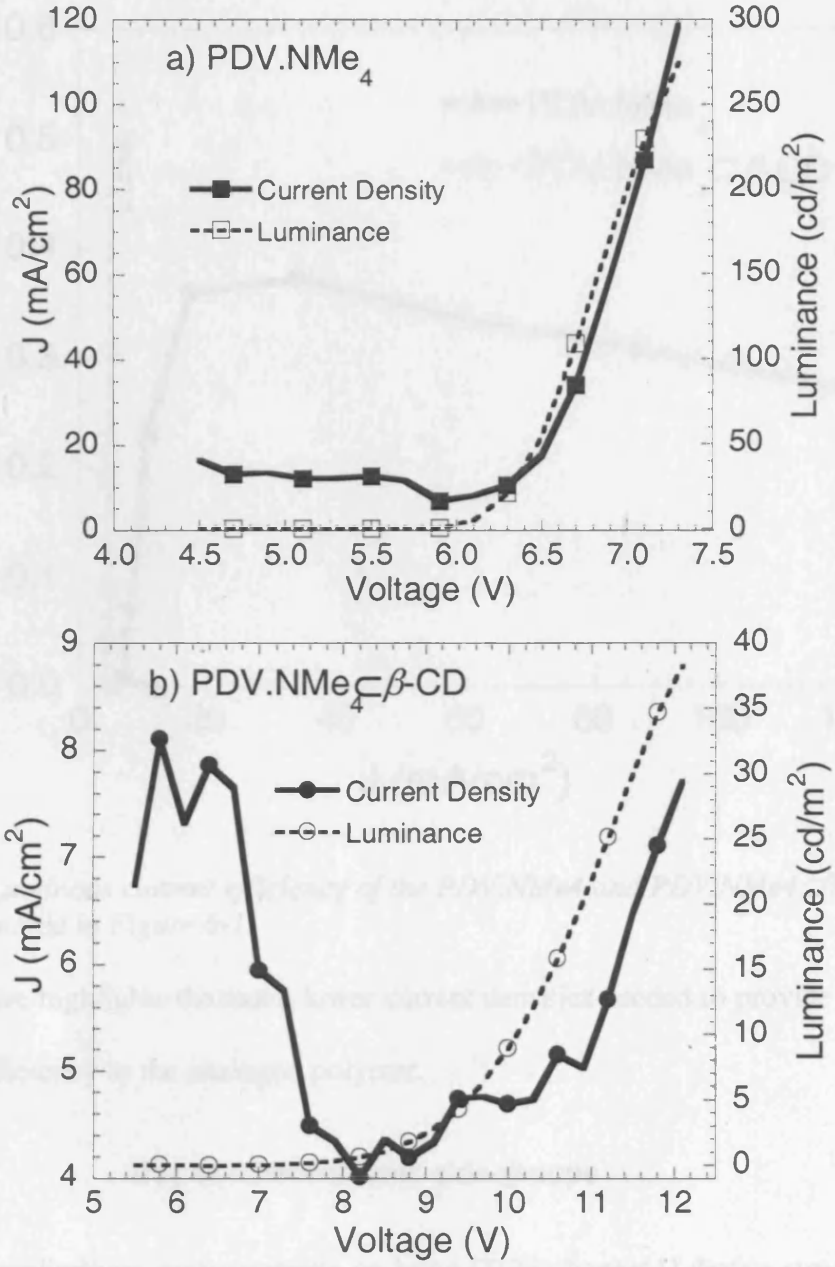

Figure 6-5 Typical current density and luminance Vs voltage graphs for a)PDV.NMe4 and b)PDV.NM4⊂β-CD. Current density and luminance is lower in the polyrotaxane compared to the analogue polymer and light emission starts at higher voltages due to the CD sheath.

Luminous current efficiencies verify that CD threading is beneficial for use of these molecular wires in light-emitting devices as the CD-threaded polyelectrolytes have higher efficiencies as shown in Figure 6-6 taken from the TMA-polymers given in Figure 6-5.

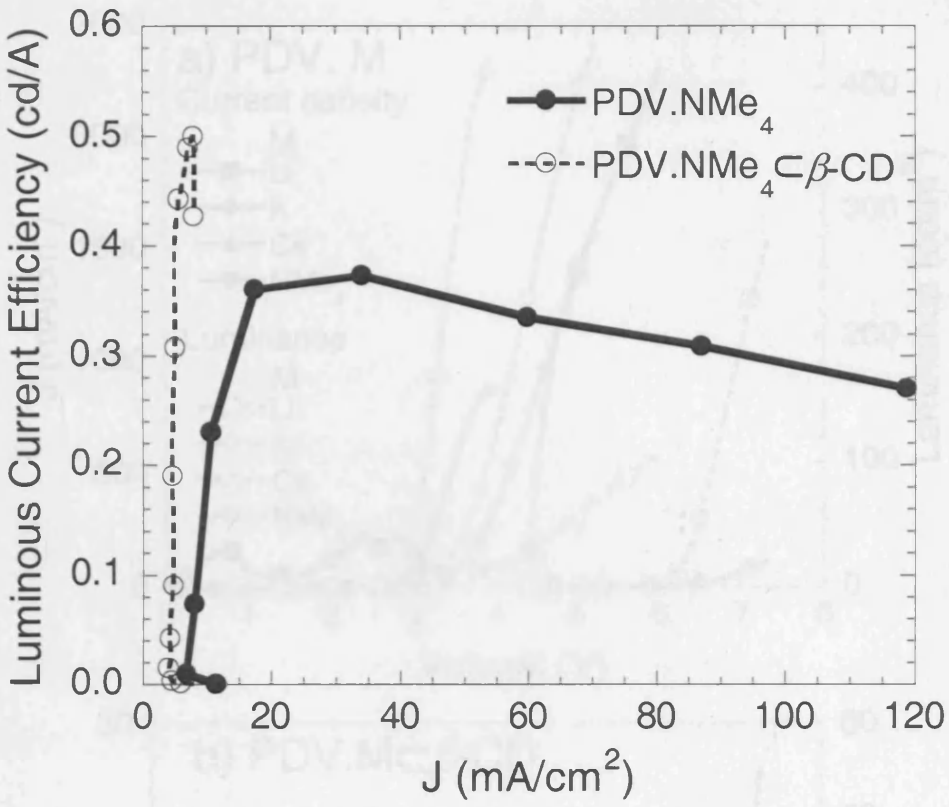

Figure 6-6 Luminous current efficiency of the PDV.NMe4 and PDV.NMe4⊂β-CD devices presented in Figure 6-1.

This figure highlights the much lower current densities needed to provide a similar operating efficiency to the analogue polymer.

6.3.2. Use of different ionic side-groups

The preliminary measurements on basic ITO/polymer/Al device structures have been followed by testing of the PDV.M and PDV.M⊂β-CD. The counter-cations are exchanged for Li and ionically bond with the SO_3^- that is tethered to the main chain. All PDV.M and PDV.M⊂β-CD devices whether with Al or LiF/Al cathodes are capable of light emission. Example graphs of J-V-L characteristics are presented in Figure 6-7a) of the analogue polymers and in Figure 6-3b) for the polyrotaxanes. The polyrotaxanes in Figure 6-7b) have threading ratios of 1.3 apart from PDV.K⊂β-CD and PDV.K@[2.2.2]⊂β-CD which have threading ratios of 2.3 per PDV repeat unit.

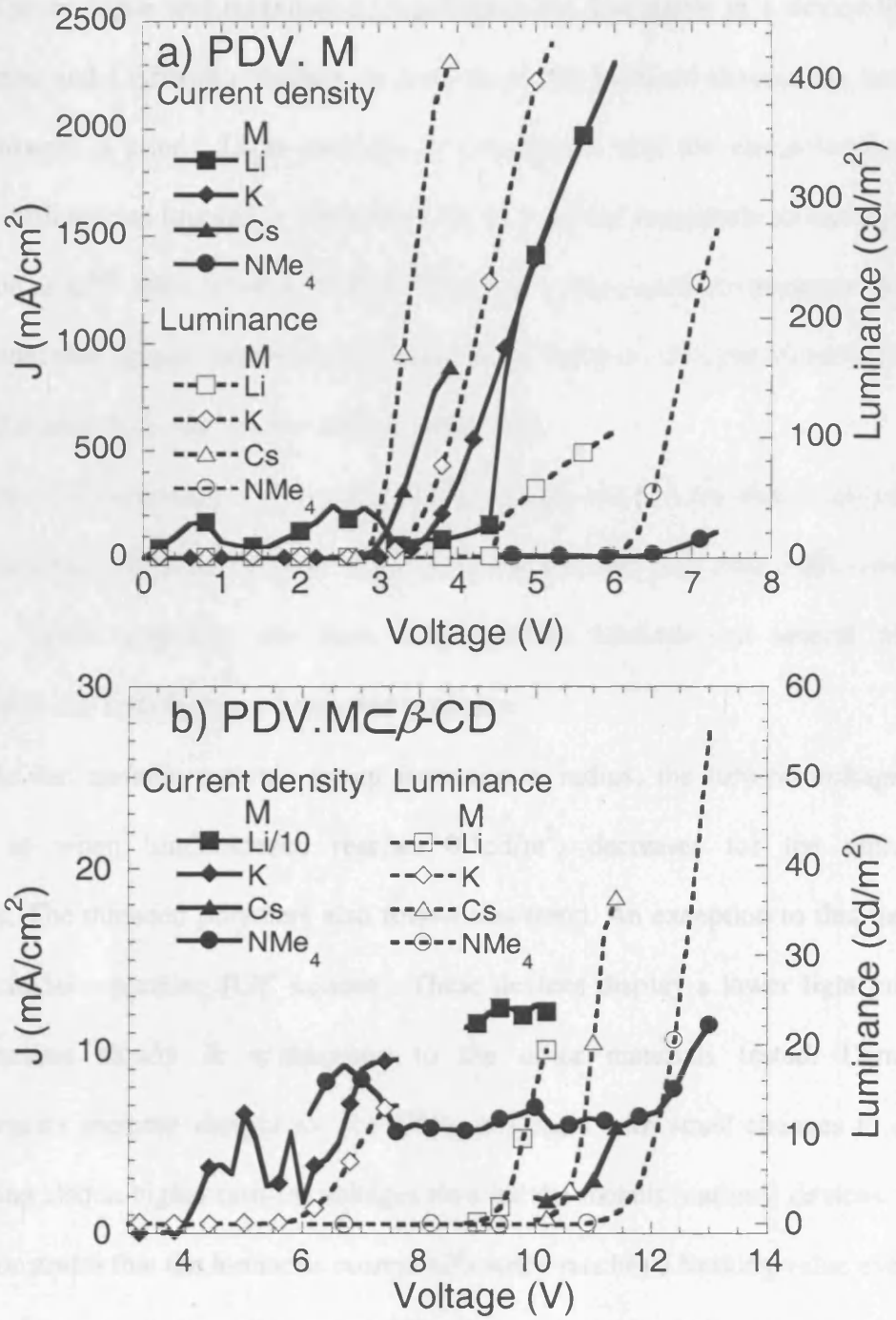

Figure 6-7 The IVL characteristics of the unthreaded polymers with different ionic groups, a) PDV.M curves and b)PDV.M⊂β-CD.

PDV.K@[2.2.2] and PDV.K@[2.2.2]⊂β-CD are not depicted in Figure 6-7 as whilst these devices exhibit light emission it was very poor and intermittent, especially so in the case of the polyrotaxane.

The analogue and rotaxinated Li-polymers are less stable in a device than the TMA-based and Cs-based polymers, as currents in the Li-based devices are noisy and light emission is poor. Light emission is comparable and the electroluminescence quantum efficiencies (quoted in Table 6-1) are of a similar magnitude to those reported by Wilson *et al*[20] after 10%b.w of PEO has been blended with the analogue polymer. Larger ionic side-groups have so far produced more stable devices than small ionic side-groups (Li) apart from the counter-cation K@[2.2.2].

Devices made from TMA- and Cs-polymers are more stable than Li-polymers as the devices can withstand several repeat IVL sweeps and will emit light over these sweeps. These polymers also have longer device lifetimes, of several minutes, compared to the Li-polymers of less than a minute.

As the metallic cationic group increases in radius, the turn-on voltage (here defined as when luminescence reaches $0.1cd/m^2$) decreases for the unthreaded polymers. The threaded polymers also follow this trend. An exception to this trend are the devices incorporating $[Li]^+$ cations . These devices display a lower light emission that increases slowly in comparison to the other materials tested. Luminance characteristics increase sharply for the NMe_4 polymers with small changes in current density and also at higher turn-on voltages than for the metallic cationic devices. Figure 6-4 demonstrates that the luminous current efficiency reaches a limiting value even with increases in cation radius. The K@[2.2.2] devices had low light emission and high current densities, data is presented in Table 6-1 and Figure 6-8, leading them to being the least efficient devices.

The threaded polymers had higher luminous current efficiencies compared with their unthreaded counterparts but the increase in efficiency lessens with increasing cationic group size, as shown in the insert to Figure 6-8. The increase from Cs to NMe_4 is minimal when compared to increase in size.

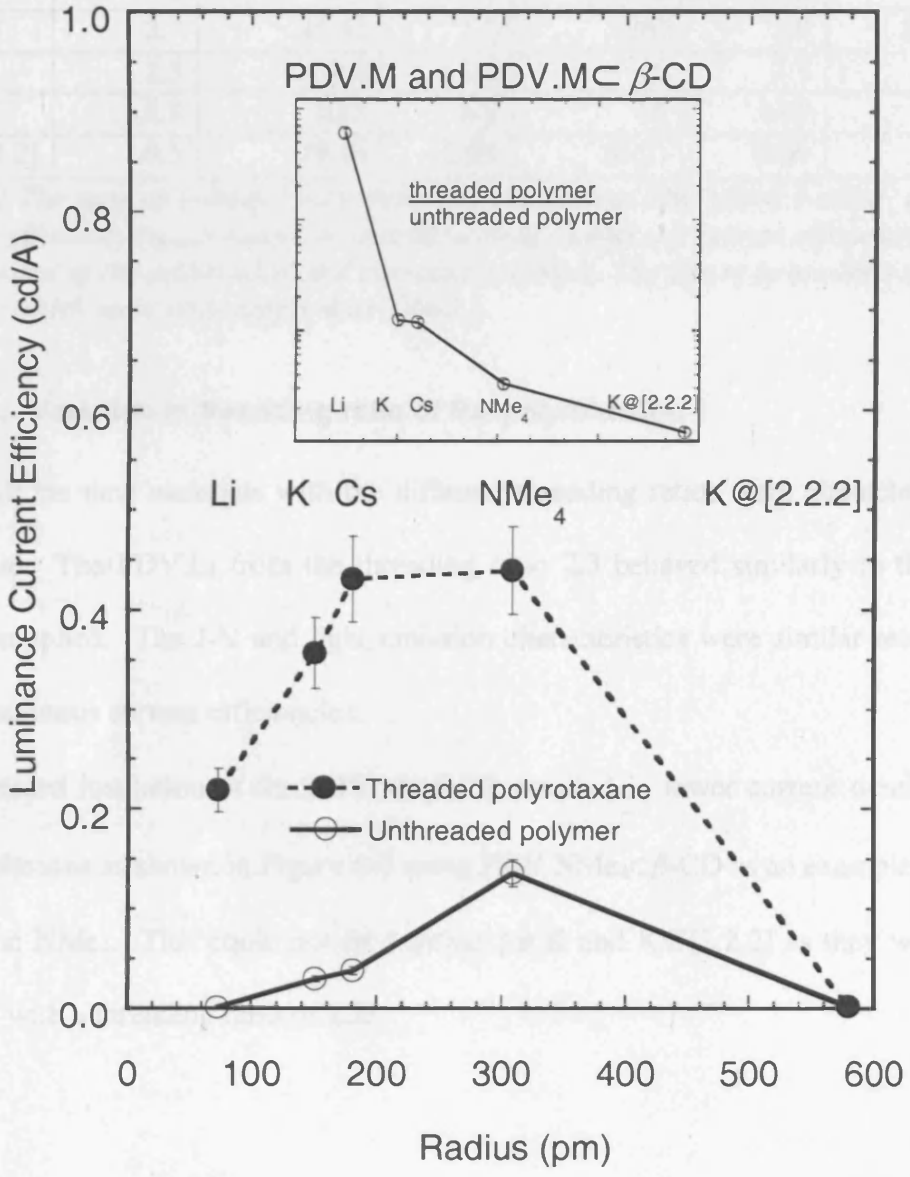

Figure 6-8 The average luminous current efficiency in cd/A as a function of the ionic (Li^+, K^+ and Cs^+) and Van der Waals (NMe_4^+ and $K@[2.2.2]^+$) radius of the unthreaded and threaded polymers over many devices is reported. In all cases in forward bias, the polyrotaxane exhibits higher efficiencies, however as the cationic group becomes larger the increase in efficiency decreases as shown in the insert.

M	V_{on} (V) at L=0.1cd/m^2		η_{max} (10^{-2} %)		Average Luminous Current Efficiency (10^{-2}cd/A)	
	PDV.M	PDV.M ⊂β-CD (TR=1.3)	PDV.M	PDV.M ⊂β-CD (TR=1.3)	PDV.M	PDV.M ⊂β-CD (TR=1.3)
Li	4.1	8.4	0.04	2.2	0.03	21.8
K	2.7	(5.6)	1.0	(26)	2.9	(35.6)
Cs	2.5	9.4	1.5	28	3.7	43.0
NMe_4	5.8	10.8	6.0	28	13.5	43.9
K@[2.2.2]	6.5	(8.9)	0.09	(0.2)	0.09	(0.1)

Table 6-1 The turn-on voltage (Von) defined as the bias at which L=0.1 cd/m^2, external quantum efficiency (η_{max}) maximum and the average luminous current efficiency over many devices of the unthreaded and threaded polymers. The figure in brackets are for polymers which were only supplied as TR=2.3.

6.3.3. Variation in threading ratio of the polyrotaxane

All the new materials with the different threading ratios were characterised for device use. The PDV.Li from the threading ratio 2.3 behaved similarly to the initial PDV.Li supplied. The J-V and light emission characteristics were similar resulting in similar luminous current efficiencies.

The increased insulation of the PDV.M⊂β-CD resulted in lower current densities and lower emissions as shown in Figure 6-9 using PDV.NMe_4⊂β-CD as an example for M = Li, Cs and NMe_4. This could not be verified for K and K@[2.2.2] as they were only available with a threading ratio of 2.3.

M	V_{on} (V) at L=0.1cd/m^2		η_{max} (10^{-2} %)		Average Luminous Current Efficiency (10^{-2}cd/A)	
	PDV.M ⊂β-CD (TR=1.3)	PDV.M ⊂β-CD (TR=2.3)	PDV.M ⊂β-CD (TR=1.3)	PDV.M ⊂β-CD (TR=2.3)	PDV.M ⊂β-CD (TR=1.3)	PDV.M ⊂β-CD (TR=2.3)
Li	8.4	8.2	2.2	2.2	21.8	2.9
K	-	5.6	-	26	-	35.6
Cs	9.4	4.6	28	0.4	43.0	0.5
NMe_4	10.8	9.4	28	20	43.9	9.5
K@[2.2.2]	-	8.9	-	0.2	-	0.1

Table 6-2 The turn-on voltage (V_{on}) defined as the bias at which L=0.1cd/m^2 for a typical device, external quantum efficiency maximum (η_{max}) and the average luminous current efficiency over many devices of the polyrotaxanes with threading ratios of 1.3 or 2.3

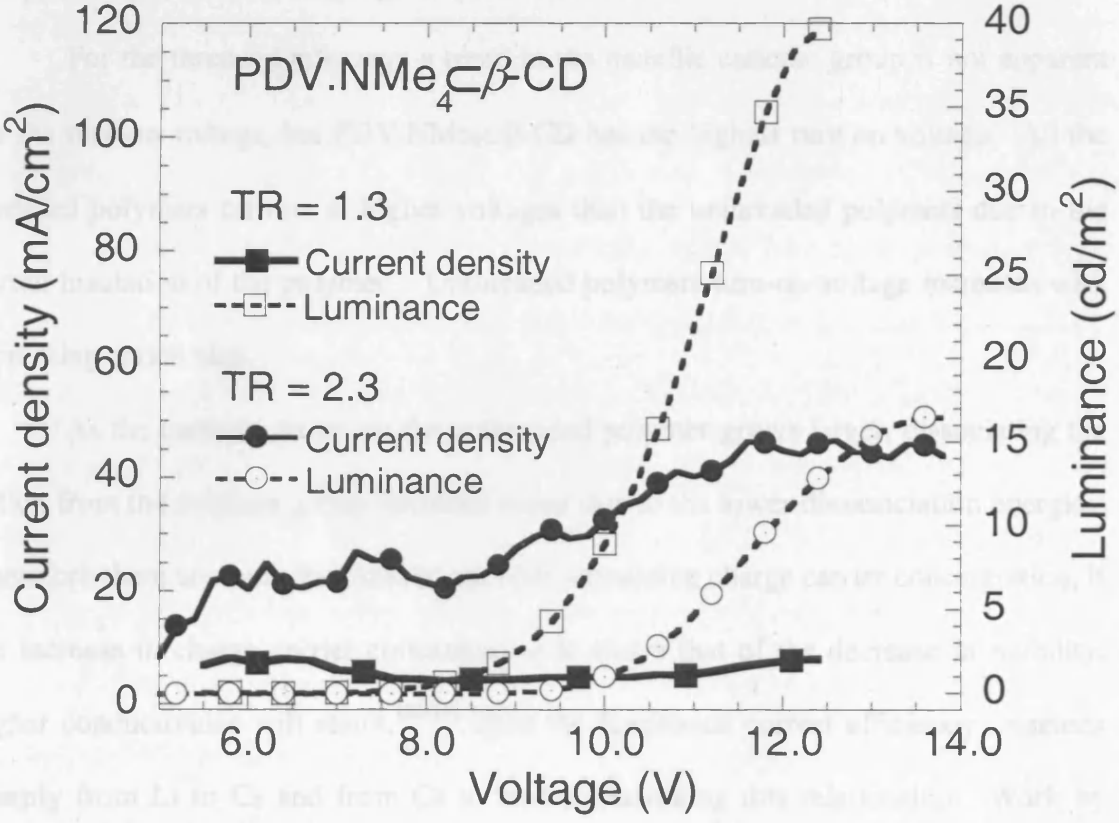

Figure 6-9 J-V-L graph of PDV.NMe_4⊂β-CD with threading ratios of 1.3 and 2.3 β-CD per PDV repeat unit.

6.4. Discussion

Improvements are seen in the electroluminescent characteristics through the tailoring of the side group of the unthreaded and threaded polymers. As the cation radius increases, luminous current efficiency also increases as documented in Table 6-1 and the non-metallic cationic group, NMe_4, has the largest luminous current efficiency overall for both the unthreaded and threaded polymers. The K@[2.2.2]-based polymers performed poorly as devices, perhaps due to limited opportunities for charge hopping due to the larger interchain distances or due to immobility of the cation. This was disappointing as they had the highest PL efficiencies.

For the threaded polymers a trend in the metallic cationic group is not apparent for the turn-on voltage, but PDV.NMe_4⊂β-CD has the highest turn on voltage. All the threaded polymers turn on at higher voltages than the unthreaded polymers due to the partial insulation of the polymer. Unthreaded polymers turn-on voltage increases with increasing cation size.

As the cationic group on the unthreaded polymer grows larger, dissociating the cation from the sulphate group becomes easier due to the lower disassociation energies. Therefore there are more free ions in the film, increasing charge carrier concentration, if the increase in charge carrier concentration is above that of the decrease in mobility, higher conductivities will result.[22-24] Here the luminance current efficiency increases sharply from Li to Cs and from Cs to NMe_4, illustrating this relationship. Work by Yang *et al*[25, 26]into exchange of counter ionic groups and the effect on the optoelectronic properties of the polymer also concludes that the size of the counter ion alters these properties. Indeed Hu *et al*[27] document that the formation and position of the *p-n* junction is highly dependent on the cation mass and mobility. Thus as the

junction is the emission zone this can lead to highly different device performance with monovalent cations which only differ in size.

K and Cs have similar radii values and so have similar efficiency values. NMe_4 hydrates poorly, it is approximately 6 times the bare radius of the Li and 3 times that of the Cs. The unthreaded luminous efficiency of the NMe_4 materials is also approximately 3 times that of the unthreaded Cs. The luminous current efficiency of the unthreaded polymers increases linearly with radius. Again this illustrates the importance of the counter-cation group.

The unthreaded polymers are useful to understand the effect of the ion and its interaction with the cyclodextrin. The β-CD is 750pm in radius, twice that of the bare radius of the NMe_4. Thus this cation will be more enclosed than the metallic cations which are 1/7 or less of the CD radius. Hence the luminance current efficiency of the threaded polymers increases linearly with metallic cation radius but stabilises with change of Cs to NMe_4. This implies that there may be a limiting radius for the cation when coupled with the CD for boosting operating efficiencies. This could be the cause for the high PL efficiency of K@[2.2.2]-substituted polymers in comparison to the other polymers studied here, whilst the EL characteristics are poor. Due to K@[2.2.2]'s size the charge mobility is low in these devices, leading to poor device characteristics. The effect of ever increasing side-groups on the EL efficency has been documented previously[28, 29]. It was found that as the side-group increased in size the EL efficiency also increased until it reached a maximum and then started to decrease. This was attributed to the large side-groups overpowering and diluting the semi-conductor properties of the material.

It is of note that the non-metallic cationic group, NMe_4, devices had longer device lifetimes than the metallic devices apart from K-based devices. This suggests

that the charge transport and ionic dissociation in this non-metallic cation is more suited for devices. The metallic ions may have undergone further redox reactions in the film or at the electrodes, removing potential charge carriers.

Previous work[30] has documented how the reduced interchain interactions caused through threading led to an increased efficiency and higher turn-on voltages as seen in Table 6-1. . In the threaded polymers the presence of the CD hinders the mobility of the larger cations as the luminous current efficiency doesn't increase as sharply for the threaded polymers as for the unthreaded polymers. This is highlighted by the decreasing ratio of threaded polymer luminous current efficiency to unthreaded efficiency, inserted in Figure 6-8.

The luminous current efficiency (cd/A) values for NMe_4 and Cs devices with TR=2.3 are smaller than the TR=1.3 values whereas for the Li-substituted devices the efficiencies are comparable. This could be attributed to the fact that the double threading affects the electroluminescent properties of the polymers with large ion side-groups more than those with small ion side-groups, such as Li, as the cations are more "frozen" in position. This follows from discussion of the CD radius and ionic radii used.

We have previously demonstrated the ability of PDV.Li and PDV.Li⊂β-CD to behave as LEC-like devices with the addition of PEO.[20] The addition of PEO reduces the electron-injection barrier thus enhancing the luminous current efficiency. It is to be expected that the ions are not very mobile as they are part of the polymeric matrix but as Figure 6-3a) shows the devices are LEC-like without the addition of extra salt or PEO.

As the cationic group grows in size the ability for reverse bias emission increases, because the cations are more easily dissociated from the main chain. Asymmetry in turn on voltages is observed with the reverse bias needing larger voltages

for emission to occur, due to the unequal lowering of the charge injection barriers because of the low mobility of the anodic polymer. Luminous current efficiency is lower in the reverse bias as reported in Figure 6-3b), especially so for the threaded polymers due to the additional CD leading to the anionic polymer chain being more fixed in place than the analogue polymer.

The LEC-like behaviour of the materials probably led to the device instabilities at room temperature. If the LEC-like behaviour could be controlled, by knowing how long the ionic rearrangement takes for example, device lifetimes may be extended.

6.5. Conclusion

It has been demonstrated that by careful choice of the cation operating efficiencies and behaviours can be modified. The CD rings also improve device performance but, if the combination of partial insulation and cation is not given due consideration the device properties can be seriously hindered. The LEC-like behaviour determines the device performance and if the device is poorly operated it severely shortens the device lifetime and decreases the device efficiency.

6.6. References

[1] J. S. Kim, M. Granstrom, R. H. Friend, N. Johansson, W. R. Salaneck, R. Daik, W. J. Feast, F. Cacialli, *Journal of Applied Physics* **1998**, *84*, 6859.

[2] Q. B. Pei, G. Yu, C. Zhang, Y. Yang, A. J. Heeger, *Science* **1995**, *269*, 1086.

[3] Y. Cao, G. Yu, A. J. Heeger, C. Y. Yang, *Applied Physics Letters* **1996**, *68*, 3218.

[4] J. Gao, A. J. Heeger, I. H. Campbell, D. L. Smith, *Physical Review B* **1999**, *59*, R2482.

[5] Q. B. Pei, Y. Yang, G. Yu, C. Zhang, A. J. Heeger, *Journal of the American Chemical Society* **1996**, *118*, 3922.

[6] D. L. Smith, *Journal Of Applied Physics* **1997**, *81*, 2869.

[7] Q. B. Pei, Y. Yang, *Synthetic Metals* **1996**, *80*, 131.

[8] J. C. deMello, N. Tessler, S. C. Graham, R. H. Friend, *Physical Review B* **1998**, *57*, 12951.

[9] J. C. deMello, J. J. M. Halls, S. C. Graham, N. Tessler, R. H. Friend, *Phys. Rev. Lett.* **2000**, *85*, 421.

[10] J. Dane, C. Tracy, J. Gao, *Applied Physics Letters* **2005**, *86*.

[11] J. Gao, J. Dane, *Applied Physics Letters* **2004**, *84*, 2778.

[12] J. Gao, J. Dane, *Applied Physics Letters* **2003**, *83*, 3027.

[13] J. C. deMello, *Physical Review B* **2002**, *66*.

[14] S. X. L. E. J.-H. Shin, *Advanced Functional Materials* **2006**, *16*, 949.

[15] M. Anni, M. E. Caruso, S. Lattante, R. Cingolani, *J. Chem. Phys.* **2006**, *124*.

[16] L. Edman, B. Liu, M. Vehse, J. Swensen, G. C. Bazan, A. J. Heeger, *Journal Of Applied Physics* **2005**, *98*.

[17] L. Edman, M. Pauchard, B. Liu, G. Bazan, D. Moses, A. J. Heeger, *Applied Physics Letters* **2003**, *82*, 3961.

[18] C. Yin, Y. Z. Zhao, C. Z. Yang, S. Y. Zhang, *Chemistry Of Materials* **2000**, *12*, 1853.

[19] Q.-D. S. J. Z. C.-Z. Y. Y.-J. B. Zhen Gu, *Journal of Applied Polymer Science* **2006**, *100*, 2930.

[20] J. S. Wilson, M. J. Frampton, J. J. Michels, L. Sardone, G. Marletta, R. H. Friend, P. Samori, H. L. Anderson, F. Cacialli, *Adv. Mater.* **2005**, *17*, 2659.

[21] P. Pachler, F. P. Wenzl, U. Scherf, G. Leising, *J. Phys. Chem. B* **2005**, *109*, 6020.

[22] S. D. Druger, M. A. Ratner, A. Nitzan, *Solid State Ion.* **1986**, *18-9*, 106.

[23] G. Dimarco, A. Bartolotta, G. Carini, *Journal Of Applied Physics* **1992**, *71*, 5834.

[24] H. T. Kim, J. K. Park, *Solid State Ion.* **1997**, *98*, 237.

[25] R. Q. Yang, A. Garcia, D. Korystov, A. Mikhailovsky, G. C. Bazan, T. Q. Nguyen, *Journal of the American Chemical Society* **2006**, *128*, 16532.

[26] R. Q. Yang, H. B. Wu, Y. Cao, G. C. Bazan, *Journal of the American Chemical Society* **2006**, *128*, 14422.

[27] Y. F. Hu, J. Gao, *Applied Physics Letters* **2006**, *89*.

[28] S. Doi, M. Kuwabara, T. Noguchi, T. Ohnishi, *Synthetic Metals* **1993**, *57*, 4174.

[29] C. Zhang, S. Hoger, K. Pakbaz, F. Wudl, A. J. Heeger, *J. Electron. Mater.* **1993**, *22*, 413.

[30] F. Cacialli, J. S. Wilson, J. J. Michels, C. Daniel, C. Silva, R. H. Friend, N. Severin, P. Samori, J. P. Rabe, M. J. O'Connell, P. N. Taylor, H. L. Anderson, *Nature Materials* **2002**, *1*, 160.

Chapter 7. Organic-soluble conjugated polyrotaxanes

Following on from synthesis of water-soluble conjugated polyelectrolytes, organic-soluble conjugated polyrotaxanes have been synthesised to circumvent the issues with solvent choice and the presence of ions which can lead to unstable devices. This would also allow the use of PEDOT:PSS as a hole transport layer.

7.1. Introduction

The water-soluble polymers have issues for use in devices arising from use of water as a solvent. Water is not volatile in comparison to some common organic solvents such as chloroform, and so when spin-coating inhomogeneous films may form. Solvent evaporation of water is slow which allows the polymers to rearrange, thus causing variation in PL spectra (as seen in chapter 5) and operational differences in LEDs. LEDs also benefit from use of multi-layered devices which can include hole or electron transporting layers. The common hole transport layer, PEDOT:PSS, is water-soluble and therefore can not be used with the water-soluble polymers as the interface between the two layer lacks a defined boundary due to the ability of the polymers to mix. Also whilst the ionic mobility in the water-soluble polymers can be a benefit, it can also cause operational instabilities due to the possibility of further electrochemical reactions and the time needed for ionic rearrangement in devices. To overcome these limitations polyrotaxanes that have been chemically modified into uncharged and counter-cation free polyrotaxanes, facilitating dissolution and processing in organic solvents, have been synthesised by the Anderson Laboratory at the University of Oxford (Frampton, Unpublished).

7.1.1. Synthesis

Synthesis of non-ionic, organic-soluble polyrotaxanes has been achieved from two different approaches. In the first approach the charged carboxyl groups were converted to methyl esters and the cyclodextrin hydroxyl functionality subjected to trihexylsilylation (THS - $Si\text{-}(C_6H_9)_3$) to form silyl ethers. In the second approach, benzylation (Bn - $CH_2\text{-}C_6H_5$) of both functionalities gave benzyl esters and benzyl ethers.

The new polymers were formed by functionalisation of the water-soluble PFBP.Li polyrotaxane. Trihexylsilylation of polyrotaxane PFBP.Li⊂*β*-CD (with a *m*-terphenylene endgroup) to give PFBP.Me⊂*β*-CD.THS was accomplished by a three-step procedure. Firstly, the free-acid PFBP.H⊂*β*-CD was obtained. Methylation of the carboxyl functionality gave the methyl ester PFBP.Me⊂*β*-CD, and finally, reaction with an excess of chlorotrihexylsilane led to silylation of the cyclodextrin hydroxyl groups. Benzylation of PFBP.Li⊂*β*-CD was accomplished at the cyclodextrin hydroxyl and carboxyl positions by reaction with benzyl chloride after first converting to the free acid PFBP.H⊂*β*-CD. An unthreaded organic-soluble polymer, PFBP.Bn, was also prepared by the chemists, with the same polymer backbone as PFBP.Bn⊂*β*-CD.Bn, and was synthesised by an analogous route, but with the omission of *β*-CD from the polymerisation reaction. The chemical structure of these polymers is given in Figure 7-1.

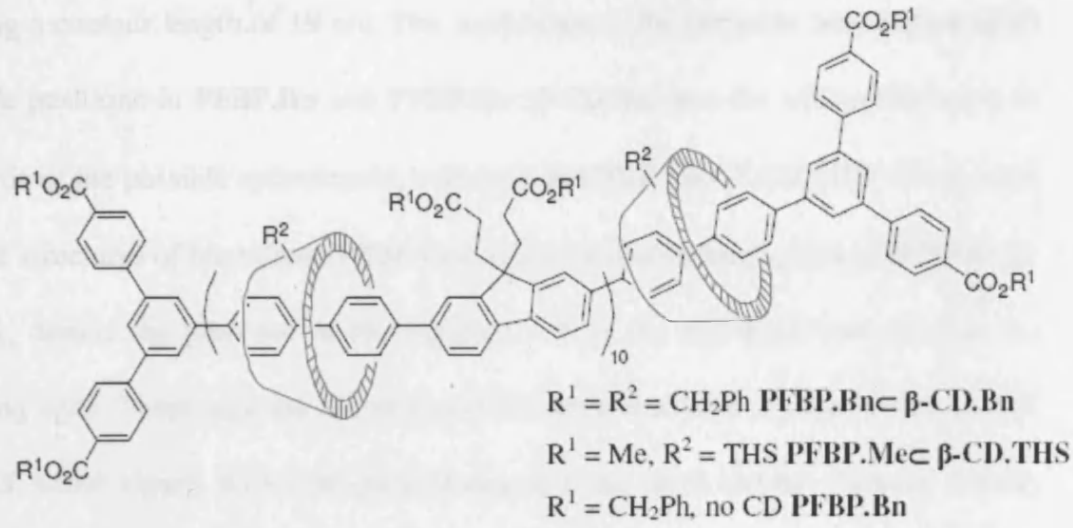

Figure 7-1 Chemical structures of PFBP.Bn⊂β-CD.Bn, PFBP.ME⊂β-CD.BnTHS and PFBP.Bn.

Molecular mechanics calculations were used by chemists at the Chemical Research Laboratories, University of Oxford to give insights into the degree of insulation in the three new organic-soluble polymers. The free acid PFBP.H⊂β-CD which was a reaction intermediate was also included as a model for an unfunctionalised polyrotaxane.

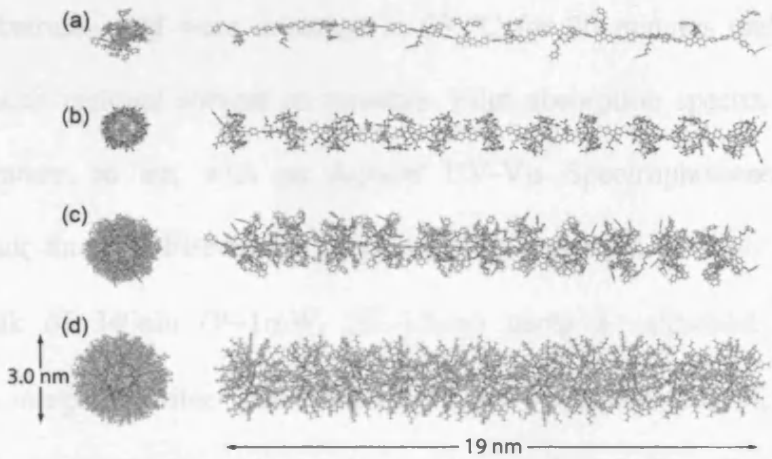

Figure 7-2 Energy-minimised structures of polymers. (a) PFBP.Bn, (b) PFBP.H⊂β-CD, (c) PFBP.Bn⊂β-CD.Bn, (d) PFB.Me⊂β-CD.THS.

The energy-minimised structures, illustrated in Figure 7-2, were determined for a polymer chain with chain length n=10, threading ratio of 1 CD per repeat unit,

revealing a contour length of 19 nm. The models allow for complete benzylation of all available positions in PFBP.Bn and PFBP.Bn⊂β-CD.Bn, and for trihexylsilylation of two thirds of the possible cyclodextrin hydroxyls in PFBP.Me⊂β-CD.THS. It is evident from the structures of benzylated PFBP.Bn⊂β-CD.Bn and unfunctionalised PFBP.H⊂β-CD that, despite the presence of the insulation, there are still significant gaps in the insulating layer. These gaps are not present in the more insulated silylated PFBP.Me⊂β-CD.THS, which clearly shows the greatest degree of coverage and has the most densely packed and thickest insulating layer, with a diameter of approximately 3.0 nm. These differences in insulation will modify the behaviour in LEDs, as seen for PDV.M⊂β-CD when the threading ratio was doubled.

7.2. Experimental details

For the preparation of thin films, materials were readily dissolved in HPLC grade chloroform at 40 °C, stirred for 24 hours and filtered through a 0.45 μm filter before preparing films. Films were typically 100 nm thick (1.5 % w/v solutions), on Spectrosil substrates, and were annealed at 60 °C for 30 minutes under nitrogen to remove as much residual solvent as possible. Film absorption spectra were taken at room temperature, in air, with an Agilent UV-Vis Spectrophotometer. PL was measured in air for the PFBP-based polymers with excitation from an UV LED with spectrum peak of 340nm (P~1mW, $\Delta\lambda$~12nm) using a calibrated Ocean Optics spectrograph, integration time varied between 2 and 5 seconds. The PL spectra of the PF-based polymers were conducted under a vacuum of approximately 10^{-5} mbar with UV excitation of 355 and 365 nm. PL efficiency was measured in air with the aid of an integrating sphere and using a He-Cd laser or UV excitation at 355 and 365 nm.[1] To fabricate light-emitting structures, thin films of PEDOT:PSS were spun onto pre-etched,

oxygen-plasma-treated ITO substrates,[2] annealed in nitrogen, and then the emissive polymers spun onto these substrates in nitrogen. Evaporation of LiF (for PFBP-based devices) cathodes (3-5 nm) with an Al capping layer (~ 100 nm thickness) or Al with thickness of 150nm (PF-based devices) was conducted at 10^{-6} mbar. Devices were transferred under nitrogen to a chamber which was then evacuated to ~10^{-2} mbar. Basic electrical characterization involved measuring the device current and light output as a function of the applied voltage. The current was measured by a Keithley 2400 source meter which also supplied the voltage. The luminous output was measured with a calibrated silicon photodiode.

7.3. Results and discussion

7.3.1. Optical Properties

Work by the Anderson group (Unpublished) has shown that in dilute solutions the shape and position of the absorption and emission spectra of the polyrotaxanes do not depend on the insulation extent and that the solution luminescence quantum yields were also similarly invariant and in the range 0.61 to 0.65. This suggests that in dilute solution, optical properties are dependent only on the nature of the polymer backbone and not on the microenvironment of the insulating layer, as observed for the thermochromic behaviour in Chapter 5. Intermolecular interactions and hence the nature of the insulation are expected to be important when the concentration of polymer is increased to the limit of the solid state. Figure 7-3 shows the thin film emission spectra of the analogue polymer and the benzylated and silylated polyrotaxane.

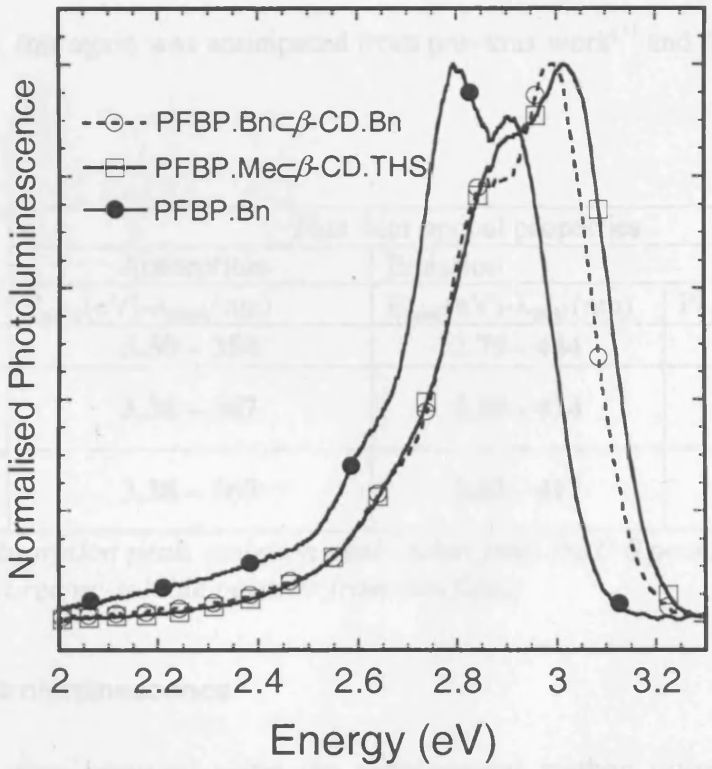

Figure 7-3 Normalised PL spectra of thin-film polymers spin coated on spectrosil substrates of PFBP.Bn⊂β-CD.Bn, PFBP.Me⊂β-CD.THS and PFBP.Bn.

The two polyrotaxanes are blue-shifted with respect to the PFBP.Bn polymer but the silyated polyrotaxane is furthest in the blue. This blue-shift of the polyrotaxanes corresponds with a reversal of the relative intensities of the 0-0 and 0-1 emission bands as seen for the water-soluble polymers. The degree of encapsulation by the insulating layer correlates with the size of the blue-shift shift in the thin film luminescence spectra and increases in the order PFBP.Bn< PFBP.Bn⊂*β*-CD.Bn < PFBP.Me⊂*β*-CD.THS.

The slight increase of the full width at half maximum (FWHM) in the red regime of the PFBP.Me⊂β-CD.THS compared to PFBP.Bn⊂β-CD.Bn is normally indicative of aggregate formation. This could be attributed to the THS chains on different chains interacting due to the close packing that is associated with thin films.

The thin-film luminescence quantum yield for the polymers shows a similar relationship. The least quenched was the trihexylsilylated polyrotaxane PFBP.Me⊂β-CD.THS suggesting the insulation prevents intermolecular non-radiative deactivation of the excited state, this again was anticipated from previous work[3] and from work in this thesis.

	Thin film optical properties		
	Absorption	Emission	
Polymer	E_{peak}(eV)-λ_{peak}(nm)	E_{peak}(eV)-λ_{peak}(nm)	PL efficiency (%)
PFBP.Bn	**3.50 – 354**	**2.79 - 444**	**33 ± 3**
PFBP.Bn ⊂*β*-CD.Bn	**3.38 – 367**	**2.99 - 414**	**49 ± 5**
PFBP.Me ⊂*β*-CD.Si	**3.38 – 367**	**3.01 - 411**	**54 ± 5**

Table 7-1 The absorption peak, emission peak (taken from the 0-0 peak) and the PL efficiency of the organic-soluble polymer from thin films.

7.3.2. Electroluminescence

Devices were prepared using the experimental method given in (7.2). The analogue polymer was capable of operation without an additional hole transport layer

however polyrotaxane devices without this layer would experience high currents and no light emission. Once polyrotaxane devices were prepared with the PEDOT:PSS they were stabilised somewhat. Figure 7-4 illustrates the typical device behaviour after the addition of PEDOT:PSS: the unthreaded derivative devices were more robust than the polyrotaxanes. This could be due to the increased insulation when compared to the water-soluble polyrotaxanes and the increased intermolecular separation due to the additional organic moieties on the CD rings, which limit the charge transport between different polymers causing device self-heating to occur rapidly.

The increased insulation results in a much higher turn-on voltage for the two polyrotaxanes compared to their analogue polymer in Table 7-2, and again the level of encapsulation can be related to turn-on voltage with PFBP.Bn< PFBP.Bn⊂β-CD.Bn< PFBP.Me⊂β-CD.THS. However the turn-on voltages are higher for all polymers when compared to the water-soluble polymer, due to the LEC-like behaviour of the water-soluble polymers lowering the turn on voltage for light emission compared to the LED-like behaviour of the organic-soluble polymers. The luminous current efficiencies are lower than previously found for the water-soluble polymers. Counterintuitively, the most insulated polymer, PFBP.Me⊂β-CD.THS has the highest luminous current efficiency. When compared to PFBP.Bn and PFBP.Bn⊂β-CD.Bn it is highly insulated and the THS group is larger than Bn. Whilst the maximum value of luminous current efficiency was achieved with the PFBP.Me⊂β-CD.THS it should be noted that few devices were stable or capable of operation so it may be presumptuous to assume that the PFBP.Me⊂β-CD.THS perform better than PFBP.Bn⊂β-CD.Bn. Further work on optimisation of the device structure will need to be conducted.

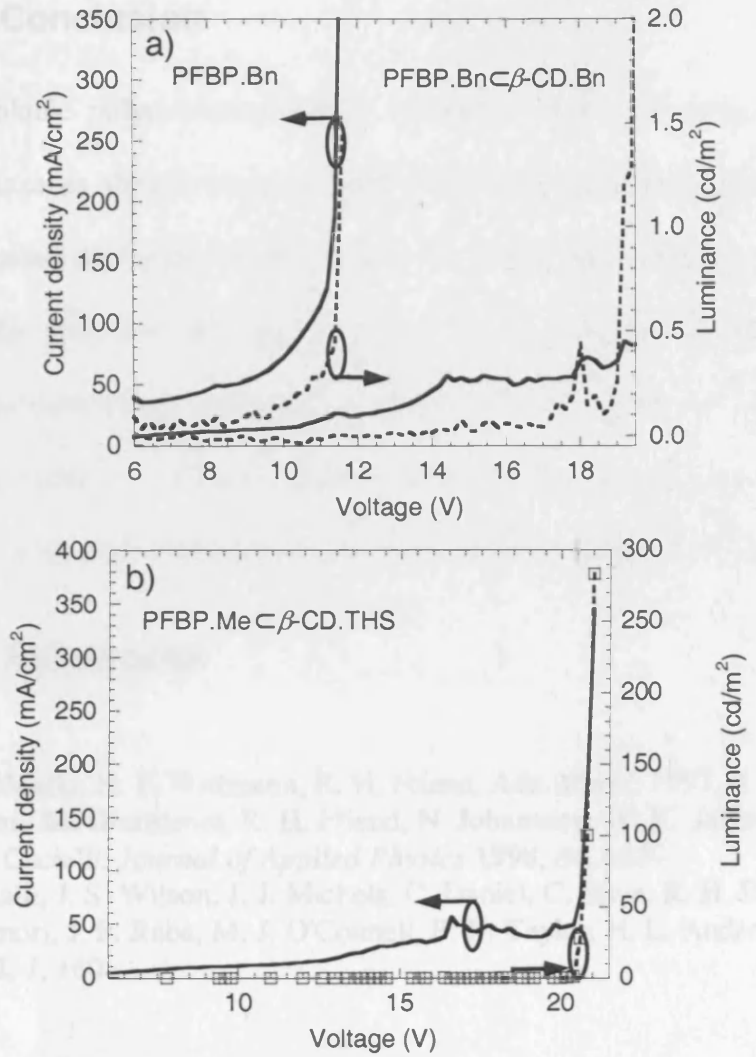

Figure 7-4 Electroluminescence and current density characteristics of a)PFBP.Bn and its corresponding polyrotaxane with b) PFBP.Me⊂β-CD.THS.

	V_{on} (V) at L=0.1cd/m	Max Luminous Current Efficiency (cd/A)
PFBP.Bn	**9.6**	**0.0003**
PFBP.Bn⊂β-CD.Bn	**17.3**	**0.003**
PFBP.Me⊂β-CD.THS	**18.2**	**0.08**

Table 7-2 Turn-on voltages and maximum luminous current efficiencies taken from Figure 7-4 which showed typical LED-like behaviour. These figures have been quoted as the devices were unstable in comparison to the water-soluble polymeric devices and so average efficiencies would have large errors.

7.4. Conclusion

The organic-soluble polyrotaxanes exhibit properties similar to those of the water-soluble polyrotaxanes, they have blue-shifted emission and absorption spectra compared to their unthreaded derivative PFBP.Bn with the blue-shift increasing with increased insulation. The polymers are capable of use as organic semiconductors with the increased insulation leading to higher turn-on voltages but further device improvements and testing are necessary. This has demonstrated that functionalisation of the CD and the end groups is possible, leading to further uses of the polymers as molecular wires.

7.5. References

[1] J. C. deMello, H. F. Wittmann, R. H. Friend, *Adv. Mater.* **1997**, *9*, 230.
[2] J. S. Kim, M. Granstrom, R. H. Friend, N. Johansson, W. R. Salaneck, R. Daik, W. J. Feast, F. Cacialli, *Journal of Applied Physics* **1998**, *84*, 6859.
[3] F. Cacialli, J. S. Wilson, J. J. Michels, C. Daniel, C. Silva, R. H. Friend, N. Severin, P. Samori, J. P. Rabe, M. J. O'Connell, P. N. Taylor, H. L. Anderson, *Nature Materials* **2002**, *1*, 160.

Chapter 8. Cross-linking of PEDOT:PSS for use with water-soluble polymers

Here a procedure to convert water-soluble PEDOT:PSS into a cross-linked matrix for use with water-soluble emissive polymers is discussed. Preliminary results of devices using this technique are presented.

8.1. Background

The benefits of a hole transport layer (HTL) have been documented in this work. Increased hole transport to the emissive layer from the ITO and additional holes from the HTL lead to increased electron-hole recombination in the emissive polymer film. PEDOT:PSS is the preferred HTL as its insolubility in organic solvents ensures a sharp boundary between the PEDOT:PSS and the emissive polymer. PEDOT:PSS also protects the emissive polymer layer from diffusion of oxygen-containing species from the ITO[1] and lowers the hole injection barrier independently from the work function of the ITO.[2]

However, PEDOT:PSS cannot be used with the polyrotaxanes in this study as both polymers are water soluble. To use PEDOT:PSS with water-soluble polymers the solvent PEDOT:PSS is dispersed in can be changed. This is not recommended due to the acidic and electrostatic nature of the polymer, as it could cause instability of the PEDOT:PSS matrix, or the PEDOT:PSS adapted so that it can become an insoluble fixed layer such as PPV in LEDs.

The possibility of cross-linking PEDOT:PSS for LEDs to provide a permanently fixed film has been successfully demonstrated by Philips Research Laboratories. Touwslager *et al*[3] used UV-irradiation of an admixed PEDOT:PSS and an bisazide- and polyazide photoinitator, 4,4'-diazido-2,2'-disulfonic acid benzalacetone disodium

salt (DAB, see Figure 8-1 for chemical structures) to crosslink the PEDOT:PSS rendering it water-insoluble.

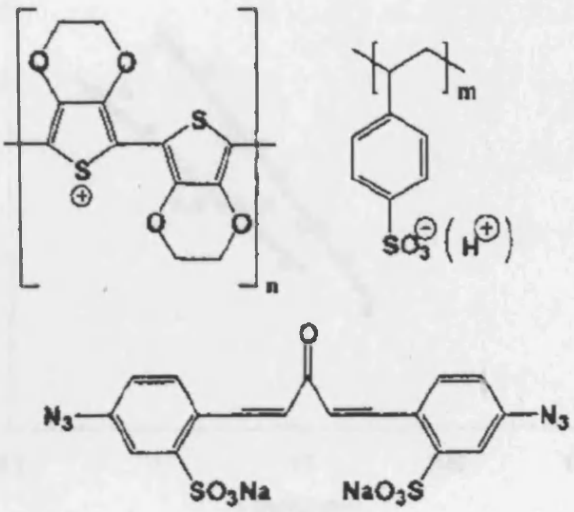

Figure 8-1 Chemical structures of PEDOT:PSS (top) and DAB (bottom).

The photocross-linking occurs when the DAB is exposed to low dose UV-radiation in the wavelengths 360-370nm. Azides photochemically decompose to nitrenes[4] which can react with C-H bonds in the PEDOT:PSS giving a cross-linked PEDOT:PSS matrix. Nitrenes are reaction intermediates and can insert into a C-H bond to form an amide or amine. The simplest nitrene is a :N-H with two electrons of the available six electrons forming a covalent bond with hydrogen, two form an electronpair and the remaining two electrons occupy two degenerate p-orbitals.[5]

Singlet and triplet nitrenes (via intersystem crossing) are formed and cross-linking, in air, occurs within minutes as shown in Figure 8-2 taken from[3]. However the nitrene may also react with oxygen,[6-9] reducing the level of cross-linking by reducing the photosensitivity of the admixed PEDOT:PSS and DAB.

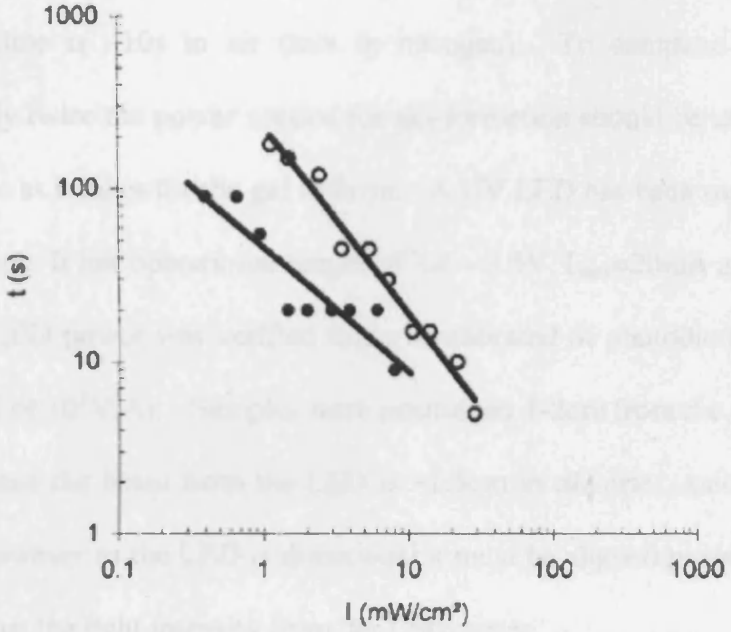

Figure 8-2 Gel-formation time as a function of intensity (λ=365nm), 0.25%b.w of DAB was used. The filled circles are for samples irradiated in nitrogen whilst the open circles indicate that irradiation took place in presence of oxygen. [3]

Touwslager produced negatively patterned circuits using this technique by using a photolithographic mask, converting the PEDOT:PSS and then washing off the unconverted material. The admixed solution was spin-coated to produce a 100nm film. After conversion, film thickness was found to decrease by ~20%. Once the DAB has been used to initialise cross-linking it is assumed to have nearly all reacted away. Any remaining unreacted initiator can be removed by baking the film after irradiation.

We needed to convert much larger areas to cross-linked PEDOT:PSS than Touwslager (~1cm^2) and ensure that throughout the depth of the film it is cross-linked to prevent "lifting" of the film during deposition of the water-soluble emissive layer.

8.2. Experimental details

The DAB is added directly to the colloidal PEDOT:PSS solution (Baytron P VP AI 4083, as supplied by H.C. Stark, is 1.6%b.w. in water or the same solution but

supplied from Sigma-Aldrich) as 0.25%b.w of the solution. Using 10mW/cm^{-1} of power, gel time is ~10s in air (less in nitrogen). To complete the cross-linking, approximately twice the power needed for gel-formation should be used to cross-link in the same time as it takes for the gel to form. A UV LED has been used with a spectrum peak of 370nm. It has operational ranges of 3.4 – 3.5V, I_{max}=20mA and P>5mW.

The LED power was verified using a calibrated Si photodiode and an amplifier (using a gain of 10^3V/A). Samples were positioned 1-2cm from the centre of the LED. At this distance the beam from the LED is ~1.5cm in diameter, suitable for Spectrosil and ITO. However as the LED is directional it must be aligned properly and it has also been noted that the light intensity from the LED varies.

Samples were irradiated for 15 minutes at 7.5mW/cm^{-1} (the calibrated photodiode area is 1cm^2) to ensure complete conversion of the film and the outlying edges which receive less irradiation from the LED. Film thicknesses across the sample vary by up to 20%, possibly due to variations in the LED intensity or from variations in the initial film from spin-coating.

After irradiation preliminary samples were spin-coated with water to determine the extent of cross-linking. Once the cross-linking of the entire film had been verified, the samples were no longer spin-coated with water. Film thicknesses decreased by 20-25% after cross-linking as found by Touwslager. Devices were prepared using the standard procedure as documented in Chapter 6, with the cross-linked PEDOT:PSS annealed in the glovebox to remove any unreacted DAB prior to spin-coating the emissive polymer and to remove moisture from the air.

Two batches of PEDOT:PSS (Baytron P VP AI 4083) have been used for cross-linking, one supplied from H.C. Stark several years ago and one from Sigma-Aldrich purchased recently. Degradation of the stability of the first, older batch led to poor

cross-linking. The contact potential differences (CPD) and devices for both batches are supplied whilst only absorption spectra of the new batch of PEDOT:PSS have been presented. Electroluminescent characteristics of the control devices are given.

8.3. Results

1.3.2. Optical Characterisation

PEDOT:PSS absorbs in the far UV whilst DAB absorbs from 325-475nm. After irradiation the PEDOT:PSS absorbance signal decreases (there is no discernible change in film thickness) and the DAB peak disappears as shown in Figure 8-3. The DAB peak at 2.8eV is large prior to irradiation but is almost not present after irradiation. The high energy peak at 5.5eV increases by 10% after cross-linking.

The spin-coating with water has been included on the absorption peak, although it was removed once the correct procedure had been determined, as it indicates the decrease in film thicknesses when the sample had not been fully converted by the lower absorbance values. When the time for cross-linking was determined if the samples were spin-coated with water, this further decrease of the absorbance spectra intensity was not observed.

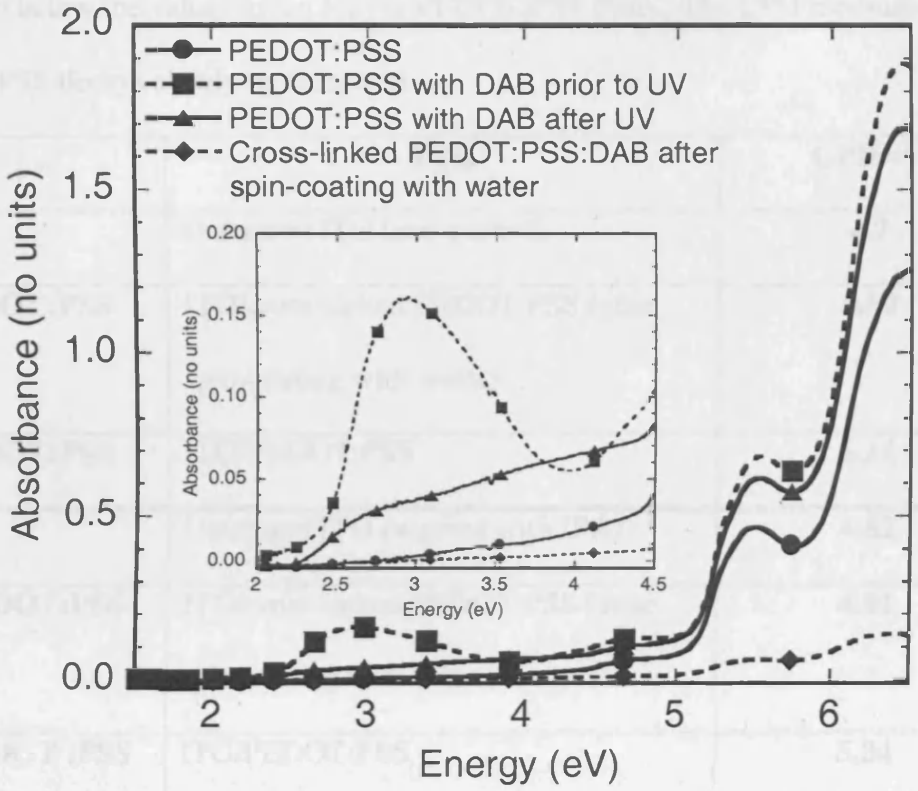

Figure 8-3 0.25% b.w. (of solution) DAB in PEDOT:PSS. Absorption spectra were taken before and after UV irradiation and after spin-coating with water. The DAB, before cross-linking exhibits a peak at 3eV. The inset is a zoom of the DAB peak, and how, after irradiation, the peak is absent.

0.5%b.w. of DAB has also been added to PEDOT:PSS as suggested by Touwslager. However this was excessive as filaments could be seen under the optical microscope be seen prior to the washing. The filaments were attributed to the DAB. These filaments were then removed by washing of the sample.

8.3.1. Kelvin Probe measurement of work function

All values have been calibrated against previous results, and as such are 0.4eV lower than the measured contact potential difference (CPD). The washing of the PEDOT:PSS decreases the CPD but the film is not annealed prior to CPD measurement, there may be moisture remaining in the film. It should be noted that whilst the CPD of the oxygen plasma cleaned ITO is very high as observed in Chapter 3, this decays

rapidly to below the values given for the PEDOT:PSS films. The CPD measured for the PEDOT:PSS decays slowly in comparison.

	Film	CPD/eV
	Untreated ITO (not washed)	**4.7**
old PEDOT:PSS	ITO/cross-linked PEDOT:PSS (after spin-coating with water)	**5.00**
old PEDOT:PSS	ITO/PEDOT:PSS	**5.14**
	Untreated ITO (washed with IPA)	**4.82**
new PEDOT:PSS	ITO/cross-linked PEDOT:PSS (after spin-coating with water)	**4.91**
new PEDOT :PSS	ITO/PEDOT:PSS	**5.04**

Table 8-1 The contact potential differences of the PEDOT:PSS after various treatments. The older PEDOT:PSS batch from H.C. Starck is presented alongside the newer batch from Sigma-Aldrich with contact potential values of ITO as reference measurements.

Table 8-1 gives the CPDs of the various PEDOT:PSS mixtures and of untreated ITO for comparison. The older PEDOT:PSS supplied directly from H.C. Starck has a CPD value of 5.14eV which is 0.1eV higher than that of the PEDOT:PSS supplied from Sigma-Aldrich. The contact potential difference of the cross-linked films are lower than for pristine PEDOT:PSS in Table 8-1for both batches. Both batches of PEDOT:PSS experience a similar relative decrease of the work function value of 0.13-0.14eV upon cross-linking.

8.3.2. Preliminary device results with F8BT

The F8BT films were deposited in the glovebox and had LiF cathodes (5nm) with Al (150nm) capping layer. Electroluminescent characteristics of the devices were tested under pressures of 10^{-2}mbr.

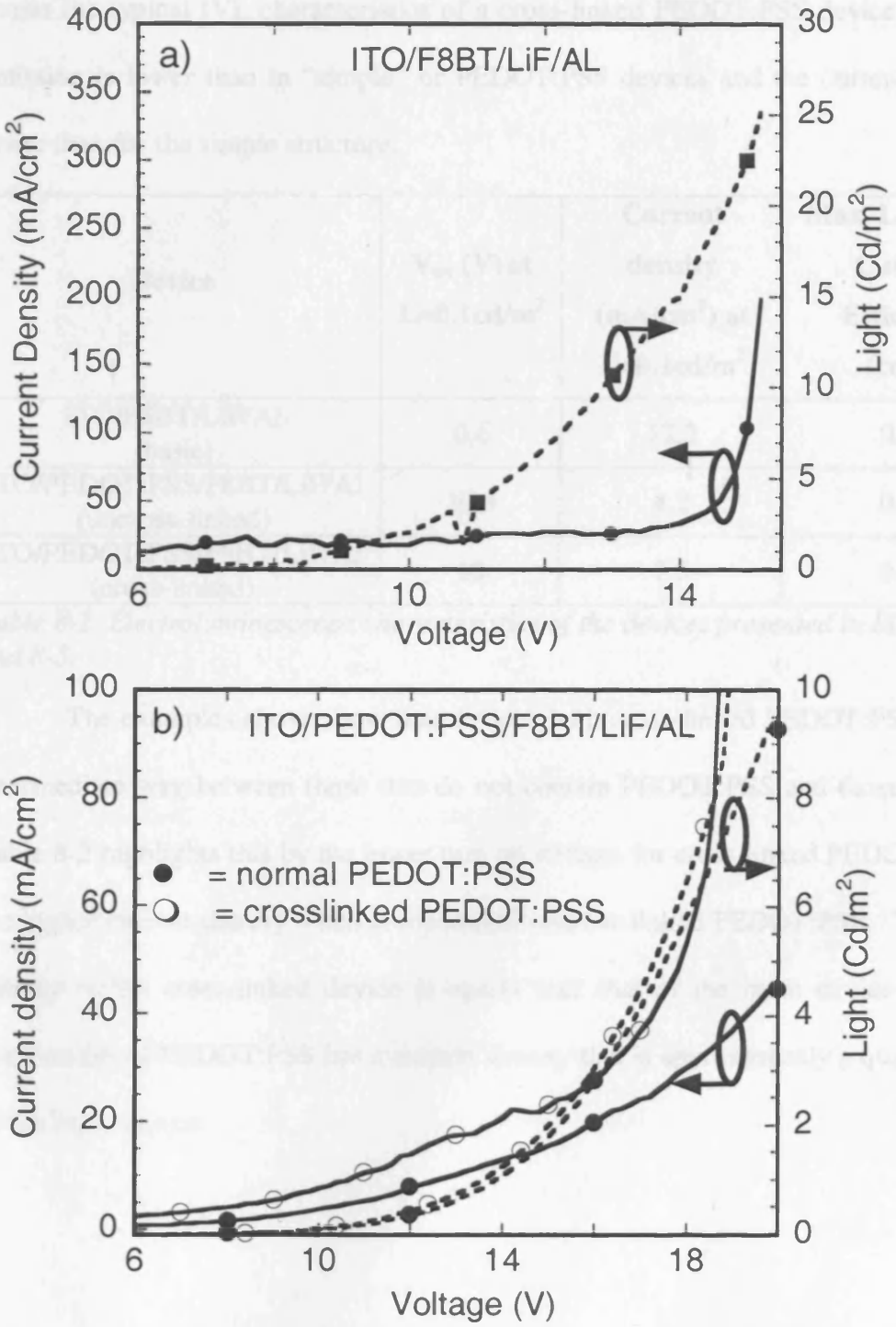

Figure 8-4 Typical IVL graphs of the 3 types of device structure employed. a) is a basic device with no PEDOT:PSS added and b) shows two devices, one with uncross-linked PEDOT:PSS and the other with cross-linked PEDOT:PSS.

The addition of PEDOT:PSS stabilised the devices, when compared to the "simple" structure (ITO/F8BT/LiF/Al): the current anomaly at low voltages is not present and the light emission is higher at similar voltages as seen in Figure 8-4. It also

shows the typical IVL characteristics of a cross-linked PEODT:PSS device. The light emission is lower than in "simple" or PEDOT:PSS devices and the current density is lower than for the simple structure.

Device	**V_{on} (V) at L=0.1cd/m^2**	**Current density (mA/cm^2) at L=0.1cd/m^2**	**Max. Luminous Current Efficiency (cd/A)**
ITO/F8BT/LiF/Al (basic)	6.6	17.2	0.05
ITO/PEDOT:PSS/F8BT/LiF/Al (uncross-linked)	10.4	4.2	0.02
ITO/PEDOT:PSS/F8BT/LiF/Al (cross-linked)	10	7.5	0.01

Table 8-2 Electroluminescence characteristics of the devices presented in Figure 8-4 and 8-5.

The examples above show that devices with cross-linked PEDOT:PSS act in an intermediate way between those that do not contain PEDOT:PSS and those which do. Table 8-2 highlights this by the lower turn on voltage for cross-linked PEDOT:PSS and the higher current density when compared to uncross-linked PEDOT:PSS. The current density in the cross-linked device is nearly half that of the basic device whilst the uncross-linked PEDOT:PSS has a current density that is approximately a quarter of that of the basic device.

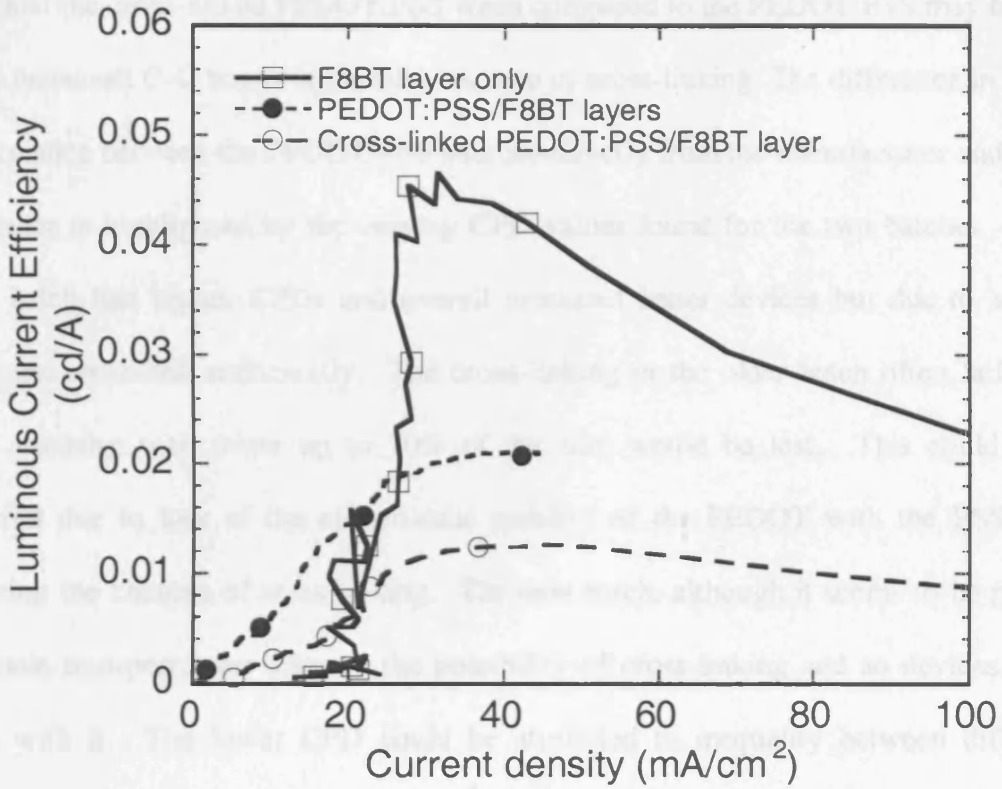

Figure 8-5 Luminous current efficiency of the three types of device made; ITO/F8BT/LiF/Al, ITO/PEDOT:PSS/F8BT/LiF/Al and ITO/cross-linked PEDOT:PSS/F8BT/LiF/Al.

The addition of PEDOT:PSS improves the device quality and stability. It can be tested multiple times before destruction. The cross-linked PEDOT:PSS devices have the lowest luminous current efficiency (~0.01 cd/A) in Table 8-2 and Figure 8-5 but the efficiency decays slowest from the three types of devices made, the stability is of a similar quality to that of uncross-linked PEDOT:PSS .

8.4. Discussion

Optical characterisation of the PEDOT:PSS during the cross-linking process verified that the DAB chemically reacts with the PEDOT:PSS, by the absence of the absorption peak in Figure 8-3 between 2.5-3.5eV. The shape of the absorption spectrum of the cross-linked PEDOT:PSS mimics that of the PEDOT:PSS closely. The seeming existence of a more intense high energy peak in the admixed PEDOT:PSS and

DAB and the cross-linked PEDOT:PSS when compared to the PEDOT:PSS may be due to the increased C-C bonds in the film because of cross-linking. The difference in batch performance between the PEDOT:PSS sourced directly from the manufacturer and from a supplier is highlighted by the varying CPD values found for the two batches. The older batch had higher CPDs and overall produced better devices but due to ageing could not cross-link sufficiently. The cross-linking in the older batch often failed so when washing with water up to 70% of the film would be lost. This could have occurred due to loss of the electrostatic stability of the PEDOT with the PSS thus lessening the chances of cross-linking. The new batch, although it seems to be poorer as a hole transport layer allowed the possibility of cross-linking and so devices were made with it. The lower CPD could be attributed to inequality between different batches of the PEDOT:PSS.

The cross-linked PEDOT:PSS performs adequately as a hole transport layer, but it has lost some of the desirable properties (increased charge transport, reduced current density to prevent heating of the device) that it had prior to the cross-linking. When the DAB cross-links it does this via the formation of nitrenes as discussed previously. These nitrenes (especially the triplet nitrenes) can react with oxygen as well as the C-H bonds, which as well as reducing the cross-linked matrix also leads to further species being present in the matrix. It also is known that due to the acidic nature of PSS in PEDOT:PSS etching of the ITO surface is possible and this reduces the hole transport due to degradation of the ITO surface.[10] The presence of these possible further species in the PEDOT:PSS could lead to increased acidic attack of the ITO. This coule be the cause of the reduced effect of the PEDOT:PSS or that by cross-linking the PEDOT:PSS it has reduced hole transport through the polymer. It is expected that they mostly insert into C-H bonds rather than react with oxygen or benzene rings. The cross-linking is

probably a random process where the nitrene inserts into whatever C-H bond happens to be closest to it at the time of its formation, since diffusion within the film is likely to be quite limited. Insertion into adjacent chains leads to cross-linking. It has been suggested that the electronic structure of the cross-linked PEDOT will not be exactly the same as the uncross-linked material, but the conjugation along the backbone ought to be maintained. It was further suggested that the cross-linking would have some kind of influence on the conformations of the polymer chains and on intermolecular interactions – this may be indicated by the decrease in thickness of the films after cross-linking.[11]

It may be beneficial to explore the surface of the cross-linked PEDOT:PSS during the cross-linking by x-ray photoelectron spectroscopy to understand the chemical reactions more and also to study the charge transport and energy level alignment of these devices by electroabsorption spectroscopy.

These preliminary results show that cross-linked PEDOT:PSS could be used to boost the operating stability of the water soluble reference polymers and polyrotaxanes by removing current anomalies and further decreasing the current density in these devices.

8.5. Conclusions

Cross-linking large areas of PEDOT:PSS has been demonstrated by observation of the absorption spectra and of trials with water. The cross-linking reduces some of the PEDOT:PSS properties in devices but they still outperform basic devices. Further investigations into the structure and behaviour of the cross-linked PEDOT:PSS may be useful to optimise performance but it is now possible to make devices with water-soluble emissive polymers and incorporate PEDOT:PSS.

8.6. References

[1] J. C. Scott, S. A. Carter, S. Karg, M. Angelopoulos, *Synthetic Metals* **1997**, *85*, 1197.
[2] T. Kugler, W. R. Salaneck, H. Rost, A. B. Holmes, *Chemical Physics Letters* **1999**, *310*, 391.
[3] F. J. Touwslager, N. P. Willard, D. M. de Leeuw, *Applied Physics Letters* **2002**, *81*, 4556.
[4] R. A. McClelland, M. J. Kahley, P. A. Davidse, G. Hadzialic, *Journal of the American Chemical Society* **1996**, *118*, 4794.
[5] K. P. C. Vollhart, N. E. Schore, *Organic Chemistry Structure and Function*, W. H. Freeman and Company, United States of America **1999**.
[6] L. N. Karyakina, A. V. Gubinov, *High Energy Chemistry* **2000**, *34*, 256.
[7] S. V. Zelentsov, N. V. Zelentsova, A. A. Shchepalov, *High Energy Chemistry* **2002**, *36*, 326.
[8] S. V. Zelentsov, N. V. Zelentsova, A. B. Zhezlov, A. V. Oleinik, *High Energy Chemistry* **2000**, *34*, 164.
[9] S. V. Zelentsov, A. B. Zhezlov, A. V. Oleinik, *High Energy Chemistry* **2001**, *35*, 247.
[10] M. P. de Jong, L. J. van Ijzendoorn, M. J. A. de Voigt, *Applied Physics Letters* **2000**, *77*, 2255.
[11] M. Frampton, University of Oxford **2006**.

Chapter 9. Conclusions and further work

This thesis has been primarily concerned with polyrotaxanes suitable for use in light emitting diodes, in particular how the counter-cation choice affects the optoelectronic properties of the polymer. Preceding this part of the work, investigations in to the longevity of the ITO work function increase by oxygen plasma treatments were reported. The thermochromic behaviour of the prototype polyrotaxanes and their analogue polymers, using lithium as the cation, in film and solution were also studied and compared to similar conjugated polymers.

The general concepts of conjugated polymers and their use as LEDs along with mention of issues which adversely affect the LED performance were introduced in Chapter 1. The terminology and uses of polyrotaxanes were given in Chapter 2. This then led onto describe the synthesis route required to make polyelectrolytic polyrotaxanes/analogue polymers, the ion-exchange process and previous work on these work on these materials.

In Chapter 3 it emerged that it is prudent to spin the emissive layer soon after oxygen plasma treatments to maximise the work function increase. An unanticipated benefit of the fast spinning of the emissive layer is that it effectively freezes the work function of the ITO. This effect is long lasting even in air.

The polyelectrolytic nature of the polyrotaxanes/analogue polymers was shown to alter its optical properties even with the use of a small cation such as lithium in Chapter 5. When used in conjunction with the cyclodextrin the thermochromism normally exhibited in similar conjugated polymers is relatively suppressed.

The substitution of small cations for larger monovalent cations proved to impact on both the optical and electronic properties of the polymers. In Chapter 4 the increasing cation size led to increasing photoluminescence efficiencies whilst in Chapter

6 the luminous current efficiency went through a maximum for the materials and rapidly decreased. This was likely due to the diluting properties and low ion mobility of the large K@[2.2.2] ion.

The last two chapters looked at two different methods to increase the operational efficiency of devices. By either making the polyrotaxanes organic-soluble so that additional layers could be added or to allow a PEDOT:PSS layer with the water-soluble polyrotaxanes via the cross-linking of the PEDOT:PSS. These methods had varying success and the more viable route is currently the PEDOT:PSS as the organic-soluble materials had very poor device characteristics.

This work has given an overview of how the use of polyelectrolytic polyrotaxanes have a future as molecular wires for molecular electronics. By the combined use of partial insulation and careful selection of cations to emphasis particular qualities of the polymers these polyrotaxanes still could feature in the ever decreasing circuitry we require. However, this work was not able to study in great details the charge transfer processes or indeed the LEC-like behaviour of the devices made which are crucial to further develop this work. There are hence many more opportunities for research in this area and I will now highlight two of them.

9.1. General characterisation

In chapter 5 it was suggested that the seemingly sharp increase in peak shift at certain temperatures could be because this coincides with the T_g/T_m point. The melting point and glassy temperature are normally determined by differential scanning calorimetry which has been previously unsuccessfully attempted on these compounds. It would be worth revisiting this experiment to gain further knowledge of these conjugated polyelectrolytes and if the morphology at room temperature can be

controlled.[1] It is also well-known that ionic transport in polyelectrolytics is highly coupled to the segmental motions of the polymer.[2] The has the effect of several restricting the cation mobility as the glass transition temperature is reached which can impede device operation. Indeed there are a few general characterisation experiments that are yet to be attempted but should be. By fully understanding the polymer it will allow better devices to be made and also how to best address the improvements needed for the devices. Cyclic voltammetry, for example, on the PDV.M and , PDV.M⊂β-CD.M may show shifting of the ionisation potentials with increasing cationic sizes or indeed show that the electronic structure remains constant.

9.2. The LEC-like nature of these materials

Once the LEC-like behaviour of these materials, even without the use of PEO was discovered we did not progress much further in the understanding of this behaviour. Pulse-radiolysis time-resolved microwave conductivity, developed by Warman, Siebbeles and co-workers,[3, 4] can be used to study the mobility of electrons and holes along isolated conjugated polymer chains such as ours. This would again allow us to study the changes in behaviour with increasing cation size as there are variations in the luminous current efficiency and the turn-on voltages vary in devices depending on the cation used and its environment (whether the polymer is threaded or not). This work may then lead on to modelling of the behaviour in devices, taking into account the cation mobility. The ionic conductivities of the various materials are unknown but impedance analysis has previously been able to give that information. This may go on to explain why K@[2.2.2] materials make poor devices.

LECs have received a lot of attention in the research community, due to the ability of the materials not necessarily having to match up the Fermi energy levels of the electrodes to the HOMO/LUMO levels of the polymer layer. Due to the two competing models there are many experiments that have been designed for LECs. Again as the charge transfer process is somewhat unknown and to further develop understanding of the role the cations play, electroabsoprtion measurements[5-8] on devices should be performed.

Work into cationic behaviour via step-voltage experiments and also direct imaging of the formation of the *p-n* junction[9-11] are another possibility to complement the work on cation choice and its affect on the device properties.

9.3. References

[1] L. Edman, B. Liu, M. Vehse, J. Swensen, G. C. Bazan, A. J. Heeger, *Journal Of Applied Physics* **2005**, *98*.
[2] S. D. Druger, M. A. Ratner, A. Nitzan, *Solid State Ion.* **1986**, *18-9*, 106.
[3] R. Hoofman, M. P. de Haas, L. D. A. Siebbeles, J. M. Warman, *Nature* **1998**, *392*, 54.
[4] P. Prins, L. P. Candeias, A. van Breemen, J. Sweelssen, P. T. Herwig, H. F. M. Schoo, L. D. A. Siebbeles, *Adv. Mater.* **2005**, *17*, 718.
[5] T. M. Brown, J. S. Kim, R. H. Friend, F. Cacialli, R. Daik, W. J. Feast, *Applied Physics Letters* **1999**, *75*, 1679.
[6] J. C. deMello, J. J. M. Halls, S. C. Graham, N. Tessler, R. H. Friend, *Phys. Rev. Lett.* **2000**, *85*, 421.
[7] J. Gao, A. J. Heeger, I. H. Campbell, D. L. Smith, *Physical Review B* **1999**, *59*, R2482.
[8] I. H. Campbell, T. W. Hagler, D. L. Smith, J. P. Ferraris, *Phys. Rev. Lett.* **1996**, *76*, 1900.
[9] J. Gao, J. Dane, *Applied Physics Letters* **2004**, *84*, 2778.
[10] J. Dane, C. Tracy, J. Gao, *Applied Physics Letters* **2005**, *86*.
[11] Y. F. Hu, J. Gao, *Applied Physics Letters* **2006**, *89*.